



City Research Online

City, University of London Institutional Repository

Citation: Muwezwa, M. E. (1986). Stability of flow in tubes and channels with slowly varying walls. (Unpublished Doctoral thesis, The City University)

This is the accepted version of the paper.

This version of the publication may differ from the final published version.

Permanent repository link: <https://openaccess.city.ac.uk/id/eprint/35222/>

Link to published version:

Copyright: City Research Online aims to make research outputs of City, University of London available to a wider audience. Copyright and Moral Rights remain with the author(s) and/or copyright holders. URLs from City Research Online may be freely distributed and linked to.

Reuse: Copies of full items can be used for personal research or study, educational, or not-for-profit purposes without prior permission or charge. Provided that the authors, title and full bibliographic details are credited, a hyperlink and/or URL is given for the original metadata page and the content is not changed in any way.

CONTENTS

STABILITY OF FLOW IN TUBES AND
CHANNELS WITH SLOWLY VARYING WALLS

TITLE	PAGE
TABLES	2
ILLUSTRATIONS	3
ACKNOWLEDGEMENTS	10
DECLARATIONS	11
ABSTRACT	12
by	
1. INTRODUCTION	14
Mwiinga E. Muwezwa	
1.1 Early Studies In Fluid Dynamics	14
1.2 Introduction to Present Thesis	14
1.21 Flow in Tubes	15
1.22 Flow in Channels	15
2. BASIC TUBE FLOW	25
2.1 Stress Function Equation	25
2.2 Exact Solution Submitted for the degree of Ph.D.	33
2.21 Series Solution	35
2.3 Slender Tube Flow	40
2.31 Exponential Tube Approximation	40
2.32 3δ Profiles as Approximations	42
3. SYSTEM STABILITY OF THE 3δ PROFILES	51
3.1 Stability	51
3.11 The City University, London,	
3.12 Department of Mathematics.	55
3.13 Numerical Solution	55
3.14 Losses	57
3.2 Losses	57
3.21 November 1986	63
4. SYSTEM STABILITY OF THE 3δ PROFILES	69
4.1 Investigation of Darcy & Poiseuille Equivalences	69
4.11 Losses	72

CONTENTS

	PAGE
TITLE	1
TABLES	5
ILLUSTRATIONS	7
ACKNOWLEDGEMENTS	10
DECLARATIONS	11
ABSTRACT	12
1. INTRODUCTION	14
1.1 Early Studies In Fluid Dynamics	14
1.2 Introduction to Present Thesis	22
1.21 Flow in Tubes	22
1.22 Flow in Channels	25
2. BASIC TUBE FLOW	28
2.1 Stream Function Equation	28
2.2 Expansion Method	33
2.21 Series Solution	35
2.3 Slender Tube Flow	40
2.31 Exponential Tube Approximation	40
2.32 DE Profiles as Approximations	42
3. SPATIAL STABILITY OF THE DE PROFILES	51
3.1 Disturbance Equation	51
3.2 Orr-Sommerfeld Equation	55
3.21 Numerical Solution	59
3.22 Least Stable Eigenvalue	63
4. TEMPORAL STABILITY OF THE DE PROFILES	69
4.1 Modification of Davey & Drazin Eigenvalues for the DE Profiles	72

4.2	Corcos-Sellars Eigenvalue Relation	80
4.21	Modification of the Corcos-Sellars Formula	81
4.3	Link Between Spatial and Temporal Roots	87
5.	BASIC CHANNEL FLOW	95
5.1	Stream Function Equation	95
5.2	Series Solution	100
6.	STABILITY EQUATIONS	103
6.1	Disturbance Equation	103
6.2	Orr-Sommerfeld Problem	109
6.21	Equation for $\phi^{(0)}$	109
6.22	Equation for $\phi^{(1)}$	115
6.23	Equation for $\phi^{(2)}$	119
7.	GROWTH RATES	123
7.1	Growth Rate Based on Stream Function	123
7.2	Growth Rate based on energy	125
7.21	Growth Rate Based on Kinetic Energy Density	127
7.22	Growth Rate Based on Relative Energy	130
7.3	Growth Rate as a Function of $f(\beta)/H$	132
7.4	Particular integral g_p	140
8.	NUMERICAL METHODS AND RESULTS	145
8.1	Numerical Methods	145
8.11	Orr-Sommerfeld Problem	145
8.12	The Eigenvalue K	149
8.13	Numerical Differentiation	151
8.14	Amplitude Functions and Growth Rates	152

1.2	Numerical Results	155
8.21	The Basic Flow	155
8.22	Growth Rate Terms	158
8.23	Growth Rates	159
9.	CONCLUSIONS	172
	REFERENCES	177
Table 2.1	Differences between the DE approximation and exact solution.	46
Table 2.2	Values of roots on branches A, B and C for $\omega = 1$, $\gamma = 0$ and $R = 500$.	73
Table 2.3	Comparison between the coefficients b and d_1 .	81
Table 4.1	Eigenvalues and estimates for γ in the range -6 to 6 when $N = 1$.	85
Table 4.2	Eigenvalues and estimates for γ in the range 0 to 3 when $N = 3$ and $N = 6$.	86
Table 4.3	Special roots q at $R = 40$, $\omega = 1$, $\gamma = 0$ with corresponding temporal roots at $R = 40$, $\omega = 1$, $\gamma = 0$.	92
Table 6.1	Roots at various values of B for $\beta = 1$ and $\delta = 2.2391$.	116
Table 8.1	The solutions ψ and θ obtained by using the Runge-Kutta routine (81) and the series (87) for $\beta = 0.5$, $\delta = 1$ at various values of γ and λ .	148
Table 8.2	The stress function and relative energy growth rates at various values of B , and λ for $\beta = 1$.	154

TABLES

	PAGE
Table 2.1 DE profiles and results (EM) from the expansion method.	43
Table 2.2 The contributions of separate powers of λ to the axial velocity profile for the tube with $H = 1 + (1/2)\tanh^2 Z$ when $\lambda = 5$.	46
Table 2.3 Differences between the DE approximation and exact solution.	50
Table 4.1 Values of roots on branches A, B and C for $\omega = 1$, $\gamma = 0$ and $R = 5000$.	73
Table 4.2 Comparison between the coefficients b and d_1 .	83
Table 4.3 Eigenvalues and estimates for γ in the range -6 to 6 when $N = 1$.	85
Table 4.4 Eigenvalues and estimates for γ in the range 0 to 3 when $N = 3$ and $N = 6$.	86
Table 4.5 Spatial roots q at $R = 40$, $\omega = 1$, $\gamma = 0$ with corresponding temporal roots at $R = 40$, $q = 1$, $\gamma = 0$.	92
Table 6.1 Roots at various values of R for $\beta = 1$ and $\beta = 1.2593$.	114
Table 8.1 The solutions ϕ_1 and ϕ_2 obtained by using the Runge-Kutta routine (RK) and the series (S) for $R = 40$, $\beta = 1$ at various values of η and Z .	148
Table 8.2 The stream function and relative energy growth rates at various values of R , and Z for $\beta = 1$.	154

	ILLUSTRATIONS	PAGE
Table 8.3	The stream function and relative energy growth rates with particular integrals P_1 and P_2 at $R = 40, 50, 60$	
Fig. 2.1	for $\beta = 1$ and $Z = 1$. velocity profile	156
Table 8.4	Values of the functions G_0, G_1 and G_2 for stream function growth rate	45
Fig. 2.2	with corresponding Poiseuille flow eigenvalues K at various values of R	48
Fig. 3.1	for $\beta = 1$ and $Z = 1$. table eigenvalue	160
Table 8.5	The second and third approximation to	82
Fig. 3.2	the critical Reynolds number at $\beta = 1$ and $Z = 1$ for the stream function and	86
Fig. 3.3	relative energy growth rate. α for $\omega = 1$	170
Fig. 3.4	Variation of q_1 with R for $\gamma = 5$ and $\omega = 1$.	56
Fig. 3.5	Variation of q_1 with ω at $\gamma = 5.5$ for $R = 200$ and $R = 300$.	57
Fig. 4.1	Branches A, B, C indicating eigenvalues $A_1, A_2, A_3, B_1, B_2, B_3, C_1, C_2$ and C_3 at $R = 3000, \omega = 1$.	70
Fig. 4.2	Variation of C_1 with γ for $\alpha = 1, R = 3000$ on A.	73
Fig. 4.3	Variation of C_1 with α at $\gamma = 5$ and $R = 3000$ for the eigenvalue AB.	77
Fig. 4.4	Variation of C_1 with γ for $\alpha = 1, R = 3000$ on B.	78
Fig. 4.5	Variation of C_1 with γ for $\alpha = 1, R = 3000$ on C.	79

ILLUSTRATIONS

	PAGE
Fig. 2.1 Second derivative of velocity profile as a function of Z at $\eta = 0$ when $\lambda = 6$.	45
Fig. 2.2 Velocity profile for Tube 2 at various values of Z when $\lambda = 10$.	48
Fig. 3.1 Contour plot of least stable eigenvalue for $\gamma = 6$, $R = 40$ and $\omega = 1$.	62
Fig. 3.2 Variation of q_i with γ at $R = 40$, $R = 60$ for $\omega = 1$.	64
Fig. 3.3 q_i at various values of γ and R for $\omega = 1$.	65
Fig. 3.4 Variation of q_i with R for $\gamma = 6$ and $\omega = 1$.	66
Fig. 3.5 Variation of q_i with ω at $\gamma = 6.6$ for $R = 200$ and $R = 300$.	67
Fig. 4.1 Branches A, B, C indicating eigenvalues $A_1, A_2, A_3, B_1, B_2, B_3, C_1, C_2$, and C_3 at $R = 5000$, $\alpha = 1$.	70
Fig. 4.2 Variation of C_i with γ for $\alpha = 1$, $R = 5000$ on A.	75
Fig. 4.3 Variation of C_i with α at $\gamma = 6$ and $R = 5000$ for the eigenvalue A_2 .	77
Fig. 4.4 Variation of C_i with γ for $\alpha = 1$, $R = 5000$ on B.	78
Fig. 4.5 Variation of C_i with γ for $\alpha = 1$, $R = 5000$ on C.	79

- Fig. 4.6 The spatial root q_1 as a function of ω when ω_r is fixed at $\omega_r = 0.5184$ and $R = 40$, $\gamma = 0$. 89
- Fig. 4.7 The spatial root q_1 as a function of ω when ω_i is fixed at $\omega_i = -0.6718$ and $R = 40$, $\gamma = 0$. 90
- Fig. 4.8 (a) The temporal roots A_1 , B_1 and C_1 at $R = 5000$, $q = 1$.
(b) The temporal roots A_1 , B_1 and C_1 at $R = 40$, $q = 1$. 93
- Fig. 6.1 Variation of the eigenfunction g_0 with η at $R = 60$ and $\beta = 1$. 112
- Fig. 8.1 Comparison of the second and third approximation for the velocity profile with appropriate Jeffery-Hamel profile at $R = 35$, $\epsilon = 0.1$ and $Z = 1$. 157
- Fig. 8.2 The Poiseuille flow stream function growth rate $G_0(R)$ as a function of R at $\beta = 1$ and $Z = 1$. 161
- Fig. 8.3 The function $G_1(R)$ in the stream function growth rate as a function of R at $\beta = 1$ and $Z = 1$. 162
- Fig. 8.4 The function $G_2(R)$ in the stream function growth rate as a function of R at $\beta = 1$ and $Z = 1$. 163
- Fig. 8.5 The second (--) and third (-) approximation for stream function growth rate $G_x(\psi)$ as a function of ϵ at $R = 60, 150$ for $\beta = 1, Z = 1$. 165

Fig. 8.6 The second (--) and third (-) approximation for relative energy growth rate $G_x(\hat{E})$ as a function of ϵ at $R = 60$ for $\beta = 1$ and $Z = 1$. 166

Fig. 8.7 The critical Reynolds number as a function of ϵ for the second (--) and third (-) approximation to the stream function growth rate at $\beta = 1$ and $Z = 1$. 167

Fig. 8.8 The critical Reynolds number as a function of ϵ for the second (--) and third (-) approximation to the relative energy growth rate at $\beta = 1$ and $Z = 1$. 168

ACKNOWLEDGEMENTS

I would like to thank my supervisor Dr. P.M. Eagles for his untiring encouragement throughout my research program. I am deeply indebted to him.

I would also like to thank Professor [REDACTED] [REDACTED] not only for inviting me to study at City University but also for his interest in my research program.

Finally I would like to thank [REDACTED]
[REDACTED] [REDACTED] and [REDACTED]
for their sponsorship.

DECLARATION

The author grants powers of discretion to the City University Librarian to allow this thesis to be copied in whole or in part without further reference to the author. This permission covers only single copies made for study purposes, subject to normal conditions of acknowledgement.

We obtain an approximation to the steady flow by expanding the stream function in powers of $\lambda^{-1/2}$. This approximation is compared with the solutions of Daniels & Eagles (1975) for exponential slender tubes ($H = \exp(\lambda x)$) and good agreement is found.

We next consider stability of the Daniels-Eagles profiles, by a quasi-parallel theory. Both spatially growing and temporally growing modes are considered, and, in addition to the case of exponential tubes, we have found no evidence of instability. In the course of this work detailed agreement was found with the eigenvalues of Davey & Drasin (1964), all of which remain stable as the parameter $\lambda \rightarrow \infty$ in the range $0 < \lambda < \infty$.

In the second part of the thesis we consider the stability of the flow in certain channels, taking into account non-parallel effects by means of a new method. Here the equations of the wall are $y = \pm \lambda^{-1/2} x^2$, where λ is independent of x . The flow is obtained to order $\lambda^{-1/2}$ as in Daniels (1971) and the corresponding stability analysis is

ABSTRACT

In the first part of the thesis we consider steady state flows in slender tubes. These tubes are characterised by having walls whose equations are $r = H(\epsilon x)$, where (r, θ, x) are cylindrical polar co-ordinates and ϵ is a small parameter proportional to $1/\bar{R}$, where \bar{R} is the Reynolds number. We obtain an approximation to the steady flow by expanding the stream function in powers of $\lambda = \epsilon \bar{R}$. This approximation is compared with the solutions of Daniels & Eagles(1979) for exponential slender tubes ($H = \exp(a\epsilon x)$) and good agreement is found.

We next consider stability of the Daniels-Eagles profiles, by a quasi-parallel theory. Both spatially growing and temporally growing modes are considered, and, contrary to expectation we have found no evidence of instability. In the course of this work detailed agreement was found with the eigenvalues of Davey & Drazin (1969), all of which remain stable eigenvalues as the parameter $\gamma = \epsilon a \bar{R}$ varies in the range $-6 < \gamma < +6$.

In the second main part of the thesis we consider the stability of the flow in certain channels, taking into account non-parallel effects by means of a new method. Here the equations of the wall are $y = \pm H(\epsilon x)$, where ϵ is independent of \bar{R} . The flow is obtained to order ϵ^2 as in Blasius(1910) and the corresponding stability analysis is

performed to same order. By comparison with earlier results of Eagles & Weissman(1975) we show that this non-parallel theory appears to give good results for the neutral stability curves for values of $\epsilon \bar{R}$ upto about 3, and we claim that this method is more satisfactory mathematically than earlier methods.

The transition of flow from laminar to turbulent flow which is fundamental to fluid dynamics, was first investigated by Reynolds(1853). He studied experimentally the stability of flow of water in tubes of various radii using dye. In these experiments he observed that the transition from laminar to turbulent type of motion depended on a parameter, R , now called the Reynolds number. This parameter denotes the ratio of viscous forces to inertia forces in the Navier-Stokes equations. It is also used to determine whether or not different flows are similar.

Reynolds(1895) carried out theoretical work on the stability of flow in tubes and concluded that the laminar pattern being a solution of the differential equations of fluid dynamics always represents a possible type of flow. It becomes unstable above a definite limit of R (the critical Reynolds number). These theoretical investigations were based on the assumption that laminar flows are affected by certain small disturbances. In the case of tube flow the disturbances may originate from the inlet while in the case of a boundary layer on a solid body placed in a stream, they may also be due to wall roughness or to irregularities in the external flow. The value of the critical Reynolds

1. INTRODUCTION

1.1 Early Studies in Fluid Dynamics

The phenomena of transition from laminar to turbulent flow which is fundamental to fluid dynamics was first investigated by Reynolds(1883). He studied experimentally the stability of flow of water in tubes of various radii using dye. In these experiments he observed that the transition from laminar to turbulent type of motion depended on a parameter, \bar{R} , now called the Reynolds number. This parameter denotes the ratio of viscous forces to inertia forces in the Navier-Stokes equations. It is also used to determine whether or not different flows are similar.

Reynolds(1895) carried out theoretical work on the stability of flow in tubes and concluded that the laminar pattern being a solution of the differential equations of fluid dynamics always represents a possible type of flow. It becomes unstable above a definite limit of \bar{R} (the critical Reynolds number). These theoretical investigations were based on the assumption that laminar flows are affected by certain small disturbances. In the case of tube flow the disturbances may originate from the inlet while in the case of a boundary layer on a solid body placed in a stream, they may also be due to wall roughness or to irregularities in the external flow. The value of the critical Reynolds

number was found experimentally to be about 1300. Later experiments by Ekman(1910) and others introduced finite amplitude effects and obtained the critical Reynolds number between 2000 and 40000.

The theory tries to follow up in time or space the behaviour of such disturbances when they are superimposed on the mean flow. The aim is to determine whether the disturbances grow or decay with time or space. If the disturbances decay, the mean flow is considered stable, on the other hand if the disturbances grow there exists the possibility of transition from laminar to turbulent flow. The process of transition from laminar to turbulent is a result of an instability in the laminar flow. The object of the theory of stability is to predict the value of the critical Reynolds number for a given flow.

Further efforts to clarify and explain theoretically the stability of flows to small disturbances were initiated by Rayleigh(1880). He published a great number of papers between 1878 and 1917 which laid a solid foundation of Reynolds hypotheses. In these studies he neglected viscous terms of the stability equation. This of course excluded the possibility of obtaining a critical Reynolds number but it was still possible to determine whether or not the laminar flow was stable.

He studied the inviscid stability of Poiseuille flow between parallel walls and found that the flow was stable to small disturbances, thus creating a paradox. Later he conjectured that the flow might be stable to small disturbances but unstable to finite ones or that the inviscid theory might be completely inapplicable to this problem. However, further work by Lin(1945) proved that plane Poiseuille flow is unstable at sufficiently high Reynolds numbers and showed that Rayleigh's idea explains the instability of plane Poiseuille flow.

Rayleigh also derived two important general theorems concerning the stability of laminar velocity profiles by inviscid theory. The theorems were later found to be valid for the case when the the effect of viscosity is taken into account. The first theorem states that the velocity profiles which possess a point of inflexion are unstable. He proved that the existence of a point of inflexion constitutes a necessary condition for the occurrence of instability. It was Tollmien(1936) who showed that this constitutes also a sufficient condition for the amplification of disturbances. These conclusions were supported by experimental investigations due to Rosenbrock(1937) who reported complete agreement between theoretical prediction and measurement. The second theorem asserts that the velocity of propagation of neutral disturbances in a boundary layer is smaller than the maximum

velocity of the mean flow. Rayleigh proved the theorem under some restricted assumptions whereas Tollmien proved it for more general conditions.

Tollmien's work was made possible by Prandtl(1904) who bridged the gap between theory and experiment. This was a significant step forward in fluid mechanics. The discrepancy between the results of classical hydrodynamics and experimental results were due in many cases to the fact that viscous terms were neglected. The reason for neglecting viscous terms was partly due to mathematical difficulties of the time and to the fact that in water and air viscous forces are very small. It was therefore difficult to understand how this could influence the motion of a fluid to such an extent. Prandtl proved theoretically and with several simple experiments that the flow about a solid body can be divided into two regions: a very thin layer(boundary layer) in the neighbourhood of a body where viscosity is important and the remaining region outside the layer where viscosity may be neglected. He further showed that the flow in the boundary layer can also be either laminar or turbulent and that the problem of separation and hence the problem of calculating the drag is governed by the critical Reynolds number.

Historically, the first application of Prandtl's boundary-layer theory was given by Blasius(1908) who

considered a boundary layer along a flat plate and obtained a series solution. Blasius(1910) also studied flows in channels and tubes with slowly varying walls. Working from first principles with the aid of the Navier-Stokes equations he obtained series solutions for flow in channels and tubes.

In our notation the channel walls would be given by $y = \pm f(\epsilon x)$, where x and y are the usual Cartesian co-ordinates, ϵ is a small parameter. We shall consider the case \bar{R} fixed as $\epsilon \rightarrow 0$. Blasius's solution is given in powers of ϵ . He calculated the first two terms and used the solution to predict the separation in an exponential channel. Patterson(1934,1935) set up experiments to test Blasius's theory and found agreement with Blasius's work for a limited range of low Reynolds numbers. Abramowitz(1949) extended Blasius' solution by obtaining a special case of the third approximation. Some years later Lucas(1972) used a computer to calculate the 13th approximation for the general shape and additional terms for special shapes.

Further advances were made by Jeffery(1915) and Hamel(1917) in the solution of flow in convergent and divergent channels. Jeffery showed that the streamlines of the motion were straight lines passing through the origin. Hamel generalised the solution and found an exact solution for flow in a divergent channel.

The stability of the Jeffery-Hamel velocity profiles was first investigated numerically by Eagles(1966) using the quasi-parallel approach. He obtained neutral curves and found fairly low critical Reynolds numbers. He also found negative wave velocities on the lower branch of the neutral curve for those profiles with regions of reversed flow. Eagles & Weissman(1975) tackled the same problem using the WKB method and obtained lower critical Reynolds numbers. The quasi-parallel growth rate turns out to be the first term in an asymptotic expansion. The method also demonstrated the dependence of the growth rate, wave number and other parameters on the cross-stream function. In an effort to make theoretical predictions much more easily amenable to experimental investigation and comparison, Eagles & Smith(1980) studied numerically the stability of flow in channels whose walls are given by $H = 1 + (1/2)\tanh \epsilon x$ using the WKB method. Their forward marching scheme showed separation at $\epsilon x \approx 0.35$ when $R \approx 15.5$ and extending over $0.2 < \epsilon x < 1.15$ when $\epsilon R \approx 18$. confirmed by Seshi & Spalberg(1982). Fekris also points out For flow in tubes the walls are defined by $r = f(\epsilon x)$, where r is the radial co-ordinate. Blasius(1910) found the first and second approximation to the solution of flow in an exponential tube. His solution was extended to $O(\epsilon^2)$ by Manton(1971) who calculated the third approximation. Kaimal(1979) has generalised Manton's results to a dilute suspension of solid particles. Eagles & Muwezwa(1986) found

the fourth approximation and used the solution to compute velocity profiles up to $\epsilon \bar{R} = 10$.

Sexl(1927) was the first to take account of the viscosity in considering the stability of axisymmetric disturbances of flow in a pipe by the method of normal modes. However, for reasons of mathematical simplicity he used artificial boundary conditions which makes his conclusions open to question, see Gill(1965). Sexl was unable to find any instability for Poiseuille flow nor was he able to prove the existence of stability for all Reynolds numbers.

However, Pretsch(1941) succeeded in proving that the analysis of the instability of these parabolic velocity profiles can be reduced to that of plane Couette flow. Since plane Couette flow is stable at all Reynolds numbers, the same applies to parabolic velocity profiles in a tube. The same conclusion was reached by Pekeris(1948) and finally confirmed by Sexl & Spielberg(1958). Pekeris also points out some of the shortcomings of Sexl's work. Sexl determined stability in the cases $R = 0$ and R large ignoring earlier experimental evidence that the flow becomes unstable at intermediate values of R . Pekeris derived an eigenvalue relation for one class of modes.

Using a different method, Corcos & Sellars(1959) confirmed earlier findings by Pekeris and obtained a similar eigenvalue relation and an additional relation for the class of modes. Further theoretical and computational work by Davey & Drazin(1969) has confirmed the results obtained by these eigenvalue relations. They also found eigenvalues in a similar pattern to that displayed by Corcos & Sellars. In addition they also found a few other modes. All the modes discovered were stable.

$$\frac{d^2 u}{dz^2} + \frac{1}{2} \frac{du}{dz} - \frac{1}{4} u^2 + 4\gamma u = 0, \quad (1.1)$$

where

$$z = \frac{y}{R},$$

$$\lambda = \frac{\alpha R}{2},$$

$$u = \frac{v}{R},$$

$$z = \frac{y}{R},$$

R is the radius of the tube, y is the downstream coordinate, α is a constant, γ is a small parameter and R is the Reynolds number. The derivatives are with respect to z . Under the basic assumption that $\lambda = \alpha R$ is of order $O(1)$ as $R \rightarrow \infty$ and $\gamma \rightarrow 0$, the velocity function u is shown (to first approximation) to satisfy the Navier-Stokes equation:

1.2 Introduction to Present Thesis

1.21 Flow in Tubes

We shall be concerned with the stability to small disturbances of the Daniels & Eagles velocity profiles, which will be referred to as the the DE profiles. Daniels & Eagles(1979) studied viscous flows in exponential tubes of varying radius. The flows were governed to a first approximation by a nonlinear ordinary differential equation

$$G'''' + \frac{1}{\eta} G''' - \frac{1}{\eta^2} G'' + 4\gamma G G' = 0, \quad (1.1)$$

where

$$\gamma = \lambda a ,$$

$$\lambda = \epsilon \bar{R} ,$$

$$H = \exp(aZ),$$

$$Z = \epsilon x ,$$

H is the radius of the tube, x is the downstream coordinate, a is a constant, ϵ is a small parameter and \bar{R} is the Reynolds number. The derivatives are with respect to η . Under the basic assumption that $\lambda = \epsilon \bar{R}$ is of $O(1)$ as $\epsilon \rightarrow 0$ and $R \rightarrow \infty$, the velocity function G is shown (to first approximation) to satisfy the Navier-Stokes equations.

For large values of Z the theory became invalid due to the exponential variation of the radius which was unbounded. This has since been modified and extended by Eagles(1982) so that the solutions may be applied to a wide variety of 'locally exponential' tubes. The modification made it applicable to tubes of infinite length and bounded radius. It is believed that the predicted flows can be attained experimentally, especially those represented by branch 1 of their solution which became Poiseuille flow when $\gamma = 0$.

Eagles predicted that the DE profiles were good approximations for more general slender tubes. To carry out the investigation, the velocity profile was expanded in terms of λ . The results of the expansion were found to be accurate for $|\gamma| \leq 3$. In Chapter 2 the basic flow is expanded in terms of λ to $O(\lambda^3)$. The results are compared with the exact solution. In addition to the exponential tubes for which the DE profiles are exact, two other tubes are examined whose walls are given by

$$H_1 = 1 + \frac{1}{2}\tanh Z \text{ and } H_2 = 1 + \frac{1}{2}\tanh^2 Z. \quad (1.2)$$

Earlier studies by Eagles(1966), Eagles & Weissman(1975) and Eagles & Smith(1980) showed that for channel flow instabilities occurred at $R = 215$ for $\alpha = 0.01$ and $R = 40$ for $\alpha = 0.1$, where α is the semi-divergence angle of the channel. A similar pattern was expected for

the DE profiles. The spatial stability of the DE profiles is presented in Chapters 3. In Chapter 4, the eigenvalues obtained by Davey & Drazin are confirmed and used as a basis for a search for eigenvalues with the DE profiles as the basic flow. The behaviour of the profiles is examined as γ varies, both by means of spatially growing modes and temporally growing modes, in both cases using quasi-parallel stability theory.

Similar growth rates are derived here by a different method and the results are compared with those obtained by Eagles & Weiseman. The results for the $O(\epsilon^2)$ theory have an order of magnitude agreement with their results, where ϵ is a small parameter, approximately equal to the semi-divergence angle of the channel.

The approach by Eagles & Weiseman assumes a relation of the form

$$\gamma = \epsilon^2 R = O(\epsilon^2) \text{ as } \epsilon \rightarrow 0$$

for the basic flow, obtaining a class of Jeffery-Hasel profiles, but treat ϵ and R as independent parameters in the disturbance equation. The present approach is a reformulation of the same problem using a different method. No assumption is made about the relationship between ϵ and R . Unlike Eagles & Weiseman we expand the basic flow in terms of ϵ with $R = O(1)$. The rationale behind the

Eagles & Weissman(1975) have studied the linear stability of a slowly varying flow in a divergent straight-walled channel to a great detail using a modification of the 'WKB' method. In this study they defined various growth rates based on the stream function, the kinetic energy density and the relative kinetic energy density. Similar growth rates are derived here by a different method and the results are compared with those obtained by Eagles & Weissman. The results for the $O(\epsilon^2)$ theory have an order of magnitude agreement with their results, where ϵ is a small parameter, approximately equal to the semi-divergence angle of the channel.

The approach by Eagles & Weissman assumes a relation of the form

$$\gamma = \epsilon \bar{R} = O(1) \quad \text{as } \epsilon \rightarrow 0$$

for the basic flow, obtaining a class of Jeffery-Hamel profiles, but treat ϵ and \bar{R} as independent parameters in the disturbance equation. The present approach is a reformulation of the same problem using a different method. No assumption is made about the relationship between ϵ and \bar{R} . Unlike Eagles & Weissman we expand the basic flow in terms of ϵ with $\bar{R} = O(1)$. The rationale behind the

present approach is that it is mathematically satisfactory and straight forward. In Eagles & Weissman's approach the term in $1/R$ in the disturbance equation was taken to be $O(1)$ even though the base flow was derived on the basis $1/\bar{R} = O(\epsilon)$, thus leading to a mathematical doubtful scheme, although the results appear to be accurate since they have been checked by Allmen(1980) using a numerical approach. The present method also removes the objections raised by Smith(1979).

In his study of the stability of flow in channels of small divergence angle Eagles(1966) used quasi-parallel theory. The limitations of this approach are well presented in Eagles & Weissman. The quasi-parallel theory is deficient in determining the growth rate as a function of the downstream co-ordinate and can only indicate whether a disturbance is growing or decaying at a particular point. To overcome this handicap, the slowly varying approach (WKB) was used to study flows in a diverging channel. Eagles & Smith(1980) applied the method to the stability of flows in curved wall channels. A similar approach was taken by Georgiou & Eagles(1985) in investigating the stability of flows in channels with small wall curvature.

The main objection to the work described above raised by Smith is about the way $1/R$ is treated in the limit as $\epsilon \rightarrow 0$. He suggests an approach that would either solve the

complete set of partial differential equations directly as in Allmen(1980) or examine the behaviour of the disturbance when the Reynolds number is asymptotically large as in Smith(1979). The method presented here is an alternative to these approaches.

The stream function equation for channel flow is discussed in Chapter 5. Here the basic flow is expanded in terms of ϵ . The resulting equations are solved in order starting with the $O(1)$ equation which represents Poiseuille flow. In Chapter 6 the disturbance equation is derived. The $O(1)$ equation is the Orr-Sommerfeld equation appropriate to strictly parallel Poiseuille flow which is solved numerically to obtain the eigenvalue, the eigenfunction and the adjoint eigenfunction. Solutions of higher order equations and growth rates are described in Chapter 6 and 7 respectively.

2. BASIC TUBE FLOW

2.1 Stream Function Equation

The stream function equation is derived from the Navier-Stokes equations with zero external forces

$$\frac{\partial \bar{U}}{\partial t'} + \bar{U} \cdot \nabla \bar{U} = - \frac{1}{\rho} \nabla P + \nu \nabla^2 \bar{U}, \quad (2.1)$$

$$\nabla \cdot \bar{U} = 0 \quad (2.2)$$

where U , ρ and P are the velocity, density and pressure of the fluid respectively, and ν is the kinematic viscosity. Taking the curl of (2.1) leads to

$$\frac{\partial \bar{W}}{\partial t'} - \nabla \wedge (\bar{U} \wedge \bar{W}) = \nu \nabla^2 \bar{W} \quad (2.3)$$

where $\bar{W} = \nabla \wedge \bar{U}$, is the vorticity vector.

For axisymmetric flows with cylindrical co-ordinates (r', θ, x') and $\bar{U} = (v', 0, u')$, a stream function $\Psi'(r', x', t')$ may be defined by

$$u' = - \frac{1}{r'} \frac{\partial \Psi'}{\partial x'}, \quad v' = \frac{1}{r'} \frac{\partial \Psi'}{\partial r'}$$

This satisfies the equation of continuity (2.2). The variables are made non-dimensional as follows :

$$x = \frac{x'}{L}, \quad r = \frac{r'}{L}, \quad \Psi = \frac{\Psi'}{M}, \quad t = \frac{Mt'}{L^3}$$

where L is the radius of the tube at $x' = 0$ and M is half the volumetric flow rate.

In terms of the non-dimensional co-ordinates equation (2.3) becomes

$$\begin{aligned} & \frac{1}{r} \frac{\partial}{\partial t} D^2 \psi + \frac{1}{r^2} \left(\psi_r \frac{\partial}{\partial x} - \psi_x \frac{\partial}{\partial r} \right) D^2 \psi \\ & + \frac{1}{r^3} (2 \psi_x \psi_{xx} + 3 \psi_x \psi_{rr} - \psi_r \psi_{rx}) - \frac{3}{r^4} \psi_x \psi_r \\ & = \frac{1}{R} \left[\frac{1}{r} D^4 \psi - \frac{2}{r^2} (\psi_{rx} + \psi_{rr}) + \frac{3}{r^3} \psi_{rr} - \frac{3}{r^4} \psi_r \right] \end{aligned} \quad (2.4)$$

where

$$R = \frac{M}{L^3}$$

is the Reynolds number and

$$D^2 = \frac{\partial^2}{\partial r^2} + \frac{\partial^2}{\partial x^2}.$$

The boundary conditions are

$$\psi = 0(r^2) \text{ as } r \rightarrow 0,$$

$$\psi_r = 0 \text{ at the tube wall,}$$

$$\psi = \frac{1}{2\pi} \text{ at the tube wall.}$$

The second condition is the no-slip condition while the last

condition follows from non-dimensionalising ψ' with respect to the volumetric flow rate.

The total stream function ψ is considered to be made of two parts, the steady-state and the time-dependent part, i.e.

$$\psi(r, x, t) = \hat{F}(r, x) + \hat{\psi}(r, x, t).$$

The solution of (2.4) will be obtained from the solutions of the equations for \hat{F} and $\hat{\psi}$. The steady-state equation which is obtained when $\frac{\partial}{\partial t} = 0$, will be considered first. Its solution will lead us to consider the DE profiles. The stability of these profiles will be investigated when the time-dependent solution is sought.

The steady-state equation is obtained by setting $\frac{\partial}{\partial t} = 0$ and letting

$$\psi(r, x, t) = \psi(r, x) = \hat{F}(r, x)$$

Daniels & Eagles derived the steady-state stream function equation for flow in tubes of slowly varying radius by defining the boundary as $r = H(Z)$, where $Z = \epsilon x$ and ϵ is a small parameter. It is convenient to make

the tube wall a co-ordinate line by letting

$$\eta = \frac{r}{H(Z)}$$

so that $\eta = 1$ on the wall. The derivatives transform as follows :

$$\frac{\partial}{\partial x} \equiv \epsilon \left(\frac{\partial}{\partial z} - \eta \frac{H'}{H} \frac{\partial}{\partial \eta} \right),$$

$$\frac{\partial}{\partial r} \equiv \frac{1}{H} \frac{\partial}{\partial \eta} .$$

This transformation introduces terms of $O(\epsilon)$ which are dominant on the left hand side of the equation (2.4), while on the right-hand side the dominant terms are of $O(1)$ times $1/\bar{R}$. In order to retain the nonlinear terms in the equations at the first approximation, Daniels & Eagles considered flows in which

$$\epsilon \bar{R} = \lambda = O(1),$$

so that the dominant terms on each side are of $O(\epsilon)$. Flows in which $\epsilon \bar{R} = \lambda$ is of $O(1)$ as $\epsilon \rightarrow 0$ satisfy boundary layer equations, (see Smith(1976)).

The steady-state stream function $\psi(\eta, Z)$ was expanded as follows,

since the boundary conditions do not contain ϵ ,

$$\psi = \psi_0(\eta, z) + \epsilon^2 \psi_2(\eta, z) + \dots$$

Substituting ψ into the steady-state equation and defining $\psi_0 = F(\eta, Z)$, the $O(1)$ equation for F becomes

$$\mathcal{L}(F) = \lambda \left[\frac{4H'}{H} \left(\frac{1}{\eta^2} (F_\eta)^2 - \frac{1}{\eta} F_\eta F_{\eta\eta} \right) + F_\eta \left(\frac{1}{\eta} F_{\eta\eta Z} - \frac{1}{\eta^2} F_{\eta Z} \right) \right. \\ \left. + F_Z \left(-\frac{1}{\eta} F_{\eta\eta\eta} + \frac{3}{\eta^2} F_{\eta\eta} - \frac{3}{\eta^3} F_\eta \right) \right] \quad (2.6)$$

where $\lambda = \epsilon R$ and

$$\mathcal{L} = \frac{\partial^4}{\partial \eta^4} - \frac{2}{\eta} \frac{\partial^3}{\partial \eta^3} + \frac{3}{\eta^2} \frac{\partial^2}{\partial \eta^2} - \frac{3}{\eta^3} \frac{\partial}{\partial \eta}.$$

The boundary conditions are

$$F = O(\eta^2) \quad \text{as } \eta \rightarrow 0,$$

$$F = 1/2\pi \quad \text{at } \eta = 1,$$

$$F_\eta = 0 \quad \text{at } \eta = 1.$$

The problem for F is called the slender tube problem and will constitute our basic flow. We shall return to this problem later in section 2.3.

For exponential tubes with $H = \exp(aZ)$, where $a = \text{constant}$, a solution independent of Z is allowable and we obtain the nonlinear ordinary differential equation

$$G'''' + \frac{1}{\eta} G''' - \frac{1}{\eta^2} G'' + 4\gamma GG' = 0 \quad (2.7)$$

where $\gamma = \lambda a$ and $G = \frac{1}{\eta} F_\eta$. The boundary conditions on G are

$$G = 0(\eta) \text{ as } \eta \rightarrow 0,$$

$$\int_0^1 \eta G d\eta = \frac{1}{2\pi},$$

$$G = 0 \text{ at } \eta = 1.$$

Equation (2.7) will be referred to as the DE equation and the associated solutions as the DE profiles, flows or velocities. The DE flows are not just small perturbations of Poiseuille flow, but the first constitute a family of flows containing not only Poiseuille flow but also flows with inflexion points and with regions of reversed flow. The case $\gamma = 0$ corresponds to Poiseuille flow, as γ increases or decreases the flows change from Poiseuille flow to other flows. Daniels & Eagles found multiple solutions for both negative and positive values of γ . The DE equation was solved numerically and several branches of the solution were given. We look at branch 1 of their solution and obtain an approximation by expanding F in terms of λ . The range of γ is restricted to $|\gamma| \leq 6$ on branch 1.

2.2 Expansion Method

The equation (2.6) precludes exact analytical solutions because it is nonlinear and has variable

coefficients. However, a good approximation to the solution may be found by seeking a parameter perturbation expansion of the form

$$F = F^{(0)} + \lambda F^{(1)} + \lambda^2 F^{(2)} + \lambda^3 F^{(3)} + \dots$$

Substituting this series into equation (2.6) leads to a sequence of differential equations and the first four of these are given below.

$$\lambda^0 : \mathcal{L}(F^{(0)}) = 0, \quad (2.8)$$

$$\begin{aligned} \lambda^1 : \mathcal{L}(F^{(1)}) = & \frac{4H'}{H} \left[\frac{1}{\eta^2} (F_{\eta}^{(0)})^2 - \frac{1}{\eta} F_{\eta}^{(0)} F_{\eta\eta}^{(0)} \right] \\ & + F_{\eta}^{(0)} \left(\frac{1}{\eta} F_{\eta\eta z}^{(0)} - \frac{1}{\eta^2} F_{\eta z}^{(0)} \right) \\ & - F_z^{(0)} \left(\frac{1}{\eta} F_{\eta\eta\eta}^{(0)} - \frac{3}{\eta^2} F_{\eta\eta}^{(0)} + \frac{3}{\eta^3} F_{\eta}^{(0)} \right), \quad (2.9) \end{aligned}$$

$$\begin{aligned} \lambda^2 : \mathcal{L}(F^{(2)}) = & \frac{4H'}{H} \left[F_{\eta}^{(0)} \left(\frac{2}{\eta^2} F_{\eta}^{(1)} - \frac{1}{\eta} F_{\eta\eta}^{(1)} \right) \right. \\ & \left. - \frac{1}{\eta} F_{\eta}^{(1)} F_{\eta\eta}^{(0)} \right] \\ & + \sum_{j=0}^1 F_{\eta}^{(1-j)} \left(\frac{1}{\eta} F_{\eta\eta z}^{(j)} - \frac{1}{\eta^2} F_{\eta z}^{(j)} \right), \\ & + \sum_{j=0}^1 F_z^{(1-j)} \left(-\frac{1}{\eta} F_{\eta\eta\eta}^{(0)} + \frac{3}{\eta^2} F_{\eta\eta}^{(0)} - \frac{3}{\eta^3} F_{\eta}^{(0)} \right), \quad (2.10) \end{aligned}$$

$$\begin{aligned} \lambda^3 : \mathcal{L}(F^{(3)}) = & \frac{4H'}{H} \left[F_{\eta}^{(0)} \left(\frac{2}{\eta^2} F_{\eta}^{(2)} - \frac{1}{\eta} F_{\eta\eta}^{(2)} \right) \right. \\ & \left. + F_{\eta}^{(1)} \left(\frac{1}{\eta^2} F_{\eta}^{(1)} - \frac{1}{\eta} F_{\eta\eta}^{(1)} \right) - \frac{1}{\eta} F_{\eta}^{(2)} F_{\eta\eta}^{(0)} \right] \end{aligned}$$

$$\begin{aligned}
 & + \sum_{j=0}^2 F_{\eta}^{(2-j)} \left(\frac{1}{\eta} F_{\eta}^{(j)} - \frac{1}{\eta^2} F_{\eta}^{(j)} \right) \\
 & + \sum_{j=0}^2 F_{\eta}^{(2-j)} \left(-\frac{1}{\eta} F_{\eta}^{(j)} + \frac{3}{\eta^2} F_{\eta}^{(j)} - \frac{3}{\eta^3} F_{\eta}^{(j)} \right). \quad (2.11)
 \end{aligned}$$

The equations together with the appropriate boundary conditions were solved successively once the solution of (2.8) was obtained. Determining equations for $F^{(0)}$ and $F^{(1)}$ was relatively simple, but it was considerably more difficult to get $F^{(2)}$ and even more laborious to derive $F^{(3)}$.

2.21 Series Solution

The solution for equation (2.8) is considered first.

$$F_{\eta}^{(0)} - \frac{2}{\eta} F_{\eta}^{(0)} + \frac{3}{\eta^2} F_{\eta}^{(0)} - \frac{3}{\eta^3} F_{\eta}^{(0)} = 0, \quad (2.12)$$

where $F^{(0)} = F^{(0)}(\eta, Z)$. The coefficients of this equation do not depend on Z and hence the equation allows solutions which are independent of Z . The boundary conditions on $F^{(0)}$ are

$$\begin{aligned}
 F^{(0)} &= O(\eta^2) \quad \text{as } \eta \rightarrow 0, \\
 F^{(0)} &= \frac{1}{2\pi} \quad \text{at } \eta = 1, \\
 F_{\eta}^{(0)} &= 0 \quad \text{at } \eta = 1.
 \end{aligned} \quad (2.13)$$

Equation (2.12) has a singularity at $\eta = 0$ and may be solved by the method of Frobenius or the Euler transformation $\eta = \exp(\omega)$ which would reduce the equation to one with constant coefficients. A solution that satisfies the boundary conditions (2.13) was found to be

$$F^{(0)} = \frac{1}{2\pi} (2\eta^2 - \eta^4). \quad (2.14)$$

The solution for equation (2.9) is obtained by substituting this value of $F^{(0)}$ into (2.9) and solving the resulting differential equation. We have after simplification

$$\begin{aligned} \mathcal{L}(F^{(1)}) &= \frac{4H'}{H} \left[\frac{1}{\eta^2} (F_{\eta}^{(0)})^2 - \frac{1}{\eta} F_{\eta}^{(0)} F_{\eta\eta}^{(0)} \right] \\ &= \frac{4H'}{H} F_{\eta}^{(0)} \left(\frac{1}{\eta^2} F^{(0)} - \frac{1}{\eta} F_{\eta\eta}^{(0)} \right). \end{aligned}$$

The derivatives of $F^{(0)}$ with respect to Z are zero since $F^{(0)}$ is not a function of Z . The boundary conditions on $F^{(1)}$ are

$$F^{(1)} \rightarrow 0 \quad \text{as} \quad \eta \rightarrow 0,$$

$$F^{(1)} = 0 \quad \text{at} \quad \eta = 1,$$

$$F_{\eta}^{(1)} = 0 \quad \text{at} \quad \eta = 1.$$

A solution that satisfies the boundary conditions was found to be

$$F^{(1)} = \frac{1}{9\pi^2} \frac{H'}{H} F_1^{(1)} \quad (2.15)$$

where $F_1^{(1)} = \eta^2 - \frac{2}{4}\eta^4 + \frac{6}{4}\eta^6 - \frac{1}{4}\eta^8$.

Having found $F^{(0)}$ and $F^{(1)}$ we can proceed to find $F^{(2)}$ and $F^{(3)}$. However, the solutions $F^{(2)}$ and $F^{(3)}$ involve derivatives of H'/H and the algebra gets quite long and tedious. When $F^{(0)}$ and $F^{(1)}$ are substituted into (2.10) the equation for $F^{(2)}$ becomes

$$\begin{aligned} \mathcal{L}(F^{(2)}) = & \frac{2}{36\pi^2} \frac{H'^2}{H^2} (f_1\eta^2 - f_2\eta^4 \\ & + f_3\eta^6 - f_4\eta^8), \end{aligned}$$

where

$$f_1 = 352 - 72Q,$$

$$f_2 = 1152 - 216Q,$$

$$f_3 = 1056 - 192Q,$$

$$f_4 = 256 - 48Q,$$

$$Q = -\frac{d}{dz} \left(\frac{H}{H'} \right).$$

The boundary conditions on $F^{(2)}$ are

$$F^{(2)} = 0 \quad \text{at} \quad \eta = 0,$$

$$F^{(2)} = F_{\eta}^{(2)} = 0 \quad \text{at} \quad \eta = 1.$$

The corresponding solution was found to be

$$F^{(2)} = \frac{331}{10800\pi^3} S^2 F_1^{(2)} - \frac{13}{1800\pi^3} S' F_2^{(2)}, \quad (2.16)$$

where $S = \frac{H'}{H},$

$$S' = \frac{dS}{dz},$$

$$F_1^{(2)} = \gamma^2 + \frac{1}{331} (-980\gamma^4 + 1100\gamma^6 - 600\gamma^8 + 165\gamma^{10} - 16\gamma^{12}),$$

$$F_2^{(2)} = \gamma^2 + \frac{1}{52} (-145\gamma^4 + 150\gamma^6 - 75\gamma^8 + 20\gamma^{10} - 2\gamma^{12}).$$

The equation for $F^{(3)}$ is obtained in a similar manner. Substitute values of $F^{(0)}, F^{(1)}$ and $F^{(2)}$ into (2.11) to obtain

$$\mathcal{L}(F^{(3)}) = \frac{16}{86400\pi^4} \frac{H'^3}{H^3} (f_5\gamma^2 - f_6\gamma^4 + f_7\gamma^6 - f_8\gamma^8 + f_9\gamma^{10} - f_{10}\gamma^{12}),$$

where $f_5 = 46256 + 1740E - 29768Q,$

$$f_6 = 230720 + 7140E - 129080Q,$$

$$f_7 = 4090600 + 10800E - 206000Q,$$

$$f_8 = 331200 + 7800E - 154800Q,$$

$$f_9 = 121680 + 2760E - 55200Q,$$

$$f_{10} = 15616 + 360E - 7088Q,$$

$$E = 2Q(1 + S^2Q).$$

A solution satisfying the boundary conditions was found to be

$$F^{(3)} = \frac{2759}{297675} \pi^4 S^3 F_1^{(3)} + \frac{281833}{38102400} \pi^4 SS' F_2^{(3)} + \frac{1459}{3175200} \pi^4 T F_3^{(3)} \quad (2.17)$$

where $T = \frac{d}{dz} \left(\frac{H'''}{H} \right),$

$$F_1^{(3)} = \eta^2 - 3.36616 \eta^4 + 4.81353 \eta^6 - 4.00156 \eta^8 + 2.13121 \eta^{10} - 0.68931 \eta^{12} + 0.12059 \eta^{14} - 0.00829 \eta^{16},$$

$$F_2^{(3)} = \eta^2 - 3.07959 \eta^4 + 3.88164 \eta^6 - 2.80526 \eta^8 + 1.34308 \eta^{10} - 0.40371 \eta^{12} + 0.06855 \eta^{14} - 0.00472 \eta^{16},$$

$$F_3^{(3)} = \eta^2 - 3.01182 \eta^4 + 3.65233 \eta^6 - 2.49786 \eta^8 + 1.13348 \eta^{10} - 0.32745 \eta^{12} + 0.05518 \eta^{14} - 0.00386 \eta^{16}.$$

Rational coefficients could not be conveniently retained in this case because the numbers involved tended to be very

large. For the special case $H'/H = \text{constant}$ the coefficients of $F_2^{(2)}$, $F_2^{(3)}$ and $F_3^{(3)}$ are zero. The remaining terms constitute an expansion in powers of $\lambda H'/H$ of the branch 1 solution of the DE equation with $\gamma = \lambda H'/H$. Extensive checks were made on the accuracy of the analysis. One method of checking was to fix η at say 0.5 and calculate numerically both sides of the equation. This method may appear simple, but its efficiency can only be appreciated in verifying the solutions $F^{(2)}$ and $F^{(3)}$.

Having calculated $F^{(0)}$, $F^{(1)}$, $F^{(2)}$ and $F^{(3)}$ we may write the approximation to F in terms of their values. The solution

$$F = F^{(0)} + \lambda F^{(1)} + \lambda^2 F^{(2)} + \lambda^3 F^{(3)} + \dots$$

constitutes the basic flow in a tube with slowly varying radius. In this case, the shape function $r = H(Z)$ is general and therefore it should be possible to compare results with specific cases. The exponential tube $H = \exp(aZ)$ and other interesting wall shapes are considered in the next section.

2.3 Slender Tube Flow

2.31 Exponential Tube Approximation

When the radius of the tube varies exponentially we have $H = \exp(aZ)$ which may represent a converging or

diverging tube depending on whether a is negative or positive. We shall confine ourselves to the case $a > 0$. Since $H'/H = a$, it follows that

$$Q = - \frac{d}{dz} \left(\frac{H}{H'} \right) = 0.$$

The solutions (2.14) - (2.17) reduce to

$$F^{(0)} = \frac{1}{2\pi} (2\eta^2 - \eta^4),$$

$$F^{(1)} = \frac{a}{9\pi^2} F_1^{(1)}(\eta),$$

$$F^{(2)} = \frac{331a^2}{10800\pi^3} F_1^{(2)}(\eta),$$

$$F^{(3)} = \frac{2759a^3}{297675\pi^4} F_1^{(3)}(\eta).$$

Writing F in terms of the velocity function $G = \frac{1}{2} F \eta$ we obtain

$$G^{(0)} = \frac{2}{\pi} (1 - \eta^2),$$

$$G^{(1)} = \frac{a}{9\pi^2 \eta} \frac{d}{d\eta} \left(F_1^{(1)} \right),$$

$$G^{(2)} = \frac{331a^2}{10800\pi^3 \eta} \frac{d}{d\eta} \left(F_1^{(2)} \right),$$

$$G^{(3)} = \frac{2759a^3}{297675\pi^4 \eta} \frac{d}{d\eta} \left(F_1^{(3)} \right). \quad (2.18)$$

$$\text{and } G = G^{(0)} + \lambda G^{(1)} + \lambda^2 G^{(2)} + \lambda^3 G^{(3)} + \dots .$$

In Table 2.1, the columns marked EM refer to our results and the Daniels & Eagles results are entered in the columns marked DE. The expansion method is shown to be quite accurate for λ in the range $-3 \leq \lambda \leq 3$. These figures indicate that we can expect accurate results from calculations using the series for G provided $|\lambda| \leq 3$. An inspection of the terms in the series shows that the coefficients of λ^n decrease rather rapidly with increasing n , and are numerically small. Thus a series might have a large range of usefulness. Since the highest derivative lies with the unknown function at each stage, the series has the general nature of a convergent series rather than merely asymptotic. For a particular value of λ if the moduli of the terms are decreasing steadily with n and if the last term is small, we may expect to have a good approximation. This has proved very useful in the flow in slender tubes and in analysing the stability of the DE profiles.

2.32 DE Profiles as Approximations

The special case for which $H = \exp(aZ)$, became invalid at large values of Z due to the exponential variation of the radius, which is unbounded. The theory has since been modified and extended by Eagles(1982) so that the solutions may be applied to a wide variety of 'locally exponential' tubes. The DE profiles are exact solutions for the slender tube equations

when $\lambda H'/H = \text{constant}$. The velocity function $G(\eta)$ satisfies equation (2.7). In more general tubes with $H'/H = f(\eta)$ they have been shown to be the first term in an asymptotic series in powers of λ , the value of λ being taken as H'/H at each value of Z . Higher order terms are shown to be numerically small, leading Eagles to conjecture that the profiles are a good approximation in more general slender tubes.

γ	$G(0)$		$G'(1)$		$G''(0)/2$	
	DE	EM	DE	EM	DE	EM
-5.0	0.558	0.550	-1.550	-1.560	-0.319	-0.262
-3.0	0.583	0.582	-1.450	-1.450	-0.412	-0.403
-1.0	0.616	0.616	-1.400	-1.340	-0.548	-0.546
1.4	0.673	0.673	-1.170	-1.170	-0.806	-0.805
3.0	0.730	0.727	-1.030	-1.040	-1.100	-1.080
5.0	0.851	0.822	-0.790	-0.826	-1.810	-1.600
6.0	0.971	0.984	-0.594	-0.706	-1.610	-1.940

Table 2.1. DE profiles and results EM from the expansion method.

Poiseuille flow.

In Table 2.2 for tube 2 with $\lambda = 3$, and selected values of η and Z we show the separate contributions of the powers of λ . The impression is of rapid convergence and we would expect higher order terms to be negligible. This is overall for this case. Here the values of H'/H are smaller

when $\lambda H'/H = \text{constant}$. The velocity function $G(\eta)$ satisfies equation (2.7). In more general tubes with $H'/H = f(\epsilon Z)$ they have been shown to be the first term in an asymptotic series in powers of ϵ , the value of γ being taken as H'/H at each value of Z . Higher order terms are shown to be numerically small, leading Eagles to conjecture that the profiles are a good approximation in more general slender tubes.

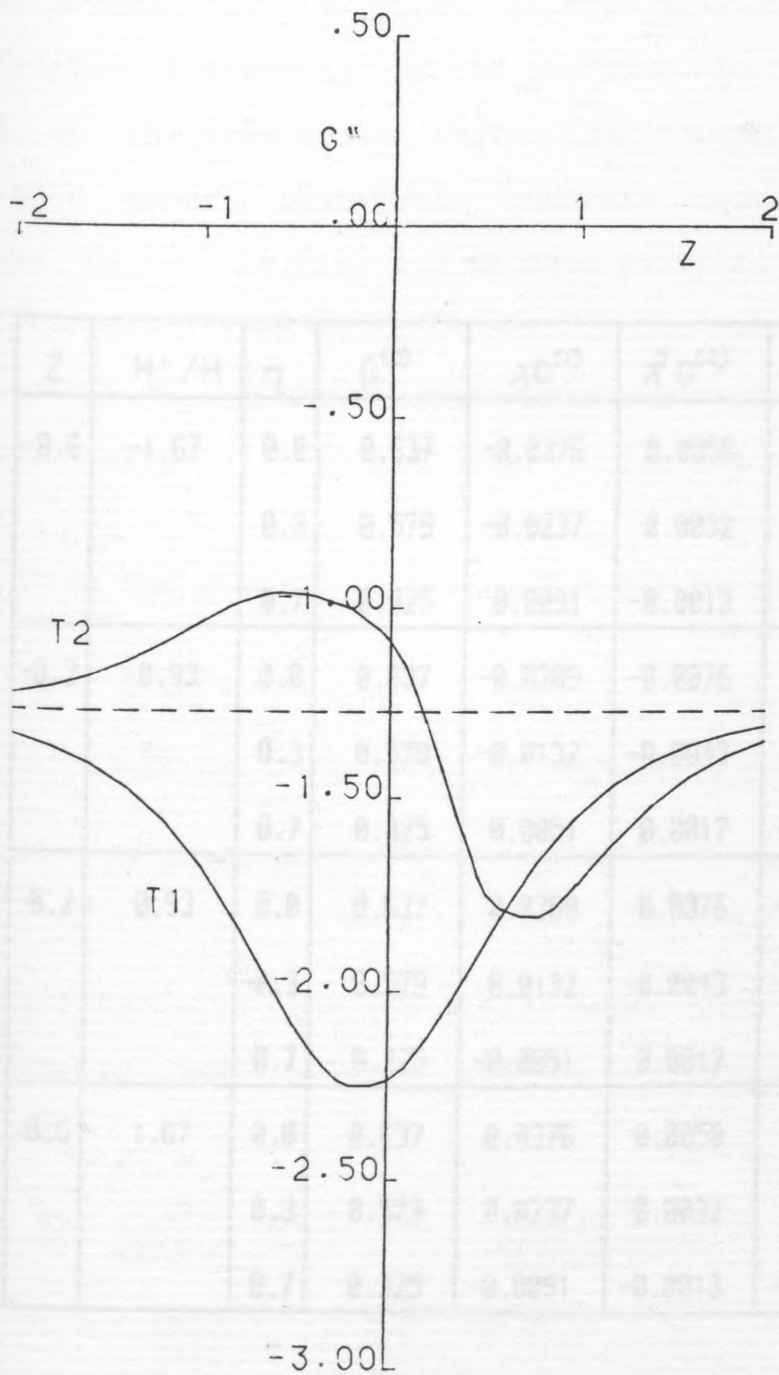
We consider two tubes whose radii are

$$H_1 = 1 + \frac{1}{2} \tanh Z$$

and $H_2 = 1 + \frac{1}{2} \tanh^2 Z$

and assess the accuracy of the approximation. The first tube, which we shall call Tube 1, is divergent and the second, Tube 2 is convergent for $Z < 0$ and divergent for $Z > 0$. In Fig. 2.1 we show the second derivative of the velocity profile as a function of Z at $\eta = 0$ when $\lambda = 6$ for Tube 1 and Tube 2. Also shown is Poiseuille flow. The profiles differ considerably from each other and from Poiseuille flow.

In Table 2.2 for Tube 2 with $\lambda = 5$, and selected values of η and Z we show the separate contributions of the powers of λ . The impression is of rapid convergence and we would expect higher order terms to be negligible. This is overall for this case. Here the values of H'/H are smaller



Z	H'/H	η	G''	$\lambda^{1/3}$	$\lambda^{2/3}$	$\lambda^{1/3}$
0.6	1.67	0.6	0.37	0.8275	0.8058	0.8004
		0.3	0.79	0.8237	0.8032	0.8002
		0.0	0.0	0.8205	0.8013	0.8001
		0.3	0.79	0.8173	0.8076	0.8076
		0.7	0.73	0.8132	0.8117	0.8115
0.7		0.8	0.77	0.8132	0.8113	0.8113
		0.7	0.73	0.8101	0.8117	0.8115
0.5	1.67	0.8	0.37	0.8076	0.8059	0.8004
		0.3	0.79	0.8037	0.8032	0.8002
		0.7	0.73	0.8001	0.8013	0.8001

Table 2.2. The contributions of separate pieces of λ

Fig. 2.1. Second derivative of velocity profile as a function of Z at $\eta = 0$ when $\lambda = 6$.

T1 : Tube 1; T2 : Tube 2; -- Poiseuille Flow.

than in Tube 1 and so the flow is closer to Poiseuille flow. Nevertheless, it is significantly different. There is a noticeable 'flattening' of the profiles in the convergent part of the tube and a 'sharpening' in the divergent part. We could expect reasonably accurate results for higher values of λ . In Fig. 2.2 we show examples of the velocity

Z	H'/H	η	$G^{(0)}$	$\lambda G^{(1)}$	$\lambda^2 G^{(2)}$	$\lambda^3 G^{(3)}$
-0.6	-1.67	0.0	0.637	-0.0376	0.0058	-0.0004
		0.3	0.579	-0.0237	0.0032	-0.0002
		0.7	0.325	0.0091	-0.0013	0.0001
-0.2	-0.93	0.0	0.637	-0.0209	-0.0076	0.0036
		0.3	0.579	-0.0132	-0.0043	0.0019
		0.7	0.325	0.0051	0.0017	-0.0008
0.2	0.93	0.0	0.637	0.0209	-0.0076	-0.0036
		0.3	0.579	0.0132	-0.0043	-0.0019
		0.7	0.325	-0.0051	0.0017	0.0008
0.6	1.67	0.0	0.637	0.0376	0.0058	0.0004
		0.3	0.579	0.0237	0.0032	0.0002
		0.7	0.325	-0.0091	-0.0013	-0.0001

Table 2.2. The contributions of separate powers of λ to the axial velocity profile for the tube with $H = 1 + (1/2)\tanh^2 Z$ when $\lambda = 5$.

than in Tube 1 and so the flow is closer to Poiseuille flow. Nevertheless, it is significantly different. There is a noticeable 'flattening' of the profiles in the convergent part of the tube and a 'sharpening' in the divergent part. We could expect reasonably accurate results for higher values of λ . In Fig. 2.2 we show examples of the velocity profiles calculated using the series for tube 2 with $\lambda = 10$. The profiles represent the velocity with respect to η at various values of Z in the range $-2 \leq Z \leq +2$.

From the general expansion for $G(\eta, Z)$ we have

$$\begin{aligned}
 G &= \frac{1}{\eta} \frac{\partial F}{\partial \eta} \\
 &= G^{(0)}(\eta) + \lambda G^{(1)}(\eta, Z) + \lambda^2 G^{(2)}(\eta, Z) \\
 &\quad + \lambda^3 G^{(3)}(\eta, Z) + \dots
 \end{aligned}$$

A comparison with equation (2.18) shows that the difference between an exact solution and the DE profile at each stage of Z is

$$\begin{aligned}
 E &= \frac{13\lambda^2}{1800\pi^3} S'G_2^{(2)}(\eta) + \frac{281833\lambda^3}{38102400\pi^4} SS'G_2^{(3)}(\eta) \\
 &\quad + \frac{1459\lambda^3}{3175200\pi^4} TG_3^{(3)}(\eta) + \dots, \quad (2.19)
 \end{aligned}$$

where $G_m^{(n)}(\eta) = \frac{1}{\eta} \frac{\partial}{\partial \eta} \left[E_m^{(n)}(\eta) \right]$.

The function E represents the series for the error which we

can write as

$$z = \lambda L^{(2)}(\eta, z) = \dots$$

The separate terms in this series have been calculated numerically for Tube 1. The results are shown in Table 2.1 for the case when $\lambda = 5$. It is apparent that for these tubes with $\lambda = 5$ the DE profiles are in extremely good

agreement. Even with $\lambda = 5$ the maximum difference between the velocity (at $\eta = 0$) of the DE profiles and the exact solution can be estimated to be less than about 1.0% and generally such low. The slight increase seen in

Table 2.1 at $Z = 0.4$ where the contribution is of about 0.1% the $\lambda = 5$ as a result of the fact that the DE profiles contain λ^{-1} as a factor and this factor is not

numerically small for negative Z values. This factor should not be taken as evidence of the divergence of the series. The case $Z = 0.4$ shows a slight indication of the convergence of the series.

For $\lambda = 10$ the DE profiles are in even better agreement with the exact solution than for $\lambda = 5$. It is plausible that the DE profiles are in good agreement with the exact solution for $\lambda = 10$.

flows in slender tubes. The stability of the flow is also a function of the stability of the flow. The stability of the flow is also a function of the stability of the flow.

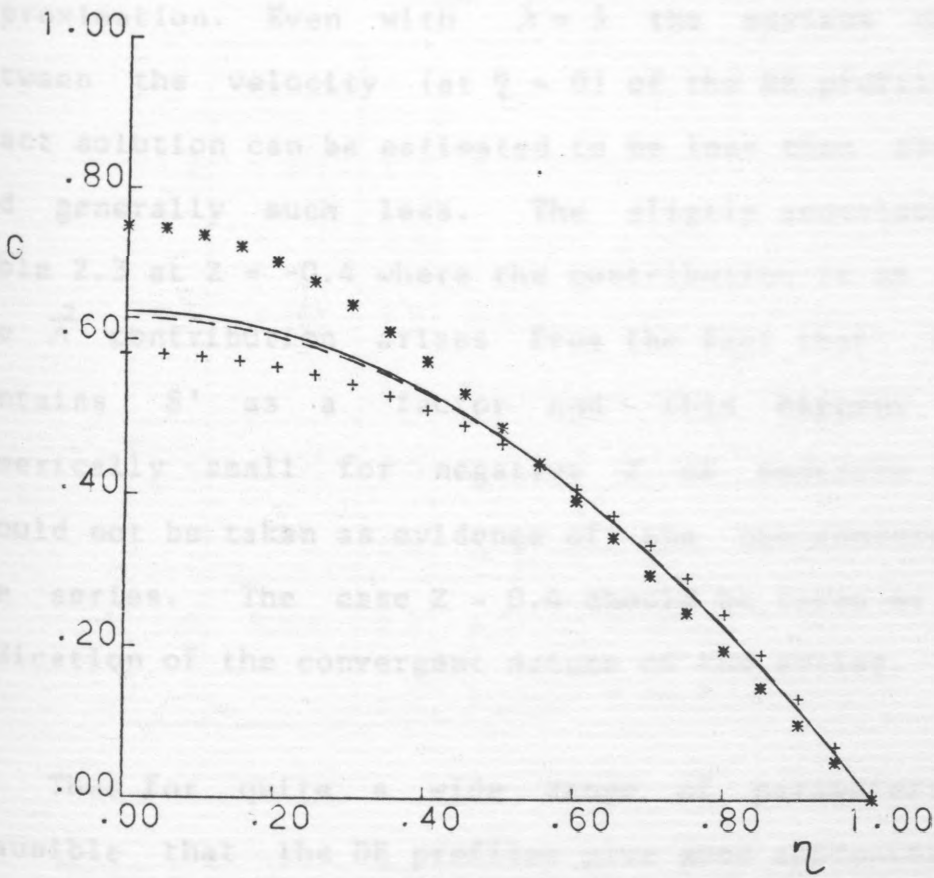


Fig. 2.2. Velocity profile for Tube 2 at various values of Z when $\lambda = 10$. - Poiseuille Flow; -- $Z = -2$; ++ $Z = -0.6$; * $Z = -0.8$.

can write as

$$E = \lambda^2 E^{(2)}(\eta, Z) + \lambda^3 E^{(3)}(\eta, Z) + \dots$$

The separate terms in this series have been calculated numerically for Tube 1. The results are shown in Table 2.3 for the case when $\lambda = 3$. It is apparent that for these tubes with $\lambda = 3$ the DE profiles are an extremely good approximation. Even with $\lambda = 5$ the maximum difference between the velocity (at $\eta = 0$) of the DE profile and the exact solution can be estimated to be less than about 1.5% and generally much less. The slightly anomalous case in Table 2.3 at $Z = -0.4$ where the contribution is as high as the λ^2 contribution arises from the fact that $E^{(2)}(\eta, Z)$ contains S' as a factor and this happens to be numerically small for negative Z of moderate size. It should not be taken as evidence of the non-convergence of the series. The case $Z = 0.4$ should be taken as a better indication of the convergent nature of the series.

Thus for quite a wide range of parameters it is plausible that the DE profiles give good approximations to flows in slender tubes. We are therefore lead to consider the stability of the DE profiles as probably giving a good guide to the stability of flow in more general tubes.

3. SPATIAL STABILITY OF THE DE PROFILES

It is known that Poiseuille flow is stable to small axisymmetric disturbances for all Reynolds numbers, the observed instabilities being attributed to finite amplitude effects. Many slender channel flows have been shown to be unstable for sufficiently high values of the parameter $\lambda H'/H$. A similar behavior would be expected for slender tube flows. Undertaken here is a study of the stability of

Z	$\lambda H'/H$	γ	DE	$\lambda^2 E^{(2)}$	$\lambda^3 E^{(3)}$
-1.0	1.017	0.0	0.66185	-0.00169	-0.00047
		0.9	0.22184	0.00040	0.00010
-0.4	1.584	0.0	0.67817	-0.00051	-0.00047
		0.9	0.21726	0.00012	0.00010
0.4	1.078	0.0	0.66348	0.00169	0.00051
		0.8	0.22137	-0.00040	-0.00011
1.0	0.456	0.0	0.64732	0.00107	0.00023
		0.8	0.22602	-0.00026	-0.00005

Table 2.3. Differences between the DE approximation and exact solution. Contributions of separate terms $\lambda^2 E^{(2)}$ and $\lambda^3 E^{(3)}$ for Tube 1, with $H = 1 + (1/2)\tanh Z$ when $\lambda = 3$.

3. SPATIAL STABILITY OF THE DE PROFILES

It is known that Poiseuille flow is stable to small axisymmetric disturbances for all Reynolds numbers, the observed instabilities being attributed to finite amplitude effects. Many slender channel flows have been shown to be unstable for sufficiently high values of the parameter $\lambda H'/H$. A similar behaviour would be expected for slender tube flows. Undertaken here is a study of the stability of the DE profiles.

3.1 Disturbance Equation

To study a small disturbance $\hat{\psi}$ to the basic steady flow \hat{F} we superimpose the disturbance on the basic flow so that the total stream function is given by

$$\psi = \hat{F}(r, x) + \hat{\psi}(r, x, t).$$

Substitute ψ into equation (2.4). Since the basic assumption is that for small disturbances the equation may be linearised, quadratic or higher order terms in the disturbance and their derivatives may be neglected. The resulting equation after substitution and simplification reduces to

$$\left[\frac{1}{r} \frac{\partial}{\partial t} + \frac{1}{r^2} \left(\hat{F}_r \frac{\partial}{\partial x} - \hat{F}_x \frac{\partial}{\partial r} \right) \right] D^2 \hat{\psi}$$

$$\begin{aligned}
& -\frac{1}{r^2} \left[\frac{\partial \hat{\Psi}_r}{\partial t} + \frac{\partial}{\partial r} (D^2 \hat{F}) \hat{\Psi}_x \right] \\
& + \frac{1}{r^3} \left[2(\hat{F}_x \hat{\Psi}_{xx} + \hat{F}_{xx} \hat{\Psi}_x) + 3(\hat{F}_x \hat{\Psi}_{rr} + \hat{F}_{rr} \hat{\Psi}_x) \right. \\
& \left. - \hat{F}_r \hat{\Psi}_{rx} - \hat{F}_{rx} \hat{\Psi}_r \right] - \frac{3}{r^4} (\hat{F}_r \hat{\Psi}_x + \hat{F}_x \hat{\Psi}_r) \\
& = \frac{1}{R} \left[\frac{1}{r} D^4 \hat{\Psi} - \frac{2}{r^2} (\hat{\Psi}_{rxx} + \hat{\Psi}_{rrr}) \right. \\
& \left. + \frac{3}{r^3} \hat{\Psi}_{rr} - \frac{3}{r^4} \hat{\Psi}_r \right] \tag{3.1}
\end{aligned}$$

where $D^2 \equiv \frac{\partial^2}{\partial r^2} + \frac{\partial^2}{\partial x^2}$.

The boundary conditions on $\hat{\Psi}$ are that $\hat{\Psi}$ is regular as $r \rightarrow 0$, $\hat{\Psi} = \hat{\Psi}_r = 0$ on the wall.

As before consider a general tube of radius $r = H(Z)$, ($Z = \epsilon x$), and let $\eta = r/H(Z)$. The stream function transforms to

$$\Psi = F(\eta, Z) + \hat{\Psi}(\eta, Z, t).$$

The disturbance equation (3.1) becomes

$$\begin{aligned}
& H^2 \eta^3 \Psi_{\eta\eta t} + H^4 \eta^3 \Psi_{zzt} + \eta^2 F_\eta \Psi_{\eta\eta z} + H^2 \eta^2 F_\eta \Psi_{zzz} \\
& - H^2 \eta^2 \Psi_{\eta t} + (-\eta^2 F_{\eta\eta\eta} + 3\eta F_{\eta\eta} - 3F_\eta) \Psi_z - \eta F_\eta \Psi_{\eta z} \\
& + \epsilon \left[\mathcal{H}(F) \{ 2H^2 \eta \Psi_{zz} + 3\eta \Psi_{\eta\eta} - \eta^2 \Psi_{\eta\eta\eta} \right. \\
& \left. - H^2 \eta^2 \Psi_{\eta zz} - 3\Psi_\eta \} - \mathcal{H}(F_\eta) \Psi_\eta \right] \\
& + \epsilon^2 \left[\mathcal{H}^2(F) \{ 2H^2 \eta \Psi_z - H^2 \eta^2 \Psi_z \} \right]
\end{aligned}$$

$$= \frac{1}{R} \left[\eta^3 \Psi_{\eta\eta\eta\eta} + 2H^2 \eta^3 \Psi_{\eta\eta z z} + H^4 \eta^3 \Psi_{z z z z} - 2H^2 \eta^2 \Psi_{\eta z z} - 2\eta^2 \Psi_{\eta\eta\eta} + 3\eta \Psi_{\eta\eta} - 3\Psi_{\eta} \right], \quad (3.2)$$

where

$$\mathcal{H} \equiv \frac{\partial}{\partial z} - \eta \frac{H'}{H} \frac{\partial}{\partial \eta}$$

with boundary conditions

$$\Psi(1, Z) = \Psi_{\eta}(1, Z) = 0$$

$$\text{and } \Psi(0, Z) = \Psi_{\eta}(0, Z) = 0$$

is the regularity condition at the centre. Note that the coefficients of the equation will now vary slowly with Z , in view of the slow variable $Z = \epsilon x$. The coefficients of the disturbance equation are independent of time, it contains time only through derivatives with respect to t . Hence we look for constant frequency solutions of the form

$$\Psi = \phi(\eta, Z) e^{i(S(x) - \beta t)} + \text{C.C.} \quad (3.3)$$

where

$$\frac{dS}{dx} = K(Z),$$

C.C. is the complex conjugate and

$$\phi = \phi^{(0)} + \epsilon \phi^{(1)} + \epsilon^2 \phi^{(2)} + \epsilon^3 \phi^{(3)} + \dots$$

Substituting this solution into (3.2) we obtain

$$\left[R^{-1} (\ell - q^2)^2 - iq \right] (G - \omega/q) (\ell - q^2)$$

$$\begin{aligned}
 & - \eta \left(\frac{G'}{\eta} \right)' \Big] \phi \\
 & + R^{-1} \eta^3 \left[\sum_{i=1}^4 \epsilon^i N_i \right] \phi - \bar{\eta}^3 \left[\sum_{i=1}^3 \epsilon^i M_i \right] \phi = 0
 \end{aligned} \tag{3.4}$$

where $R = \frac{\bar{R}}{H}$,

$$\omega = \beta H^3,$$

$$q = KH,$$

are the local Reynolds number, frequency and wave number respectively;

$$l = \frac{\partial^2}{\partial \eta^2} - \frac{1}{\eta} \frac{\partial}{\partial \eta}.$$

M_i and N_i are operator functions of η , H and \mathcal{H} . These have been derived, but the details are not needed here. The boundary conditions on ϕ are

$$\phi = \phi_\eta = 0 \quad \text{at } \eta = 0,$$

$$\phi = \phi_\eta = 0 \quad \text{at } \eta = 1.$$

Equation (3.4) represents a sequence of differential equations of which the $O(1)$ equation is the familiar Orr-Sommerfeld equation. We shall be concerned mainly with the solutions of the

Orr-Sommerfeld equation written here as

$$(\ell - q^2)^2 \phi^{(0)} - iqR \left[(G - \omega/q)(\ell - q^2) - \eta \left(\frac{G'}{\eta} \right)' \right] \phi^{(0)} = 0 \quad (3.5)$$

with boundary conditions

$$\begin{aligned} \phi^{(0)} = \phi_{\eta}^{(0)} = 0 & \quad \text{at } \eta = 0, \\ \phi^{(0)} = \phi_{\eta}^{(0)} = 0 & \quad \text{at } \eta = 1. \end{aligned} \quad (3.6)$$

In other words we shall be using the usual quasi-parallel assumption for studying the stability, and it is brought out here that to obtain this approximation we must treat R in the disturbance equation as $O(1)$, even though the base flow was derived on the basis of $R = O(\epsilon^{-1})$. This feature is common in most quasi-parallel stability analysis but it is argued in Eagles & Weissman(1975) that the method is allowable, and produces accurate results at least for channel flows.

3.2 Orr-Sommerfeld Equation

The solution of the Orr-Sommerfeld equation for specified real ω and R gives a complex eigenvalue q and a complex eigenfunction. In general, the equation will have four linearly independent solutions, so that

$$\phi^{(0)} = A_1 \phi_1 + A_2 \phi_2 + A_3 \phi_3 + A_4 \phi_4$$

where A_i are arbitrary constants and ϕ_i are independent solutions. A series solution of (3.5) enabled us to eliminate immediately those solutions which were not regular near the centre of the tube. A linear combination of the remaining solutions yielded

$$\phi^{(0)} = A_1 \phi_1 + A_2 \phi_2.$$

By applying the boundary conditions (3.6) we obtained two homogeneous equations for the constants A_1 and A_2 . For non-trivial solution to exist the determinant of the coefficients A_1 and A_2 must vanish, leading to

$$F(R, \omega, q) = \phi_1(1) \phi_2'(1) - \phi_1'(1) \phi_2(1) = 0.$$

The eigenvalues q must be determined for selected real positive values of R and ω . If $q = q_r + iq_i$, q_i determines whether or not the basic flow is stable to small disturbances. If q_i is positive the flow is considered to be stable. If it is negative the flow is unstable. The case $q_i = 0$ indicates neutral stability. In general a number of types of modes are possible each with a spectrum of eigenvalues, (See Drazin & Reid(1981)). Searching for the least stable or unstable eigenvalue is by no means an easy task.

On expanding equation (3.5) we obtain

$$\left[\eta^4 D^4 - 2\eta^3 D^3 + (3 - A\eta^2)\eta^2 D^2 + (-3 + A\eta^2)\eta D + (B + iqRU)\eta^4 \right] \phi^{(0)} = 0,$$

where

$$D \equiv \frac{d}{d\eta},$$

$$A = 2q^2 + iqR(G - \omega/q),$$

$$B = q^4 + iqR(G - \omega/q),$$

$$U = \eta \left(\frac{G'}{\eta} \right)'. \quad (3.7)$$

with boundary conditions $\phi^{(0)}$, $\phi_{\eta}^{(0)}$, regular at $\eta = 0$ and $\phi^{(0)}(1) = \phi_{\eta}^{(0)}(1) = 0$ on the walls. The velocity function $G(\eta)$ was defined in (2.18) for the DE profiles. The following alternative form was more convenient to use for the series solution in powers of η which will be used for small values of η

$$G = 2 \sum_{k=1}^{\infty} (-1)^{k+1} k g_k \eta^{2k-2},$$

$$U = 8 \sum_{k=1}^{\infty} k(k-1)(k-2) g_k (-1)^{k+1} \eta^{2k-4}$$

where g_k are the coefficients of $\eta/2k$ in (2.18).

Equation (3.7) is an ordinary differential equation which may be solved by the Frobenius method. Let

$$\phi^{(0)} = \sum_{r=0}^{\infty} A_r \eta^{5+r}.$$

On substituting the series into (3.5) we obtain a series solution with four arbitrary constants,

$$\begin{aligned} \phi^{(0)} = & A_0(\eta^4 \log \eta + \dots) + A_1(\eta^2 + \dots) \\ & + A_2(\eta^4 + \dots) + A_4(\eta^2 \log \eta + \dots). \end{aligned}$$

The boundary conditions at the centre of the tube require that A_0 and A_3 are both zero. The appropriate solution that satisfies the boundary conditions is given by

$$\phi^{(0)} = A_1 \phi_1 + A_2 \phi_2, \quad (3.8)$$

where for small values of η

$$\phi_1 = \eta^2 - \frac{1}{192} Q \eta^6 + \frac{1}{1152} (M - \frac{1}{8} PQ) \eta^8 + \dots,$$

$$\phi_2 = \eta^4 + \frac{8}{192} P \eta^6 + \frac{1}{1152} (P^2 - Q - N) \eta^8 + \dots,$$

$$P = 2q^2 + iqR(2g_1 - \omega/q),$$

$$Q = q^4 + iqR(2g_1 - \omega/q),$$

$$M = 4iqR(g_2 q^2 - 12g_3),$$

$$N = iqR(32g_2).$$

This series was used to calculate starting values for the Runge-Kutta integration scheme. The fourth-order Runge-Kutta routine in double precision was used for all calculations to minimise both truncation and roundoff errors. A step length of 1/20 was used throughout with some numerical checks made on a step length of 1/40.

3.21 Numerical solution

The Orr-Sommerfeld equation was considered in the form

$$\eta^4 \phi^{iv} = 2\eta^3 \phi''' - \eta^2 y_1 \phi'' - \eta y_2 \phi' - y_3 \phi$$

where

$$y_1 = 3 - A\eta^2,$$

$$y_2 = -y_1,$$

$$y_3 = (B + iqRU)\eta^4.$$

The equation was integrated in double precision from 0.05 to 1 in view of the singularity at $\eta = 0$, the series solution (3.8) being used up to $\eta = 0.05$. For the solution $\phi^{(0)} = A_1 \phi_1 + A_2 \phi_2$, the computer considered two stages initially to obtain two independent solutions. The stages are : $A_1 = 1, A_2 = 0$ and $A_1 = 0, A_2 = 1$. Later an attempt was made to satisfy the boundary conditions at $\eta = 1$.

At each stage integration proceeded using a fourth-order Runge-Kutta procedure evaluating ϕ , ϕ' , ϕ'' and ϕ''' until $\eta = 1$. These values were stored. The stored values were used to obtain the eigenvalue relation

$$F(R, \omega, q) = \phi_1(1) \phi_2'(1) - \phi_1'(1) \phi_2(1) = 0.$$

For fixed values R and ω , the eigenvalues of q must be found by searching iteratively for the zeroes of F . In order to effect the procedure we needed values of R , ω and needed a good estimate of q .

Although the above procedure is simple its numerical implementation can lead to serious difficulties especially when R is large. The difficulty arises from the fact that although the solutions ϕ_1 and ϕ_2 are numerically satisfactory near $\eta = 0$, they both contain some multiple of the rapidly growing viscous solution and causes loss of linear independence near $\eta = 1$. One of the methods of overcoming this difficulty, proposed by Nachtsheim(1964), is based on the method of matched initial-value problems. In this method, in addition to forward integration from $\eta = 0$, a backward integration is also made from $\eta = 1$ and the eigenvalue relation is then obtained by matching the results at an interior point of the interval, e.g. the midpoint. Other methods for dealing with this difficulty include filtering as in Kaplan(1964).

In the present study R was first kept reasonably low at $R = 40$ and the frequency was fixed at $\omega = 1$. The search was made by plotting contour lines $F_r = 0$, $F_i = 0$ in the complex q -plane, where F_r and F_i are the real and imaginary parts of F . Any intersection of the contour lines $F_r = 0$ and $F_i = 0$ indicates the approximate location of a root. A typical contour plot is shown in Fig. 3.1 for the first and fourth quadrants. The approximate root found in this way was used as an estimate for the eigenvalue q . A more accurate value was obtained by a root finding routine based on successive linear interpolation. In the range $-10 \leq q_r \leq 10$ and $-4 \leq q_i \leq 4$ no unstable roots were found for $R = 40$, $\omega = 1$ at both $\gamma = 0$ and $\gamma = 6$. Two stable roots were found in the first quadrant, of which the least stable root is shown in Fig. 3.1. The second root was also confirmed by an independent program used by Eagles (Private communication). The roots were determined by the root finding routine at $\gamma = 0$, $R = 40$, $\omega = 1$ as $q_1 = (1.74912, 1.32565)$ and $q_2 = (1.82435, 3.34520)$. In the next section we look at the behaviour of the least stable eigenvalue as R , ω and γ are varied.

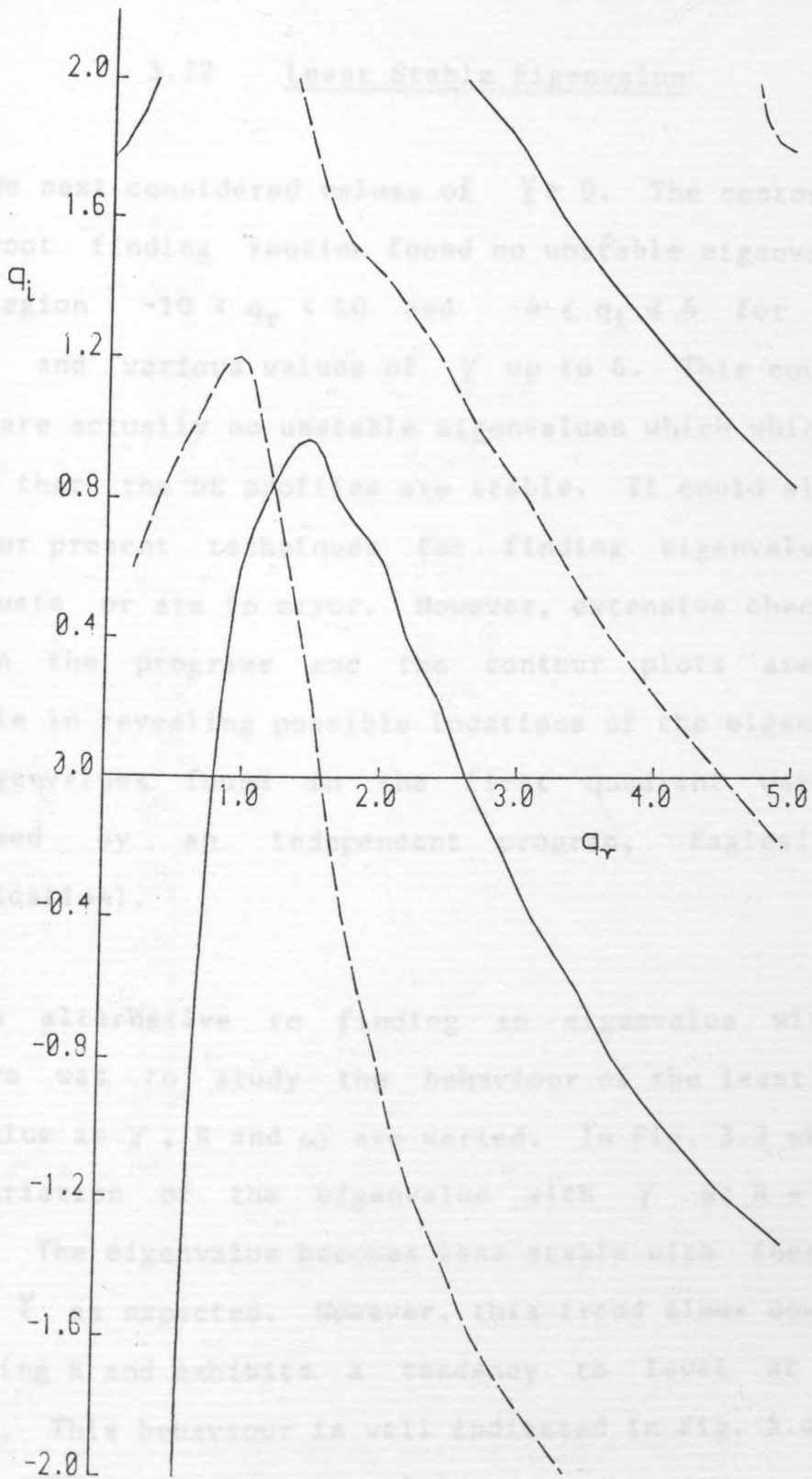


Fig. 3.1. Contour plot of least stable eigenvalue for $\chi = 6$, $R = 40$ and $\omega = 1$. - F_1 ; -- F_2 .

3.22 Least Stable Eigenvalue

We next considered values of $\gamma > 0$. The contour plots and root finding routine found no unstable eigenvalues in the region $-10 < q_r < 10$ and $-4 \leq q_i \leq 4$ for $R = 40$, $\omega = 1$ and various values of γ up to 6. This could mean there are actually no unstable eigenvalues which would imply that the DE profiles are stable. It could also mean that our present techniques for finding eigenvalues are inadequate or are in error. However, extensive checks were made on the programs and the contour plots are quite reliable in revealing possible locations of the eigenvalues. The eigenvalues found in the first quadrant were also confirmed by an independent program, Eagles(private communication).

An alternative to finding an eigenvalue with q_i negative was to study the behaviour of the least stable eigenvalue as γ , R and ω are varied. In Fig. 3.2 we show the variation of the eigenvalue with γ at $R = 40$ and $R = 60$. The eigenvalue becomes less stable with increasing R and γ as expected. However, this trend slows down with increasing R and exhibits a tendency to level at about $R = 400$. This behaviour is well indicated in Fig. 3.4 where q_i begins to level around $R = 210$. A scatter diagram of the eigenvalue at various values of R is given in Fig. 3.3. It is interesting to note that the least stable root remains stable at Reynolds numbers as high as $R = 450$ at $\gamma = 6.6$.

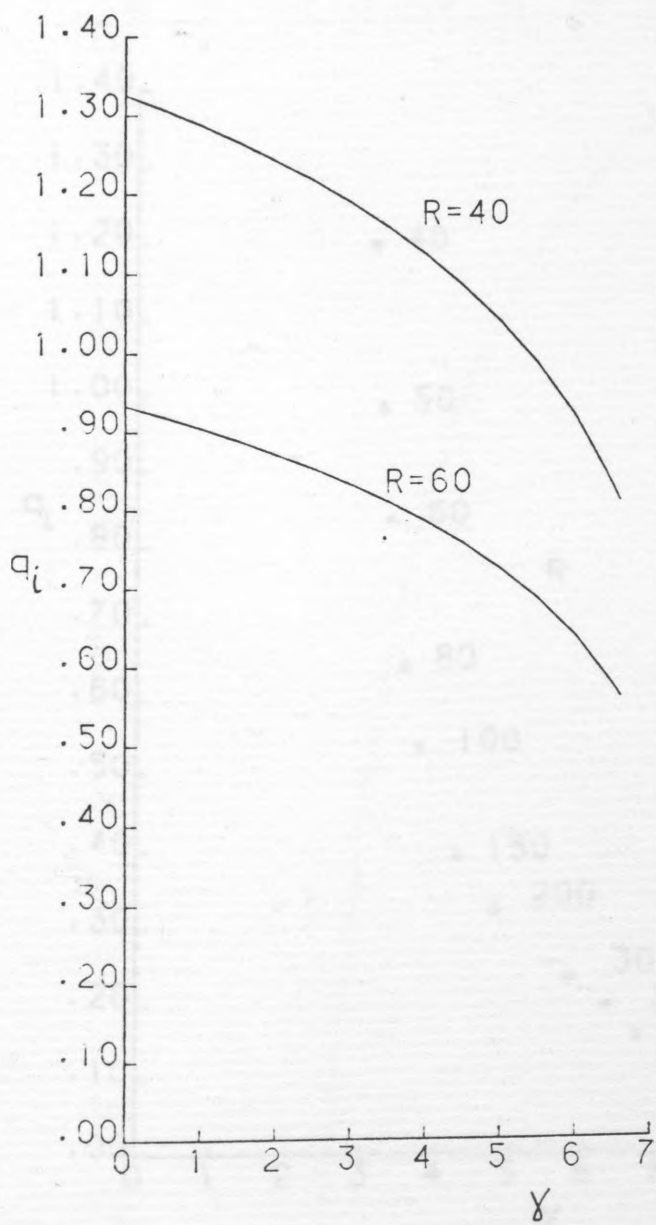


Fig. 3.2. Variation of q_i with γ at $R = 40$ and $R = 60$ For $\omega = 1$.

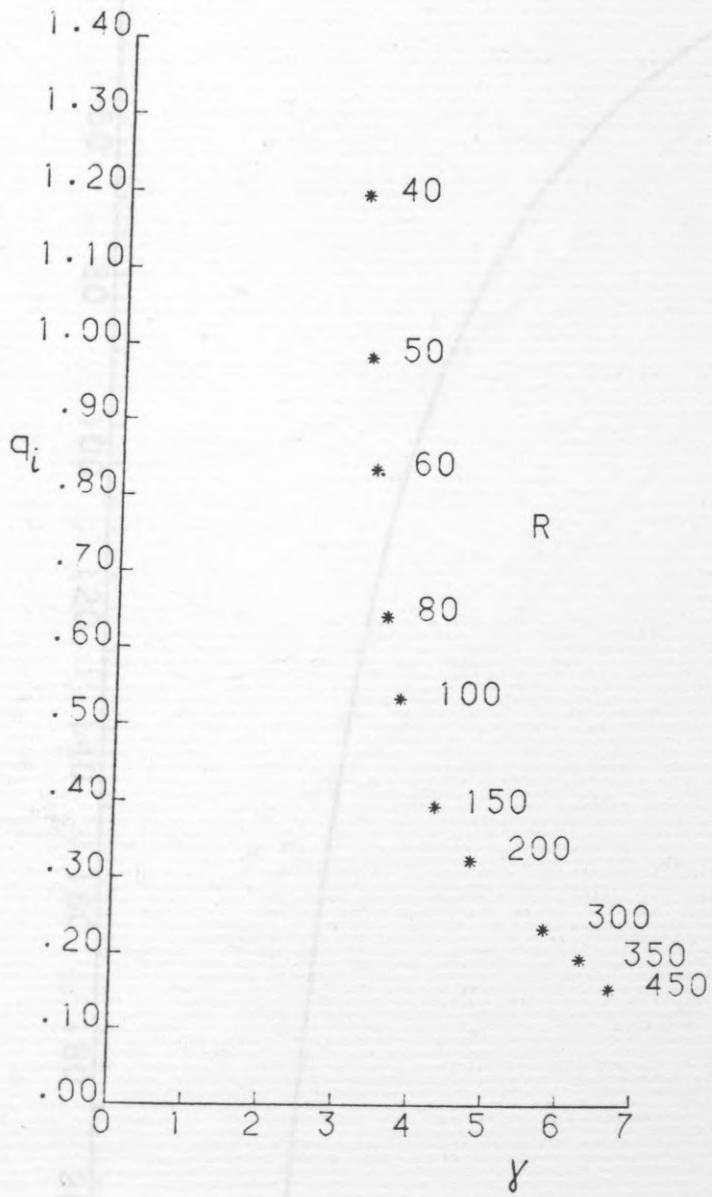


Fig. 3.3. q_i at various values of γ and R , $\omega = 1$.

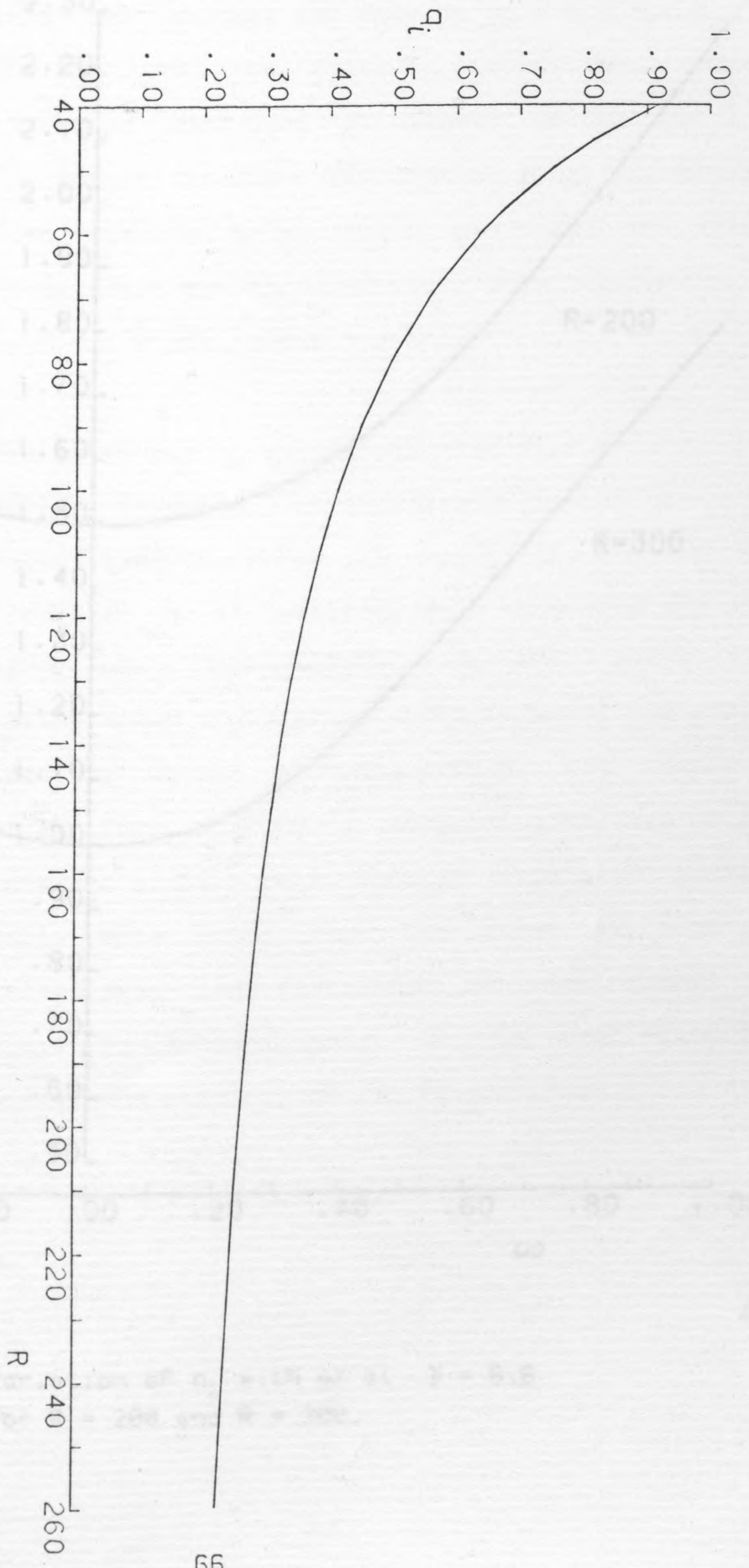


Fig. 3.4. Variation of q_l with R for $\gamma = 6$ and $\omega = 1$.

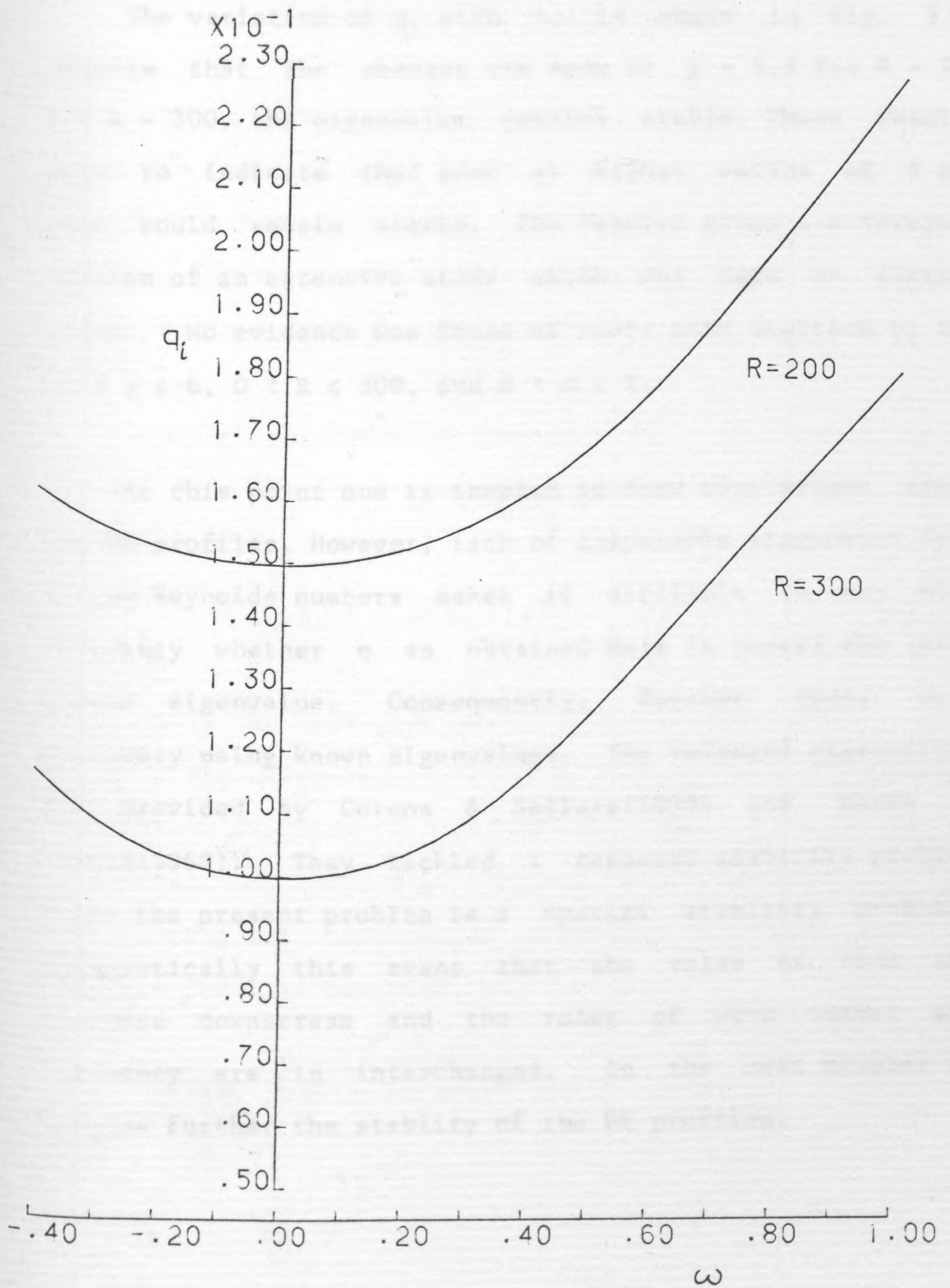


Fig. 3.5. Variation of q_i with ω at $\gamma = 6.6$
For $R = 200$ and $R = 300$.

The variation of q_i with ω is shown in Fig. 3.5. Despite that the changes are made at $\gamma = 6.6$ for $R = 200$ and $R = 300$, the eigenvalue remains stable. These results seem to indicate that even at higher values of R the root would remain stable. The results given are merely a section of an extensive study which was made on similar lines. No evidence was found of roots with negative q_i for $-6 \leq \gamma \leq 6$, $0 < R \leq 500$, and $0 < \omega \leq 1$.

At this point one is tempted to draw conclusions about the DE profiles. However, lack of comparable eigenvalue data at low Reynolds numbers makes it difficult to say with certainty whether q as obtained here is indeed the least stable eigenvalue. Consequently, further tests were necessary using known eigenvalues. The relevant eigenvalues are provided by Corcos & Sellars(1959) and Davey & Drazin(1969). They tackled a temporal stability problem while the present problem is a spatial stability problem. Mathematically this means that the roles of time and distance downstream and the roles of wave number and frequency are in interchanged. In the next chapter we examine further the stability of the DE profiles.

4. TEMPORAL STABILITY OF THE DE PROFILES

Davey & Drazin(1969) have confirmed the various classes of modes found by Pekeris(1948) and Corcos & Sellars(1959). In addition they also found a few other modes not known before. The relationship between these classes of modes was displayed in a diagram, similar to Fig. 4.1.

Consider axisymmetric flow in a tube of radius H as before and let the transformed disturbance stream function be of the form

$$\Psi(\eta, Z, t) = \phi(\eta, Z)e^{i\alpha(x - Ct)} + \text{C.C.} \quad (4.1)$$

where α is the real wave number and C is the complex wave speed. The disturbance function is similar to the spatial disturbance function (3.3) except that this formulation is convenient for treating temporal stability problems. On substituting the disturbance function Ψ into (3.2) we obtain a familiar equation

$$\begin{aligned} (\ell - \alpha^2)^2 \phi &= i\alpha R \left[(G - C)(\ell - \alpha^2) \right. \\ &\quad \left. - \eta \left(\frac{G}{\eta} \right)' \right] \phi \end{aligned} \quad (4.2)$$

where

$$G = \frac{2}{\pi}(1 - \eta^2)$$

with boundary conditions

$$\phi(1) = \phi'(1) = 0,$$

and ϕ, ϕ' are regular at $\eta = 0$.

This is equation (3.5) with q replaced by C_T and ω/q replaced by C_T .

where C_r and C_i are the real and imaginary parts of the eigenvalue C .

The eigenvalue C determines whether or not the basic flow is stable. If C_i is negative the flow is considered to be stable. The case $C_i = 0$ represents neutral stability.

Davy & Drain used $G = 1 - \eta^2$ for the basic flow along a different non-dimensionalisation.

Their eigenvalues will therefore be multiplied by η^2 to give the values shown in Fig. 4.1.

In Fig. 4.1 we display our roots which will be examined in detail in the next section.

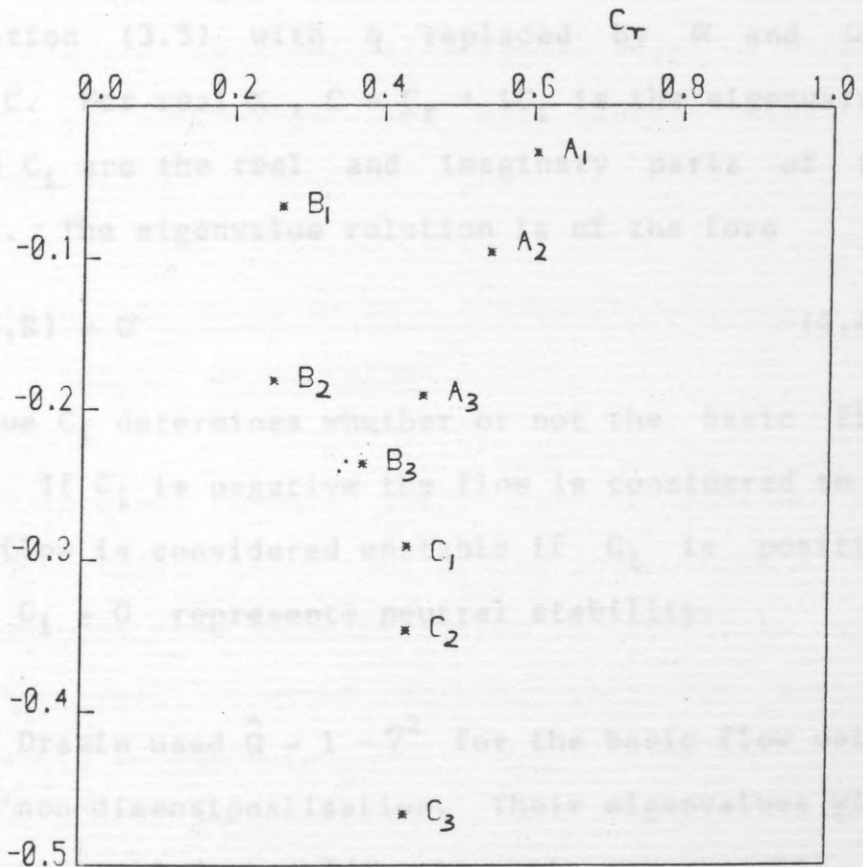


Fig. 4.1. Branches A, B, C indicating eigenvalues

$A_1, A_2, A_3, B_1, B_2, B_3, C_1, C_2$ and C_3

at $R = 5000, \alpha = 1, \gamma = 0$.

with boundary conditions

$$\phi(1) = \phi_{\eta}(1) = 0,$$

and ϕ , ϕ_{η} are regular at $\eta = 0$. (4.3)

This is equation (3.5) with q replaced by α and ω/q replaced by C . For real α , $C = C_r + iC_i$ is the eigenvalue, where C_r and C_i are the real and imaginary parts of the eigenvalue C . The eigenvalue relation is of the form

$$F(\alpha, C, R) = 0 \quad (4.4)$$

The eigenvalue C_i determines whether or not the basic flow is stable. If C_i is negative the flow is considered to be stable. The flow is considered unstable if C_i is positive and the case $C_i = 0$ represents neutral stability.

Davey & Drazin used $\hat{G} = 1 - \eta^2$ for the basic flow using a different non-dimensionalisation. Their eigenvalues will therefore be multiplied by $2/\pi$ to get our results at $\gamma = 0$. In Fig. 4.1 we display our roots which will be examined in this Chapter. Three branches labelled A, B, and C are shown. These are the same branches obtained by Davey & Drazin in addition to two other branches which will not concern us here. The branches A and B were also displayed by Corcos & Sellars.

On each branch we shall consider three roots which will be referred to as A_1, A_2, A_3 on A, B_1, B_2, B_3 on B and C_1, C_2, C_3 on C. Branch A contains the least stable root A_1

which raises the possibility of instability for higher values of γ . The values of these roots are given in Table 4.1. The table also includes the Davey & Drazin roots (DD) calculated from our results. The calculated roots (DD) compare very well with Figure 3.(b) of Davey & Drazin (1969), an indication that our results (EM) are reasonably accurate.

4.1 Modification of Davey & Drazin Eigenvalues for the DE Profiles

Our main interest in this study was to observe the stability of the least stable root A_1 and other roots as the DE profiles changed from Poiseuille flow to the flow with $\gamma = 6$. If the root remained stable, then our earlier observation would be confirmed.

The relation between our results and those obtained by Davey & Drazin was derived as follows. Let \hat{G} be the basic flow used by Davey & Drazin and let G be our basic flow. Equation (4.2) is written in terms of G and \hat{G} as follows

$$l^2 \phi = i \alpha R \left[(G - C) l \phi - \eta \left(\frac{G'}{\eta} \right)' \phi \right]$$

$$l^2 \phi = i \hat{\alpha} \hat{R} \left[(\hat{G} - \hat{C}) l \phi - \eta \left(\frac{\hat{G}'}{\eta} \right)' \phi \right]$$

where

$$l \equiv \frac{\partial^2}{\partial \eta^2} - \frac{1}{\eta} \frac{\partial}{\partial \eta} - \alpha^2$$

From the above system, we obtain the relations

$$\alpha = \beta,$$

$$\alpha \gamma = \beta \delta,$$

$$\alpha \rho = \beta \sigma.$$

From which

$$\beta = \frac{\alpha \gamma}{\delta}$$

$$\alpha = \frac{\beta \delta}{\gamma}$$

	EM		DD	
A ₁	0.6047	-0.0321	0.9499	-0.0504
A ₂	0.5410	-0.0959	0.8498	-0.1507
A ₃	0.4567	-0.1953	0.7174	-0.3068
B ₁	0.2579	-0.0712	0.4032	-0.1118
B ₂	0.2166	-0.1862	0.3402	-0.2924
B ₃	0.3745	-0.2393	0.5883	-0.3758
C ₁	0.4302	-0.2952	0.6757	-0.4637
C ₂	0.4283	-0.3506	0.6727	-0.5507
C ₃	0.4272	-0.4716	0.6711	-0.7408

Table 4.1. Values of roots on branches A, B and C for $\alpha = 1$, $\gamma = 0$ and $R = 5000$. DD are the Davey & Drazin roots calculated from our results (EM).

From the above system, we obtain the relations

$$\alpha = \hat{\alpha},$$

$$\alpha RG = \hat{\alpha} \hat{R} \hat{G},$$

$$\alpha RC = \hat{\alpha} \hat{R} \hat{C}$$

from which

$$R = \frac{\hat{G} \hat{R}}{G}$$

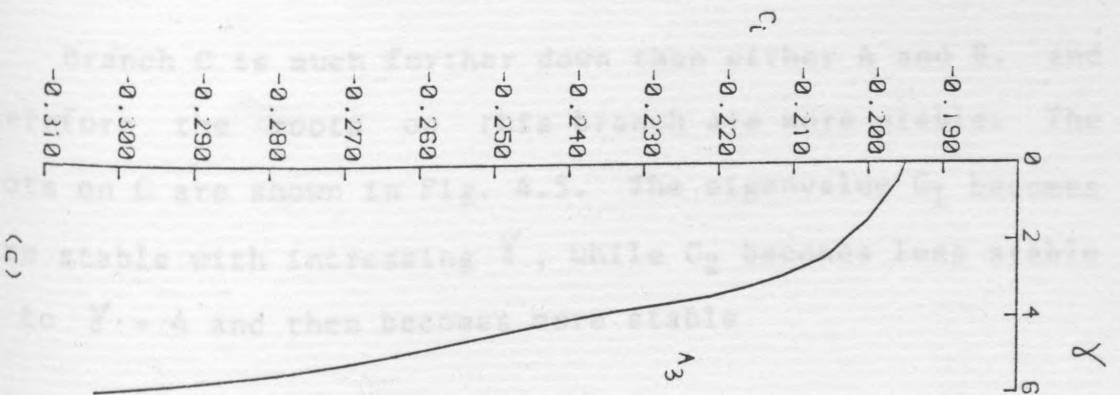
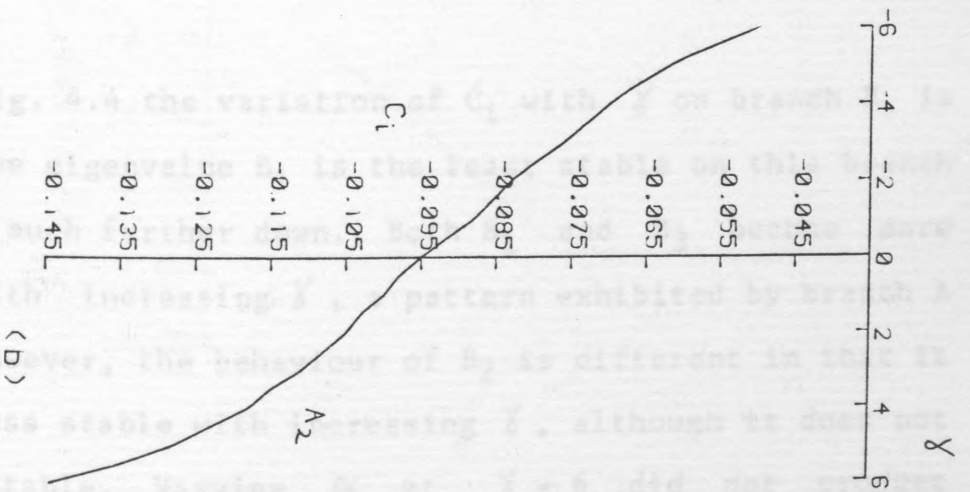
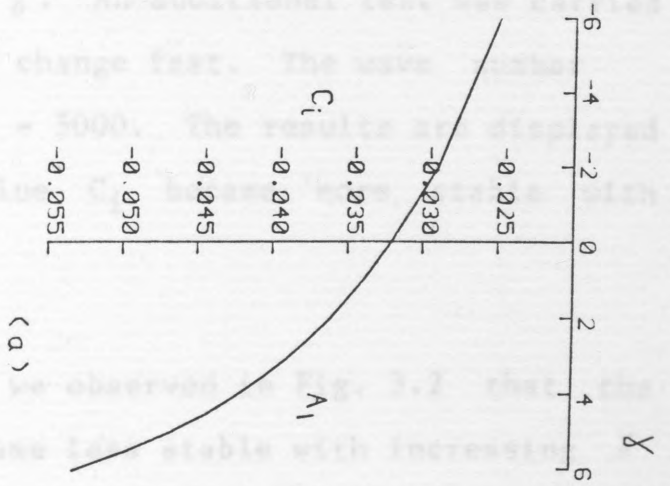
and

$$\begin{aligned} C &= \frac{\hat{R} \hat{C}}{R} \\ &= \frac{2 \hat{C}}{\pi} \end{aligned}$$

Our eigenvalues were obtained at $\alpha = 1$, $\gamma = 0$ and $R = 5000$ at which values the use double precision computing was just sufficient to obtain accurate results. Note that Davey & Drazin also obtained the eigenvalues at $\alpha = 1$ and $R = 5000$.

The roots on branch A were considered first. These are displayed in Fig. 4.2. The eigenvalue A_1 becomes more stable as γ increases from -6 to +6. This was unexpected behaviour from the least stable root. Further tests were carried out on A_2 and A_3 . The behaviour of A_2 was similar to that of A_1 except that it becomes more stable faster. The root A_3 as shown in Fig. 4.1 is much further down and

Fig. 4.2. Variation of C_i with λ for $\alpha = 1$, $R = 5000$ on A.



hence more stable than the other two. It also becomes more stable with increasing γ . An additional test was carried out on A_2 which seemed to change fast. The wave number was varied at $\gamma = 6$, $R = 5000$. The results are displayed in Fig. 4.3. The eigenvalue C_1 became more stable with increasing α .

In spatial stability we observed in Fig. 3.2 that the least stable root q_1 became less stable with increasing γ even though it did not become unstable. The unexpected results observed here needed further investigation to confirm the trends so far observed.

In Fig. 4.4 the variation of C_1 with γ on branch B is shown. The eigenvalue B_1 is the least stable on this branch and B_3 is much further down. Both B_1 and B_3 become more stable with increasing γ , a pattern exhibited by branch A roots. However, the behaviour of B_2 is different in that it becomes less stable with increasing γ , although it does not become unstable. Varying α at $\gamma = 6$ did not produce instability.

Branch C is much further down than either A and B. and therefore the roots on this branch are more stable. The roots on C are shown in Fig. 4.5. The eigenvalue C_1 becomes more stable with increasing γ , while C_2 becomes less stable up to $\gamma = 4$ and then becomes more stable

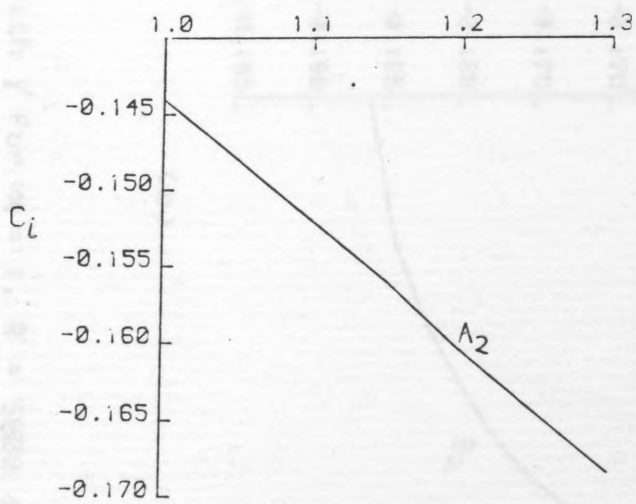


Fig. 4.3. Variation of C_i with α at $\gamma = 6$ and $R = 5000$ for the eigenvalue λ_2 .

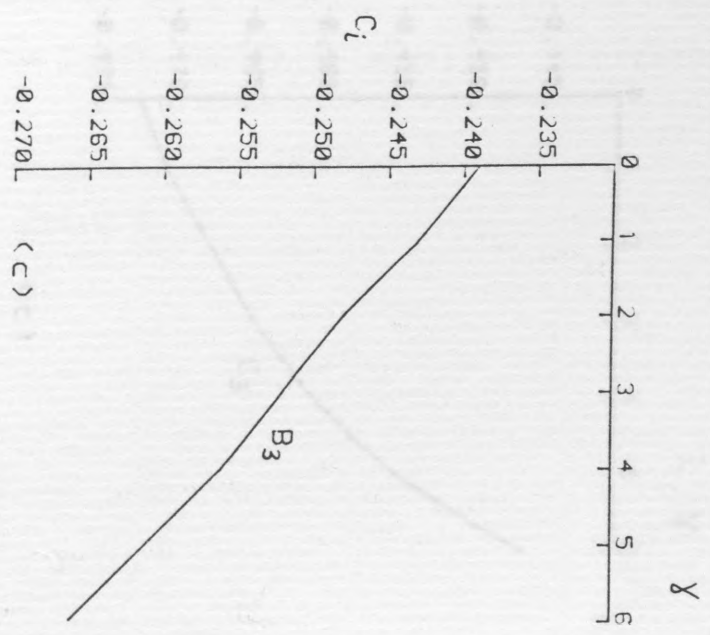
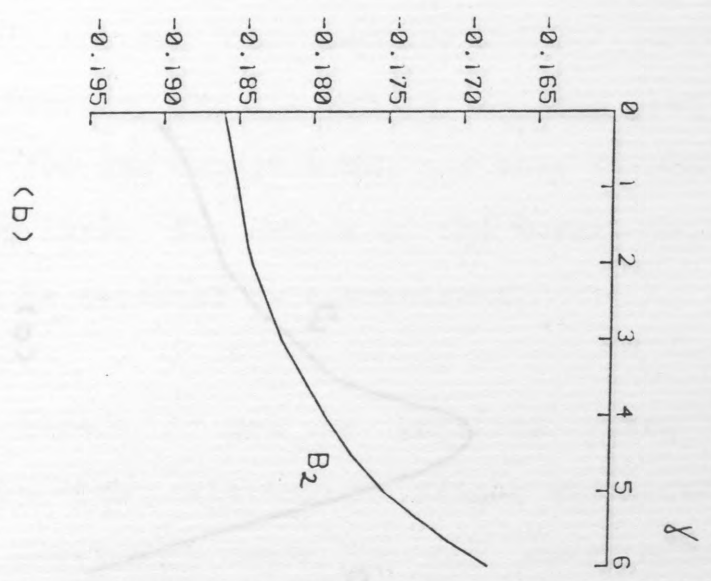
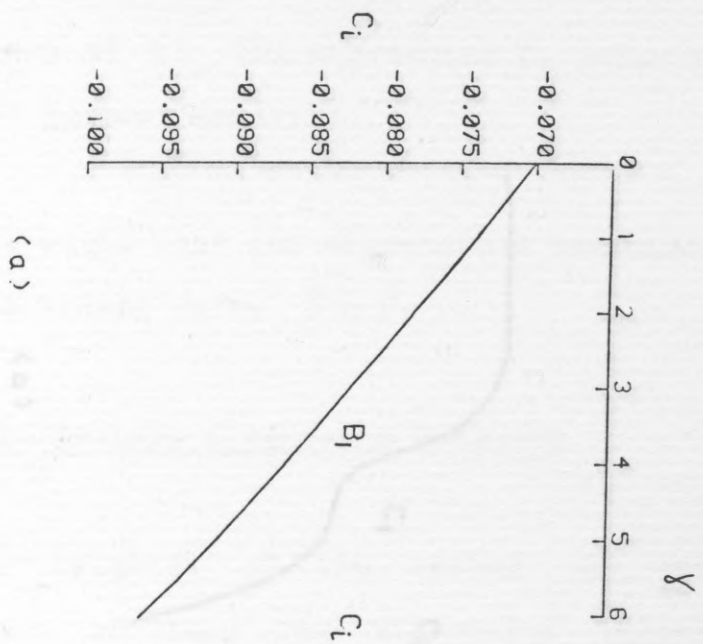
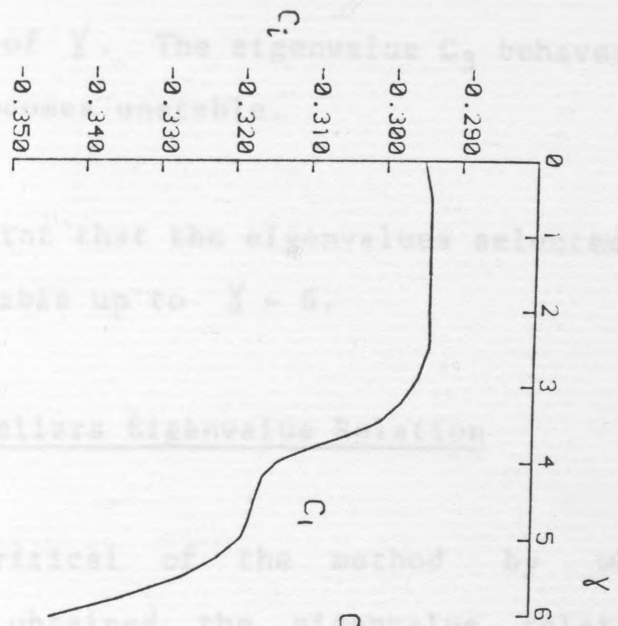
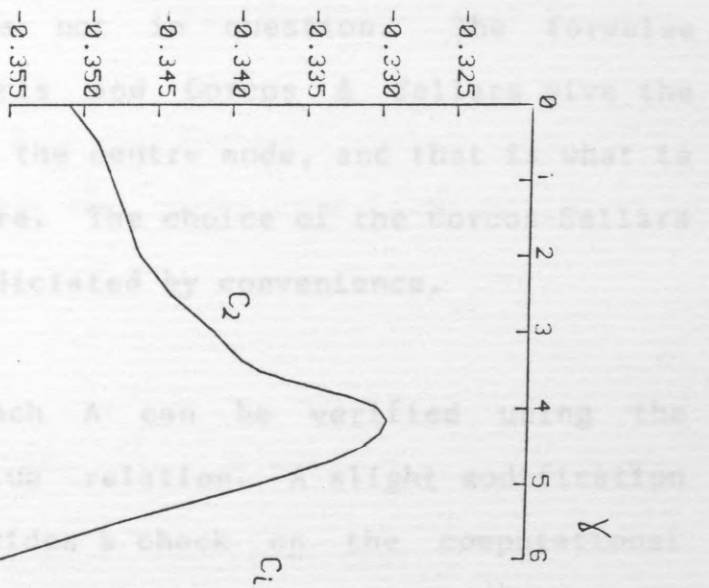


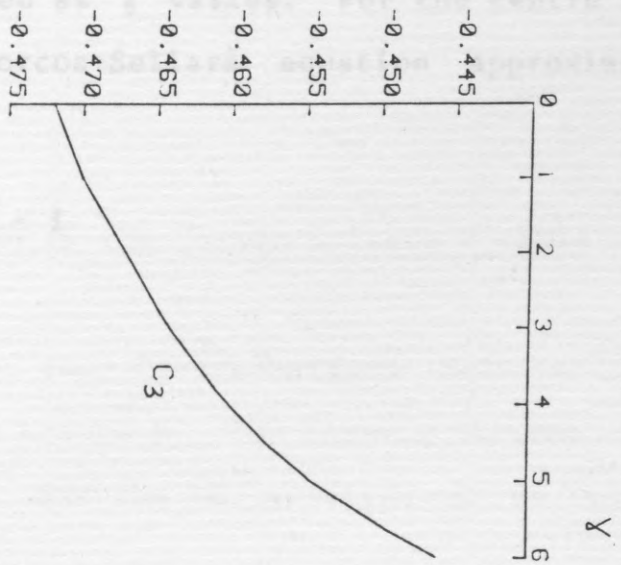
Fig. 4.4. Variation of C_i with γ for $\alpha = 1$, $R = 5000$ on B.



(a)



(b)



(c)

FIG. 4.5. Variation of C_i with γ for $\alpha = 1$, $R = 5000$ on B.

with further increases of χ . The eigenvalue C_3 behaves as B_2 although it never becomes unstable.

We note at this point that the eigenvalues selected on all the branches are stable up to $\chi = 6$.

4.2 Corcos-Sellars Eigenvalue Relation

Gill(1965) was critical of the method by which Corcos & Sellars(1959) obtained the eigenvalue relation. The formula itself is not in question. The formulae derived by both Pekeris and Corcos & Sellars give the correct eigenvalues for the centre mode, and that is what is relevant in our case here. The choice of the Corcos-Sellars eigenvalue relation is dictated by convenience.

The roots on branch A can be verified using the Corcos-Sellars eigenvalue relation. A slight modification to the formula also provides a check on the computational results so far obtained as χ varies. For the centre mode when R is large the Corcos-Sellars equation approximates to

$$(1 - e^Q) e^P \approx -i$$

Equation (4.7) is the Corcos-Sellars formula that generates the roots on branch A. The formula becomes less accurate as N increases. For the W profile G is given below

where

$$Q = 2 \int_k^0 \sqrt{[i \alpha R (G - C)]} dr,$$

$$P = \int_k^1 \sqrt{[i \alpha R (G - C)]} dr,$$

$$K^2 = 1 - C, \tag{4.5}$$

$G = 1 - r^2$ is the basic flow,

$\psi = \phi(r) e^{i\alpha(x - Ct)}$ is the disturbance function,

α is the wave number, R is the Reynolds number and C is the eigenvalue. The term e^P grows very large as $R \rightarrow \infty$ so that

$$e^Q = 1;$$

$$Q = -2\pi iN, \quad N = 1, 2, 3, \dots \tag{4.6}$$

It follows from equations (4.5) and (4.6) that

$$C = 1 + \frac{4Ne^{-0.25(3\pi i)}}{\sqrt{\alpha R}} \tag{4.7}$$

4.21 Modification of the Corcos-Sellars Formula

Equation (4.7) is the Corcos-Sellars formula that generates the roots on branch A. The formula becomes less accurate as N increases. For the DE profiles G is given below

$$G = a - b\eta^2 + d_1\eta^4 - d_2\eta^6 + \dots$$

where, approximately, from section 2.31

$$a = \frac{2}{\pi} + \frac{8\gamma}{36\pi^2} + \frac{2}{25}T\gamma^2f_1 + \frac{2}{300\pi}T\gamma^3L_0,$$

$$b = \frac{2}{\pi} + \frac{\gamma}{\pi^2} + \frac{4}{25}T\gamma^2f_2 + \frac{4}{300\pi}T\gamma^3L_1,$$

$$d_1 = \frac{\gamma}{\pi^2} + \frac{6}{25}T\gamma^2f_3 + \frac{6}{300\pi}T\gamma^3f_7,$$

$$(f_1, f_2, f_3, f_4, f_5, f_6, f_7, f_8, f_9, f_{10}, f_{11}, f_{12}) = (2648, 7840, 8800, 4800, 1320, 128, 46256, 230720, 409600, 331200, 121680, 15611),$$

$$T = \frac{1}{3456\pi^3},$$

$$L_0 = f_7 - \frac{2}{6}f_8 + \frac{3}{20}f_9 - \frac{4}{50}f_{10} + \frac{5}{105}f_{11} - \frac{6}{196}f_{12},$$

and

$$L_1 = 2f_7 - \frac{3}{6}f_8 + \frac{4}{20}f_9 - \frac{5}{50}f_{10} + \frac{6}{105}f_{11} - \frac{7}{196}f_{12}.$$

In making the modification to the Corcos-Sellars eigenvalue equation, a further approximation was necessary to facilitate evaluation of the integrals. This is justified since the coefficients d_i of η are small in comparison with a and b . The largest of these is d_1 which can be compared with b at selected values of η as shown in Table 4.2.

For

$$0 = 2 \int_0^1 [(1-x^2)(1-c) - c] dx$$

Let

$$c = a + b\eta^2$$

hence

$$0 = 2 \int_0^1 [(1-x^2)(a + b\eta^2) - (a + b\eta^2)] dx$$

γ	η	a	b	d_1	$b\eta^2$	$d_1\eta^4$
0.1	0.1	0.6389	0.6487	0.0103	0.00649	0.00000
	0.5			.	0.16217	0.00350
2.0	0.1	0.6911	0.8963	0.3035	0.00896	0.00003
	0.5				0.22405	0.01897
3.0	0.1	0.7271	1.09050	0.5555	0.01090	0.00006
	0.5				0.27013	0.03472

Table 4.2. Comparison between the coefficients of b and d_1 .

At first sight this approximation might appear severe on the velocity function G was also shown to be accurate in the range $-3 \leq \gamma \leq 3$. The estimates indicate to the contrary. Despite these limitations, it does provide a good check on the behaviour of the eigenvalues as γ varies from -6 to 6 . A program was written to evaluate G , a and b for N up to 10, with $N = 1$ representing the least stable root. A comparison with the estimate and the root as calculated by the main program is shown in Tables 4.3 and 4.2, for $N = 1, K = 5000$.

For

$$Q = 2 \int_k^0 \sqrt{[i \alpha R (G - C)]} d\eta,$$

let $G = a - b\eta^2,$

hence

$$Q = 2 \sqrt{i \alpha R} \int_k^0 (a - C - b\eta^2)^{\frac{1}{2}} d\eta$$

$$= e^{5\pi i/4} (\alpha R)^{\frac{1}{2}} \frac{\pi}{2} K^2 b^{\frac{1}{2}}$$

where

$$K^2 = (a - c)/b.$$

Since $Q = -2\pi iN$ we obtain the formula

$$C = a - 2N(1 + i) \frac{\sqrt{2b}}{\sqrt{\alpha R}}.$$

At first sight this approximation might appear severe on the formula which is already restricted to small N . The velocity function G was also shown to be accurate in the range $-3 \leq \gamma \leq 3$. The estimates indicate to the contrary. Despite these limitations, it does provide a good check on the behaviour of the eigenvalues as γ varies from -6 to 6 . A program was written to evaluate C , a and b for N up to 10 , with $N = 1$ representing the least stable root. A comparison with the estimate and the root as calculated by the main program is shown in Tables 4.3 and 4.4, for $\alpha = 1, R = 5000$.

γ	EIGENALUE		ESTIMATE		DIFFERENCE	
-6.0	0.5253	-0.025018	0.5149	-0.016660	0.0104	0.00835
-5.0	0.5346	-0.025997	0.5292	-0.020495	0.0054	0.00540
-4.0	0.5451	-0.026971	0.5428	-0.023208	0.0023	0.00366
-3.0	0.5570	-0.027502	0.5563	-0.025406	0.0007	0.00250
-2.0	0.5706	-0.029162	0.5705	-0.027439	0.0001	0.00172
-1.0	0.5861	-0.030533	0.5863	-0.029549	0.0002	0.00098
-0.5	0.5951	-0.031305	0.5951	-0.030691	0.0000	0.00061
-0.1	0.6028	-0.031951	0.6027	-0.031663	0.0001	0.00028
0.0	0.6048	-0.032116	0.6047	-0.031915	0.0001	0.00002
0.1	0.6069	-0.032287	0.6067	-0.032171	0.0001	0.00000
0.5	0.6153	-0.032997	0.6152	-0.033235	0.0001	0.00000
1.0	0.6268	-0.033954	0.6266	-0.034662	0.0002	0.00000
2.0	0.6544	-0.036144	0.6532	-0.037870	0.0012	0.00100
3.0	0.6991	-0.039909	0.6955	-0.041579	0.0026	0.00100
4.0	0.7330	-0.042159	0.7247	-0.045803	0.0083	0.00300
5.0	0.7978	-0.046745	0.7719	-0.050534	0.0259	0.00300
6.0	0.7959	-0.144205	0.9282	-0.055752	0.0323	0.09900

Table 4.3. Eigenvalues and estimates For γ in the range -6 to 6 when $N = 1$.

N	γ	EIGENVALUE		ESTIMATE		DIFFERENCE	
3	0.0	0.5410	-0.09594	0.5409	-0.09575	0.0001	0.0002
	0.1	0.5426	-0.09634	0.5424	-0.09651	0.0002	0.0002
	0.5	0.5492	-0.09802	0.5487	-0.09970	0.0005	0.0016
	1.0	0.5583	-0.10030	0.5573	-0.10400	0.0010	0.0037
	2.0	0.5802	-0.10530	0.5775	-0.11360	0.0027	0.0083
	3.0	0.6074	-0.11120	0.6024	-0.12470	0.0050	0.0135
6	0.0	0.4567	-0.19530	0.4451	-0.19150	0.0116	0.0038
	0.1	0.4577	-0.19560	0.4459	-0.19300	0.0118	0.0026
	0.5	0.4617	-0.19670	0.4490	-0.19940	0.0127	0.0027
	1.0	0.4672	-0.19830	0.4533	-0.20800	0.0139	0.0094
	2.0	0.4793	-0.20280	0.4639	-0.22720	0.0154	0.0244
	3.0	0.4911	-0.21190	0.4776	-0.24950	0.0135	0.0376

Table 4.4. Eigenvalues and estimates for γ in the range 0 to 3 when $N = 3$ and $N = 6$.

The Corcos-Sellars eigenvalue relation was used to check on the various trends of the eigenvalues as γ varied from -6 to +6. This was a necessary independent check since we required confidence in the program's ability to locate eigenvalues as γ varied. The main program uses the exact solution for the basic flow while the modified eigenvalue relation uses only a very approximate solution obtained by the expansion method. The results in both cases have been remarkably close as shown by the estimates in Tables 4.3 and 4.4.

The investigations carried out so far in both spatial and temporal stability indicate that the DE profiles are stable to small disturbances for γ in the range $-6 \leq \gamma \leq 6$.

4.4 Link Between Spatial and Temporal Roots

We conclude this Chapter by considering the link between spatial and temporal roots. We shall begin by considering the link between our least stable spatial root given by

$$q_1 = (1.74916, 1.32567)$$

for $\gamma = 0$, $\omega = (1, 0)$, $R = 40$ and the least stable temporal root given by $\omega_1 = (0.518428, -0.671796)$ for $\gamma = 0$, $q = (1, 0)$, $R = 40$. The temporal root was traced from the Davey & Drazin root A_1 given in Fig 4.1 and Table 4.1. The root was traced from $R = 5000$ to $R = 40$ by reducing R by small steps of

$R = 10$ and checked by drawing a continuous graph of the root as a function of R . Contour plots were also used to confirm the root obtained by tracing.

We pose the question: are these special values q_1 and ω_1 consistent with a functional relationship of the form

$$q = f(\omega) ?$$

If so, then we would be able to change ω by small steps to move from one root to the other in such a way that q varies continuously and smoothly. In the first case consider ω_r fixed at $\omega_r = 0.518428$ while ω_i varies in small steps, where ω_r and ω_i are the real and imaginary parts of ω respectively. The results are given in Fig. 4.6. As ω_i varies from 0 to -0.671796 , q changes smoothly to $q = (1,0)$. Note that q attains the value $q = (1,0)$ when $\omega = \omega_1$. In the second case consider ω_i fixed at $\omega_i = -0.671796$ while ω_r is allowed to vary. In Fig. 4.7 ω_r is reduced from 1 to 0.517828 and again $q = (1,0)$ when $\omega = \omega_1$. If instead we consider a relationship of the form

$$\omega = f(q)$$

we obtain the same result where ω attains a value of $\omega = (1,0)$ when $q = q_1$. This is an indication that the two roots are connected.

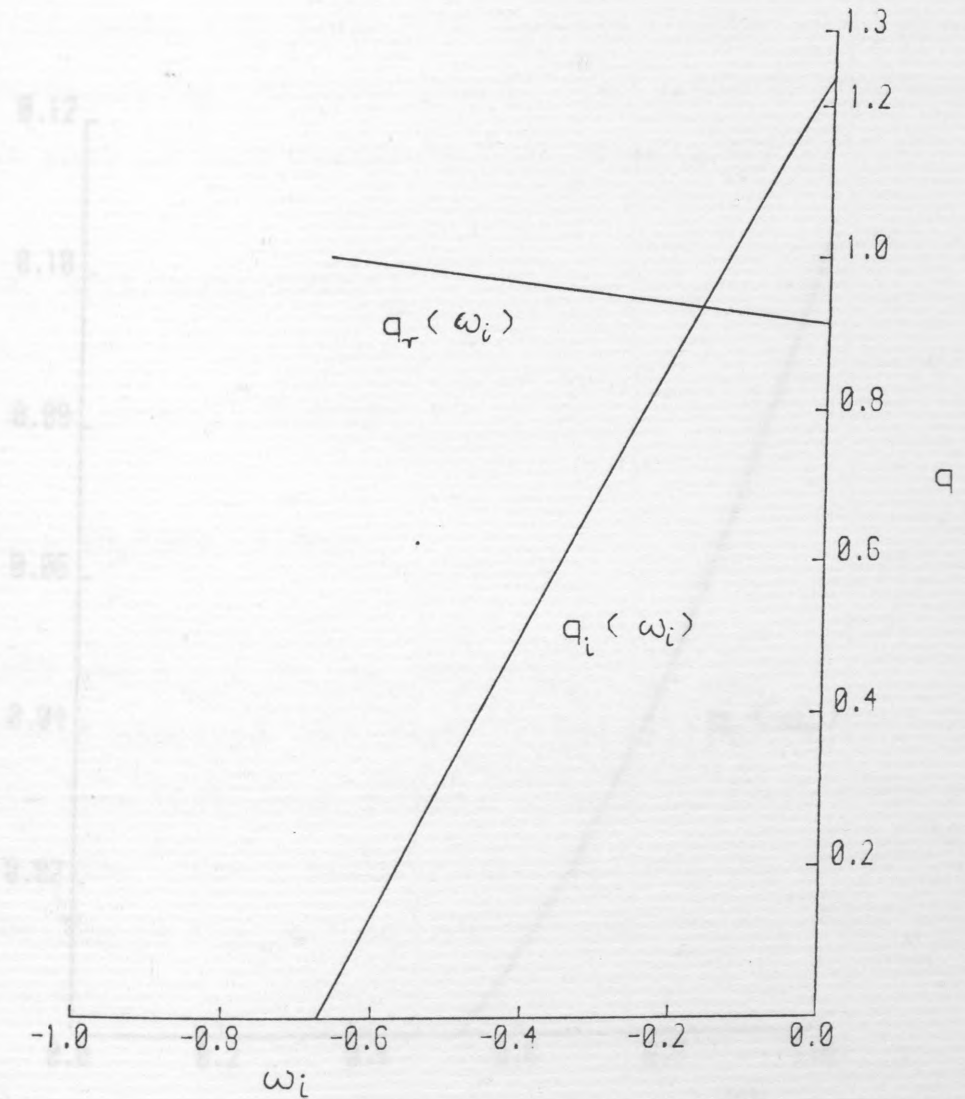


Fig. 4.6. The spatial root q as a function of ω when ω_r is fixed at $\omega_r = 0.5184$ and $R = 40$, $\gamma = 0$.

Using similar methods, it was possible to find continuous smooth connections between other temporal roots and spatial roots. In Table 4.5 spatial roots are given with corresponding temporal roots. The roots to represent the first root of each branch (A,B,C) being given by

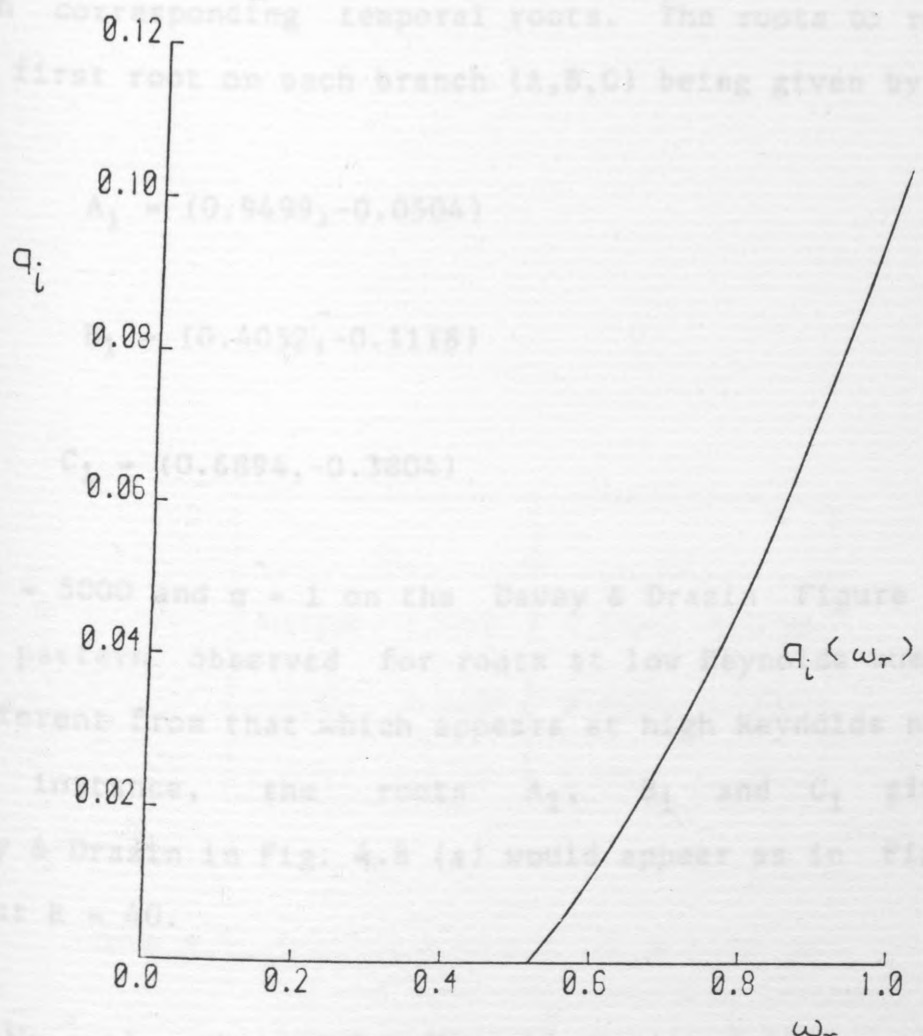


Fig. 4.7. The spatial root q as a function of ω when ω_i is fixed at $\omega_i = -0.6718$ and $R = 40$, $\gamma = 0$.

We notice that at low Reynolds numbers the roots are together. The effect of raising the Reynolds number brings the roots close together in a small area. At very high Reynolds numbers most of the roots will lie within a square root of unity of the real axis. Thus we tend to have small regions of stability at high Reynolds numbers and unstable regions at low Reynolds numbers. The process of finding roots at high Reynolds numbers is

Using similar methods it was possible to find continuous smooth connections between other temporal roots and spatial roots. In Table 4.5 spatial roots are given with corresponding temporal roots. The roots ω represent the first root on each branch (A,B,C) being given by

$$A_1 = (0.9499, -0.0504)$$

$$B_1 = (0.4052, -0.1118)$$

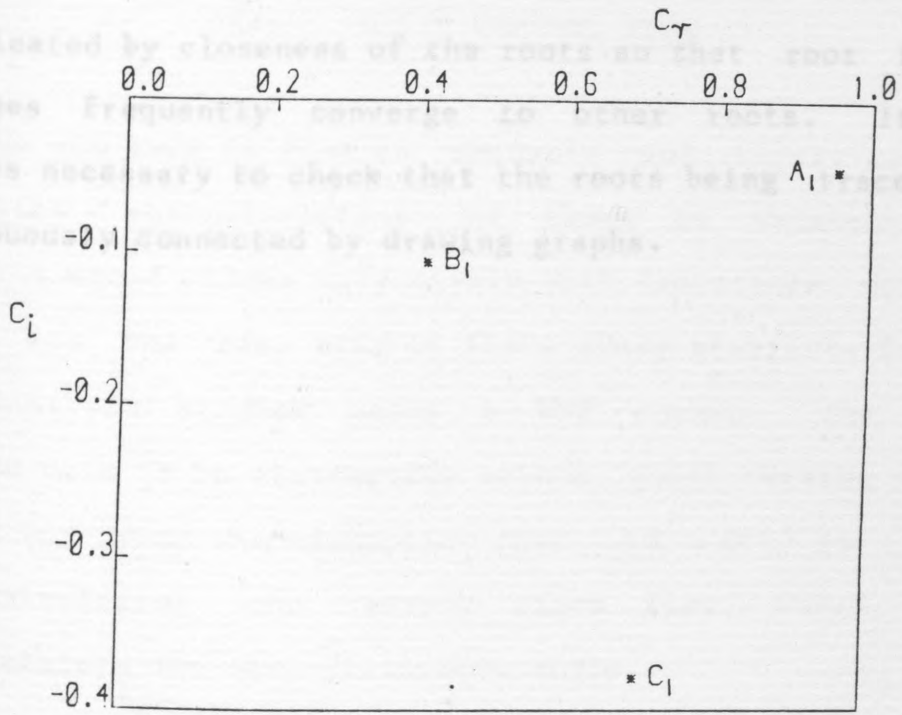
and $C_1 = (0.6894, -0.3804)$.

at $R = 5000$ and $q = 1$ on the Davey & Drazin Figure 3.(b). The pattern observed for roots at low Reynolds numbers is different from that which appears at high Reynolds numbers. For instance, the roots A_1 , B_1 and C_1 given by Davey & Drazin in Fig. 4.8 (a) would appear as in Fig. 4.8 (b) at $R = 40$.

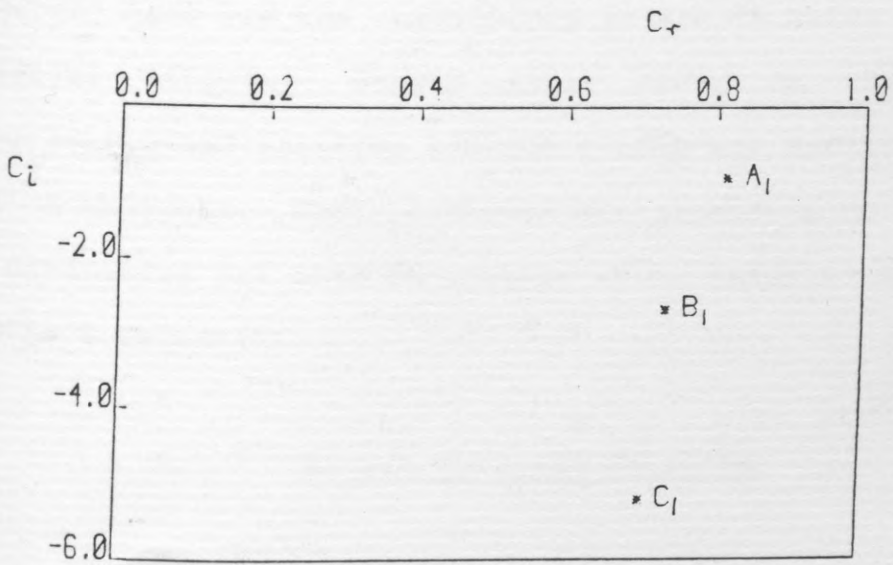
We notice that at low Reynolds numbers the roots are spaced out, whereas at high Reynolds numbers they are close together. The effect of raising the Reynolds number brings the roots close together in a small area. At very high Reynolds numbers most of the roots will lie within a square unit close to the real axis. Thus we tend to have small eigenvalues at high Reynolds numbers and somehow larger eigenvalues at low Reynolds numbers. The process of tracing roots at high Reynolds numbers is

q		ω	
1.74916	1.32567	0.51843	-0.67180
1.81368	3.31609	0.46288	-1.77669
1.71517	5.67301	0.44614	-3.35712

Table 4.5. Spatial roots q at $R = 40$, $\omega = 1$, $\gamma = 0$ with corresponding temporal roots at $R = 40$, $q = 1$, $\gamma = 0$.



(a)



(b)

Fig. 4.8. (a) The temporal roots A_1 , B_1 and C_1 at $R = 5000$, $q = 1$. (b) The temporal roots A_1 , B_1 and C_1 at $R = 40$, $q = 1$.

complicated by closeness of the roots so that root finding routines frequently converge to other roots. It then becomes necessary to check that the roots being traced are continuously connected by drawing graphs.

These are the same kind of roots whose stability Egglee & Weissenberg (1975) studied using a WKB method. The method adopted here is an alternative method, which retains the WKB method but drops the assumption that $\epsilon \ll 1$ in calculating the growth rate σ , where σ is approximately the real divergence rate.

In the present approach the growth rate σ is the basic flow rate U , i.e. we have $\sigma = U$ with ϵ small. Of interest here are the conditions for growth due to nonparallel effects. Growth rates have been calculated using energy and relative kinetic energy and are defined by Egglee & Weissenberg. Growth rates corresponding to $\sigma = U$ and these quantities are used to compare with results obtained by Egglee & Weissenberg.

5.1. Growth rate calculation

The vorticity equation together with the continuity and continuity were defined in Chapter 2 equations (2.2) and (2.3). They are recalled here for your reference. The equations are:

5. BASIC CHANNEL FLOW

We now turn to flow in channels and investigate the stability characteristics of flows in straight-walled channels whose widths vary slowly with downstream distance. These are the same kind of flows whose stability Eagles & Weissman(1975) studied using a WKB method. The method adopted here is an alternative method, which retains the WKB method but drops the assumption that $\epsilon R = O(1)$ as $\epsilon \rightarrow 0$ in calculating the steady state flow, where ϵ is approximately the semi-divergence angle.

In the present approach the restrictions imposed on the basic flow are dropped, i.e. we take $\epsilon \rightarrow 0$ with R fixed. Of interest here are the corrections to growth rates due to nonparallel effects. Growth rates based on amplitude, kinetic energy and relative kinetic energy are defined as in Eagles & Weissman. Neutral curves corresponding to each of these quantities are used to compare with results obtained by Eagles & Weissman.

5.1 Stream Function Equation

The vorticity equation together with the equation of continuity were defined in Chapter 2 equations (2.2) and (2.3). They are recalled here for easy reference. The equations are

$$\frac{\partial \bar{w}}{\partial t'} - \nabla \wedge (\bar{u} \wedge \bar{w}) = \gamma \nabla^2 \bar{w}, \quad (5.1)$$

$$\nabla \cdot \bar{u} = 0.$$

Consider a two dimensional flow with co-ordinates $(x', y', 0)$ and $\bar{u} = (u', v', 0)$. We can define a stream function as before by

$$u' = \frac{\partial \psi'}{\partial y'}, \quad v' = -\frac{\partial \psi'}{\partial x'}.$$

The equation was nondimensionalised as follows,

$$x = \frac{x'}{L}, \quad y = \frac{y'}{L}, \quad \hat{\psi} = \frac{\psi'}{M}, \quad t = t' \frac{M}{L^2}$$

$$u = u' \frac{M}{L}, \quad v = v' \frac{M}{L}$$

where L is half the channel width at $x' = 0$, M is half the volumetric flow rate per unit thickness.

Substituting into the equations of motion (5.1) we obtain

$$\frac{\partial}{\partial t} (\nabla^2 \hat{\psi}) + \left(\hat{\psi}_y \frac{\partial}{\partial x} - \hat{\psi}_x \frac{\partial}{\partial y} \right) \nabla^2 \hat{\psi} = \frac{1}{R} \nabla^4 \hat{\psi} \quad (5.2)$$

where $R = M/\gamma$ is the Reynolds number and

$$\hat{\psi} = \hat{\psi}(x, y, t).$$

The boundary conditions on $\hat{\psi}$ are

$$\hat{\psi} = \hat{\psi}_y = 0 \quad \text{at the walls.}$$

To transform equation (5.2) into the equation for a channel with varying walls, let

$$Z = \epsilon x$$

be a slow variable as before and let $y = \pm H(Z)$ be the equation of the wall. Also define

$$\eta = y/H(Z).$$

The derivatives transform as follows:

$$\frac{\partial}{\partial x} \equiv \epsilon \left(\frac{\partial}{\partial Z} - \eta \frac{H'}{H} \frac{\partial}{\partial \eta} \right),$$

$$\frac{\partial}{\partial y} \equiv \frac{1}{H} \frac{\partial}{\partial \eta}.$$

Equation (5.2) may now be expressed in terms of η and Z . Let

$$\hat{\psi}(x, y, t) = \psi(\eta, Z, t).$$

The various terms in the equation expand as follows.

$$\begin{aligned} \frac{\partial}{\partial t} (\nabla^2 \hat{\psi}) &\equiv \frac{1}{H^2} \psi_{\eta\eta t} + \epsilon^2 \left[\psi_{ZZt} \right. \\ &\quad + \eta \left(2 \frac{H'^2}{H^2} - \frac{H''}{H} \right) \psi_{\eta t} - 2 \eta \frac{H'}{H} \psi_{\eta Z t} \\ &\quad \left. + \eta^2 \frac{H'^2}{H^2} \psi_{\eta\eta t} \right] + O(\epsilon^3), \end{aligned}$$

$$\frac{\partial}{\partial x} (\nabla^2 \hat{\psi}) = \epsilon \left(-2 \frac{H'}{H^3} \psi_{\eta\eta} + \frac{1}{H^2} \psi_{\eta\eta z} - \eta \frac{H'}{H^3} \psi_{\eta\eta\eta} \right) + O(\epsilon^3),$$

$$\begin{aligned} \frac{\partial}{\partial y} (\nabla^2 \hat{\psi}) &= \frac{1}{H^3} \psi_{\eta\eta\eta} + \frac{\epsilon^2}{H} \left[\psi_{\eta z z} + \eta \left(2 \frac{H'^2}{H^2} - \frac{H''}{H} \right) \psi_{\eta\eta} \right. \\ &\quad + \left(2 \frac{H'^2}{H^2} - \frac{H''}{H} \right) \psi_{\eta} - 2 \frac{H'}{H} \psi_{\eta z} - 2 \eta \frac{H'}{H} \psi_{\eta\eta z} \\ &\quad \left. + 2 \eta \frac{H'^2}{H^2} \psi_{\eta\eta} + \eta^2 \frac{H'^2}{H^2} \psi_{\eta\eta\eta} \right] + O(\epsilon^3), \end{aligned}$$

$$\begin{aligned} \nabla^4 \hat{\psi} &= \frac{1}{H^4} \psi_{\eta\eta\eta\eta} + \frac{\epsilon^2}{H^2} \left[\psi_{\eta\eta z z} + 2 \left(2 \frac{H'^2}{H^2} - \frac{H''}{H} \right) \psi_{\eta\eta} \right. \\ &\quad + \eta \left(2 \frac{H'^2}{H^2} - \frac{H''}{H} \right) \psi_{\eta\eta\eta} - 4 \frac{H'}{H} \psi_{\eta\eta z} \\ &\quad - 2 \eta \frac{H'}{H} \psi_{\eta\eta\eta z} + 2 \frac{H'^2}{H^2} \psi_{\eta\eta} + 4 \eta \frac{H'^2}{H^2} \psi_{\eta\eta\eta} \\ &\quad \left. + \eta^2 \frac{H'^2}{H^2} \psi_{\eta\eta\eta\eta} \right] + O(\epsilon^3). \end{aligned} \quad (5.3)$$

Consider the stream function ψ to be made up of the steady state and the time dependent stream functions thus

$$\psi(\eta, z, t) = F(\eta, z) + \Psi(\eta, z, t).$$

The aim of this investigation is to study stability of F in the presence of a small disturbance Ψ . We begin by solving the steady state equation, which is the equation for F and later find the solution Ψ .

The basic flow F is obtained by setting $\frac{\partial}{\partial t} \equiv 0$ and $\Psi = 0$, and substituting equations (5.3) into (5.2). The resulting equation is

$$\begin{aligned}
 E_{\eta\eta\eta} &+ \epsilon \left[2RH'E_{\eta\eta} E_{\eta} + RH(E_z E_{\eta\eta\eta} - E_{\eta} E_{\eta\eta z}) \right] \\
 &+ \epsilon^2 H^2 \left[E_{\eta\eta z z} + 2 \left(\frac{3H'^2}{H^2} - \frac{H'''}{H} \right) E_{\eta\eta} \right. \\
 &+ \eta \left(\frac{6H'^2}{H^2} - \frac{H'''}{H} \right) E_{\eta\eta\eta} + \eta^2 \frac{H'^2}{H^2} E_{\eta\eta\eta\eta} \\
 &\left. - \frac{2H'}{H} (2E_{\eta\eta z} + \eta E_{\eta\eta\eta z}) \right] = 0,
 \end{aligned}$$

$$\begin{aligned}
 (1 + \epsilon^2 \eta^2 H'^2) E_{\eta\eta\eta\eta} &+ \left[\epsilon RH'E_z + \epsilon^2 \eta (6H'^2 - HH''') \right] E_{\eta\eta\eta} \\
 &+ \left[2\epsilon RH'E_{\eta} + 2\epsilon^2 (3H'^2 - HH''') \right] E_{\eta\eta} \\
 &- (\epsilon RHE_{\eta} + 4\epsilon^2 HH') E_{\eta\eta z} - 2\epsilon^2 HH' \eta E_{\eta\eta\eta z} \\
 &+ \epsilon^2 H^2 E_{\eta\eta z z} + O(\epsilon^3) = 0
 \end{aligned} \tag{5.4}$$

The boundary conditions on F are

$$F = \pm 1 \quad \text{at} \quad \eta = \pm 1,$$

$$E_{\eta} = 0 \quad \text{at} \quad \eta = \pm 1.$$

The solution F is obtained by expanding in powers of the parameter ϵ

$$F = F(0) + \epsilon F(1) + \epsilon^2 F(2) + \dots$$

Substituting the series into (5.4) leads to a sequence of equations by equating powers of ϵ . The equations are solved in order beginning with the $O(1)$ equation.

5.2 Series Solutions

$O(1)$ Equation

The equation for $F^{(0)}$ is

$$F_{\eta\eta\eta\eta}^{(0)} = 0$$

with boundary conditions

$$F^{(0)} = 1 \text{ at } \eta = 1,$$

$$F_{\eta}^{(0)} = 0 \text{ at } \eta = 1,$$

$$F^{(0)} = -1 \text{ at } \eta = -1,$$

$$F_{\eta}^{(0)} = 0 \text{ at } \eta = -1,$$

and the solution is

$$F^{(0)} = \frac{1}{2}(3\eta - \eta^3). \quad (5.5)$$

$O(\epsilon)$ Equation

The equation for $F^{(1)}$ is

$$F_{\eta\eta\eta\eta}^{(1)} + 2RH'F_{\eta}^{(0)}F_{\eta\eta}^{(0)} + RH(F_{\eta\eta}^{(0)}F_{\eta\eta\eta}^{(0)} - F_{\eta}^{(0)}F_{\eta\eta\eta}^{(0)}) = 0,$$

with boundary conditions

$$F^{(1)} = F_{\eta}^{(1)} = 0 \quad \text{at } \eta = 1,$$

$$F^{(1)} = F_{\eta}^{(1)} = 0 \quad \text{at } \eta = -1.$$

We obtain

$$F_{\eta\eta\eta\eta}^{(1)} = 9RH(\eta - \eta^3)$$

and hence

$$F^{(1)} = \frac{RH'}{280} (15\eta - 33\eta^3 + 21\eta^5 - 3\eta^7). \quad (5.6)$$

$O(\epsilon^2)$ Equation

The equation for $F^{(2)}$ is

$$\begin{aligned} F_{\eta\eta\eta\eta}^{(2)} + \eta^2 H'^2 F_{\eta\eta\eta\eta}^{(0)} + RH(F_Z^{(0)} F_{\eta\eta\eta}^{(1)} + F_Z^{(1)} F_{\eta\eta\eta}^{(0)}) \\ + \eta(6H'^2 - HH'') F_{\eta\eta\eta}^{(0)} \\ + 2RH'(F_{\eta}^{(0)} F_{\eta\eta}^{(1)} + F_{\eta}^{(1)} F_{\eta\eta}^{(0)}) \\ + 2(3H'^2 - HH'') F_{\eta\eta}^{(0)} + H^2 F_{\eta\eta Z Z}^{(0)} \\ - 2HH'\eta F_{\eta\eta\eta Z}^{(0)} - 4HH' F_{\eta\eta Z}^{(0)} \\ - RH(F_{\eta}^{(0)} F_{\eta\eta Z}^{(1)} + F_{\eta}^{(1)} F_{\eta\eta Z}^{(0)}) = 0. \end{aligned} \quad (5.7)$$

with boundary conditions

$$F^{(2)} = F_{\eta}^{(2)} = 0 \quad \text{at } \eta = 1,$$

$$F^{(2)} = F_{\eta}^{(2)} = 0 \quad \text{at } \eta = -1.$$

Hence we find

$$F_{\eta\eta\eta\eta}^{(2)} = -a_1(-19\eta + 68\eta^3 - 63\eta^5 + 14\eta^7) - a_2(7\eta - 23\eta^3 + 21\eta^5 - 5\eta^7) + a_3 9\eta$$

where

$$a_1 = \frac{9R^2 H'^2}{70},$$

$$a_2 = \frac{9R^2 H H''}{70},$$

$$a_3 = 9(4H^2 - H H'')$$

and the solution is eventually found to be

$$\begin{aligned} F^{(2)} &= \frac{1}{55440} a_1 (2875\eta - 8222\eta^3 + 8778\eta^5 - 4488\eta^7 \\ &\quad + 1155\eta^9 - 98\eta^{11}) \\ &\quad - \frac{1}{55440} a_2 (1213\eta - 3279\eta^3 + 3234\eta^5 - 1518\eta^7 \\ &\quad + 385\eta^9 - 35\eta^{11}) \\ &\quad + \frac{1}{55440} a_3 (462\eta - 924\eta^3 + 462\eta^5). \end{aligned} \quad (5.7)$$

The growth rates will be evaluated to $O(\epsilon^2)$ and therefore we only require the expansion for F to $O(\epsilon^2)$. The solution to $O(\epsilon)$ was Blasius' (1910) approximation who used it to predict the separation in an exponential channel. Graphs of the first, second and third approximation to F are given in Fig. 8.1 together with the appropriate Jeffery-Hamel profile. The time-dependent stream function Ψ is dealt with in the next Chapter.

6. STABILITY EQUATIONS

6.1 Disturbance Equations

The steady state equation (5.4) was solved to $O(\epsilon^2)$ by expanding the base flow F in terms of ϵ . A similar approach will be taken here in deriving the disturbance equation. As remarked earlier we look at a small two dimensional disturbance Ψ from the base flow F . The assumption that the disturbances be small implies that the equations be linearised by neglecting quadratic and higher order terms in the disturbances and their derivatives. The total stream function was defined as

$$\hat{\Psi} = \hat{F}(x, y) + \hat{\psi}(x, y, t)$$

where \hat{F} satisfies the steady state equation.

On substituting $\hat{\Psi}$ into equation (5.2) we obtain

$$\begin{aligned} \frac{\partial}{\partial t} \nabla^2(\hat{F} + \hat{\psi}) + \left[\frac{\partial}{\partial y}(\hat{F} + \hat{\psi}) \frac{\partial}{\partial x} \right. \\ \left. - \frac{\partial}{\partial x}(\hat{F} + \hat{\psi}) \frac{\partial}{\partial y} \right] \nabla^2(\hat{F} + \hat{\psi}) \\ = \frac{1}{R} \nabla^4(\hat{F} + \hat{\psi}). \end{aligned} \quad (6.1)$$

When quadratic terms in $\hat{\psi}$ and its derivatives are neglected the equation reduces to

$$\begin{aligned}
 & \frac{\partial}{\partial t} \nabla^2 \hat{\psi} + \left(\hat{F}_y \frac{\partial}{\partial x} - \hat{F}_x \frac{\partial}{\partial y} \right) \nabla^2 \hat{\psi} \\
 & + \left(\hat{\psi}_y \frac{\partial}{\partial x} - \hat{\psi}_x \frac{\partial}{\partial y} \right) \nabla^2 \hat{F} \\
 & = \frac{1}{R} \nabla^4 \hat{\psi}, \tag{6.2}
 \end{aligned}$$

with boundary conditions

$$\hat{\psi} = \hat{\psi}_y = 0 \quad \text{at the walls.}$$

The variables η and Z were defined in section 5.1.

Let

$$\mathcal{H} \equiv \frac{\partial}{\partial Z} - \eta \frac{H'}{H} \frac{\partial}{\partial \eta}.$$

The various terms in equation (6.2) are defined below to $O(\epsilon^2)$. We set the steady state solution $\hat{F}(x,y) = F(\eta,Z)$ and then find

$$\begin{aligned}
 \nabla^2 \hat{F} &= \left[\epsilon^2 \mathcal{H}^2 + \frac{1}{H^2} \frac{\partial^2}{\partial \eta^2} \right] F \\
 &= \epsilon^2 \left[F_{ZZ} + \eta \left(\frac{2H'^2}{H^2} - \frac{H''}{H} \right) F_\eta - 2\eta \frac{H'}{H} F_{\eta Z} \right. \\
 &\quad \left. + \frac{\eta^2 H'^2}{H^2} F_{\eta\eta} \right] + \frac{1}{H^2} F_{\eta\eta} + \dots,
 \end{aligned}$$

$$\frac{\partial}{\partial x} \nabla^2 \hat{F} = \frac{\epsilon}{H^3} \left[-2H' F_{\eta\eta} + H F_{\eta\eta Z} - \eta H' F_{\eta\eta\eta} \right] + \dots,$$

$$\frac{\partial}{\partial y} \nabla^2 \hat{F} = \frac{\epsilon^2}{H} \left[F_{\eta ZZ} + \left(\frac{2H'^2}{H^2} - \frac{H''}{H} \right) F_\eta \right]$$

$$\begin{aligned}
 & + \eta \left(\frac{2H'^2}{H^2} - \frac{H''}{H} \right) E_{\eta\eta} - \frac{2H'}{H} E_{\eta z} - 2\eta \frac{H'}{H} E_{\eta\eta z} \\
 & + 2\eta \frac{H'^2}{H^2} E_{\eta\eta} + \eta^2 \frac{H'^2}{H^2} E_{\eta\eta\eta} \left. \right] + \frac{1}{H^3} E_{\eta\eta\eta} + \dots
 \end{aligned}$$

Equation (6.2) may be written as

$$\begin{aligned}
 & \hat{\Psi}_{xxt} + \hat{\Psi}_{yyt} + \hat{F}_y (\hat{\Psi}_{xx} + \hat{\Psi}_{yy}) \\
 & - \hat{F}_x (\hat{\Psi}_{xxy} + \hat{\Psi}_{yyx}) + \hat{\Psi}_y \frac{\partial}{\partial x} \nabla^2 \hat{F} \\
 & - \hat{\Psi}_x \frac{\partial}{\partial y} \nabla^2 \hat{F} \\
 & = \frac{1}{R} (\hat{\Psi}_{xxxx} + 2\hat{\Psi}_{xxyy} + \hat{\Psi}_{yyyy}). \tag{6.3}
 \end{aligned}$$

This equation together with boundary conditions governs the disturbance $\hat{\Psi}$. The disturbance here is a function of time as well as the coordinates x, y . Hence we would expect the disturbance to grow or decay with time or distance or both along the channel. The type of small disturbance considered in this case is one which is travelling in the direction of flow having a stream function of the form

$$\Psi = \phi(\eta, z) e^{\sigma} + \text{C.C.} \tag{6.4}$$

where C.C. is the complex conjugate,

$$\sigma = i(S(x) - \omega t),$$

and $\frac{dS}{dZ} = q(Z)$.

This may be termed the WKB method, as used by Eagles & Weissman and others. Remember here that $Z = \epsilon x$ is a slow variable. We expand $\phi(\eta, Z)$ in the form

$$\phi = \phi^{(0)} + \epsilon \phi^{(1)} + \epsilon^2 \phi^{(2)} + \dots$$

We now proceed to write equation (6.3) in terms of ϕ and the variables η, Z . We have $\frac{\partial}{\partial x} \rightarrow \epsilon \mathcal{H}$, $\frac{\partial}{\partial y} \rightarrow \frac{1}{H} \frac{\partial}{\partial \eta}$ when applied to $\phi(\eta, Z)$

and so

$$\hat{\Psi}_x = (iq\phi + \epsilon \mathcal{H}\phi) e^\sigma,$$

$$\hat{\Psi}_{xx} = [-q^2\phi + \epsilon i(2q\mathcal{H}\phi + q'\phi) + \epsilon^2 \mathcal{H}^2\phi] e^\sigma,$$

$$\hat{\Psi}_{xxt} = [i\omega q^2\phi + \epsilon \omega(2q\mathcal{H} + q')\phi - \epsilon^2 i\omega \mathcal{H}^2\phi] e^\sigma,$$

$$\begin{aligned} \hat{\Psi}_{xxx} = & [-iq^3\phi - \epsilon(3qq'\phi + 3q^2\mathcal{H}\phi) \\ & + \epsilon^2 i(q''\phi + 3q'\mathcal{H}\phi + 3q\mathcal{H}^2\phi) + \epsilon^3 \mathcal{H}^3\phi] e^\sigma, \end{aligned}$$

$$\begin{aligned} \hat{\Psi}_{xxxx} = & [q^4\phi - \epsilon i(6q^2q' + 4q^3\mathcal{H})\phi \\ & - \epsilon^2(3q'^2 + 4qq'' + 12qq'\mathcal{H} \\ & + 6q^2\mathcal{H}^2)\phi] e^\sigma, \end{aligned}$$

$$\begin{aligned} \hat{\Psi}_{xxy} = & \frac{1}{H} \left[-q^2 \phi_\eta + \epsilon i \left(2q \frac{\partial}{\partial \eta} (\mathcal{H}\phi) + q' \phi_\eta \right) \right. \\ & \left. + \epsilon^2 \frac{\partial}{\partial \eta} (\mathcal{H}^2\phi) \right] e^\sigma, \end{aligned}$$

$$\hat{\Psi}_{xxyy} = \frac{1}{H^2} \left[-q^2 \phi_{\eta\eta} + \epsilon i (2q \frac{\partial^2}{\partial \eta^2} (\mathcal{H}\phi) + q' \phi_{\eta\eta}) + \epsilon^2 \frac{\partial^2}{\partial \eta^2} (\mathcal{H}^2 \phi) \right] e^\sigma,$$

$$\hat{\Psi}_y = \frac{1}{H} \phi_\eta e^\sigma,$$

$$\hat{\Psi}_{yy} = \frac{1}{H^2} \phi_{\eta\eta} e^\sigma,$$

$$\hat{\Psi}_{yyx} = \epsilon \left[\mathcal{H} \left(\frac{1}{H^2} \right) \phi_{\eta\eta} + \frac{1}{H^2} \mathcal{H} \cdot (\phi_{\eta\eta}) \right] e^\sigma + \frac{i}{H^2} q \phi_{\eta\eta} e^\sigma,$$

$$\hat{\Psi}_{yyt} = -\frac{i}{H^2} \omega \phi_{\eta\eta} e^\sigma,$$

$$\hat{\Psi}_{yyy} = \frac{1}{H^3} \phi_{\eta\eta\eta} e^\sigma,$$

$$\hat{\Psi}_{yyyy} = \frac{1}{H^4} \phi_{\eta\eta\eta\eta} e^\sigma. \quad (6.5)$$

On substituting the terms in (6.5) into equation (6.3) we get a sequence of equations as before with the Orr-Sommerfeld equation as the $O(1)$ equation. The important differences from the work of Eagles & Weissman(1975) and Eagles & Smith(1980) are that

(i) R is independent of ϵ in deriving the base flow, so that the first equation is the Orr-Sommerfeld equation with Poiseuille flow as the base flow. Eagles & Weissman took $\epsilon R = \lambda$ in deriving the base flow, yet ignored this relation in deriving the disturbance equation.

(ii) The expansion is taken to $O(\epsilon^2)$, whereas earlier work was only to $O(\epsilon)$ in the disturbance equations,

although terms $\epsilon^2 R^2$, $\epsilon^3 R^3$... etc were implicitly contained in the base (Jeffery-Hamel) flow.

Having obtained $\hat{\Psi}$, \hat{F} and their derivatives in terms of the variables η , Z we may substitute these into (6.3) to obtain the following disturbance equation to $O(\epsilon^2)$.

$$\begin{aligned}
 & \left[i\omega q^2 + \epsilon\omega(2q\mathcal{H} + q') - \epsilon^2 i\omega\mathcal{H}^2 \right] \phi - \frac{i\omega}{H^2} \phi_{\eta\eta} \\
 & + \frac{1}{H} E_\eta \left\{ \left[-iq^3 - \epsilon(3qq' + 3q^2\mathcal{H}) \right. \right. \\
 & + \left. \left. \epsilon^2 i(q'' + 3q'\mathcal{H} + 3q\mathcal{H}^2) \right] \phi \right. \\
 & + \left. \left[\frac{iq}{H^2} + \epsilon \left(\mathcal{H} \left(\frac{1}{H^2} \right) + \frac{1}{H^2} \mathcal{H} \right) \right] \phi_{\eta\eta} \right\} \\
 & - \left(E_z - \eta \frac{H'}{H} E_\eta \right) \left\{ \frac{1}{H} \left[-q^2 \phi_\eta + \epsilon i \left(2q \frac{\partial}{\partial \eta} (\mathcal{H}\phi) \right. \right. \right. \\
 & + \left. \left. q' \phi_\eta \right) + \epsilon^2 \frac{\partial}{\partial \eta} (\mathcal{H}^2 \phi) \right] + \frac{1}{H^3} \phi_{\eta\eta\eta\eta} \right\} \\
 & + \frac{1}{H} \phi_\eta \left[\frac{\epsilon}{H^3} \left(-2H'E_{\eta\eta} + HE_{\eta\eta z} - \eta H'E_{\eta\eta\eta} \right) \right] \\
 & - (iq + \epsilon\mathcal{H}) \phi \left\{ \frac{\epsilon^2}{H} \left[E_{\eta z z} + \left(\frac{2H'^2}{H^2} - \frac{H''}{H} \right) E_\eta \right. \right. \\
 & + \left. \left. \eta \left(\frac{2H'^2}{H^2} - \frac{H''}{H} \right) E_{\eta\eta} - \frac{2H'}{H} E_{\eta z} - 2\eta \frac{H'}{H} E_{\eta\eta z} \right. \right. \\
 & + \left. \left. 2\eta \frac{H'^2}{H^2} E_{\eta\eta} + \eta^2 \frac{H'^2}{H^2} E_{\eta\eta\eta} \right] + \frac{1}{H^3} E_{\eta\eta\eta\eta} \right\} \\
 & = \frac{1}{R} \left\{ \left[q^4 - \epsilon i(6q^2 q' + 4q^3 \mathcal{H}) \right. \right.
 \end{aligned}$$

$$\begin{aligned}
 & - \epsilon^2 (3q'^2 + 4qq'' + 12qq' \mathcal{H} + 6q^2 \mathcal{H}^2) \\
 & + \frac{2}{H^2} \left[-q^2 \phi_{\eta\eta} + \epsilon i \left(2q \frac{\partial^2}{\partial \eta^2} (\mathcal{H} \phi) + q' \phi_{\eta\eta} \right) \right. \\
 & \left. + \epsilon^2 \frac{\partial^2}{\partial \eta^2} (\mathcal{H}^2 \phi) \right] + \frac{1}{H^4} \phi_{\eta\eta\eta\eta} \Bigg] . \quad (6.6)
 \end{aligned}$$

The boundary conditions on ϕ are

6.2 Orr-Sommerfeld Problem

From the equation (6.6) we can obtain the equations for $\phi^{(0)}$, $\phi^{(1)}$ and $\phi^{(2)}$ required in the stability analysis. The functions F and ϕ as indicated earlier are expanded in terms of ϵ .

6.2.1 Equation for $\phi^{(0)}$

By equating terms in ϵ^0 in equation (6.6), we obtain

$$L \phi^{(0)} \equiv 0 \quad (6.7)$$

where

$$L \equiv (D^2 - K^2)^2 - iKR \left[(E_\eta^{(0)} - \beta/K)(D^2 - K^2) \right] \quad (6.8)$$

where $E_\eta^{(0)}$ is a solution of the Orr-Sommerfeld equation at some fixed Z and A_0 is the amplitude function associated with $E_\eta^{(0)}$. The eigenfunction $E_\eta^{(0)}$ is not

$D \equiv \frac{\partial}{\partial \eta}$, arbitrarily, a convenient choice is to let

$$\beta(Z) = \omega H^2(Z), \quad (6.12)$$

and

$$K(Z) = q(Z)H(Z). \quad (6.9)$$

The boundary conditions on $\phi^{(6)}$ are

$$\phi^{(6)} = \phi_{\eta}^{(6)} = 0 \quad \text{at } \eta = 1,$$

$$\phi_{\eta}^{(6)} = \phi_{\eta\eta}^{(6)} = 0 \quad \text{at } \eta = 0. \quad (6.10)$$

These are the boundary conditions for a symmetric disturbance which is known to be the most unstable. The functions β and K as defined in (6.9) are called the local frequency and wave number. They are functions of Z and therefore for fixed Z (6.7) is the local Orr-Sommerfeld equation. For given ω we have an eigenvalue problem to determine K as a function of β and R .

The slow variable Z appears only as a parameter in the equation, so that a solution may be found of the form

$$\phi^{(6)} = A_0(Z)g_0(\eta, Z) \quad (6.11)$$

where g_0 is a solution of (6.7) at some fixed Z and A_0 is an amplitude function associated with g_0 . The eigenfunction g_0 is normalised arbitrarily, a convenient choice is to let

$$\phi(\eta, Z) = 1 \quad \text{at } \eta = 0 \quad (6.12)$$

from which $\phi^{(0)} = 1$ and $g_0(0, Z) = 1$ so that

$$A_0(Z) = 1 \quad \text{at } Z = 1.$$

The eigenfunction g_0 is displayed in Fig. 6.1. for $R = 60$ and $\beta = 1$.

The Orr-Sommerfeld equation was solved numerically starting with a root traced from a known root obtained by Eagles (Private communication). The local frequency was defined as in Eagles & Weissman (1975) by

$$\beta(Z) = \omega e^{2Z}.$$

Using the Jeffery-Hamel profile as the basic flow he calculated the root for equation (6.7) at $Z = 0.92$ for $R = 65$ and $\omega = 0.2$ as $K = (1.6025, -0.02055)$. The root was traced to Poiseuille flow at $\beta = 1.2593$ and β was gradually adjusted to $\beta = 1$. As the parameter μ varies from 0 to 1 the basic flow

$$F = (1 - \mu)J(\eta) + \mu P(\eta)$$

changes from the ... flow, $P(\eta)$. The ... given in Table 6.1.

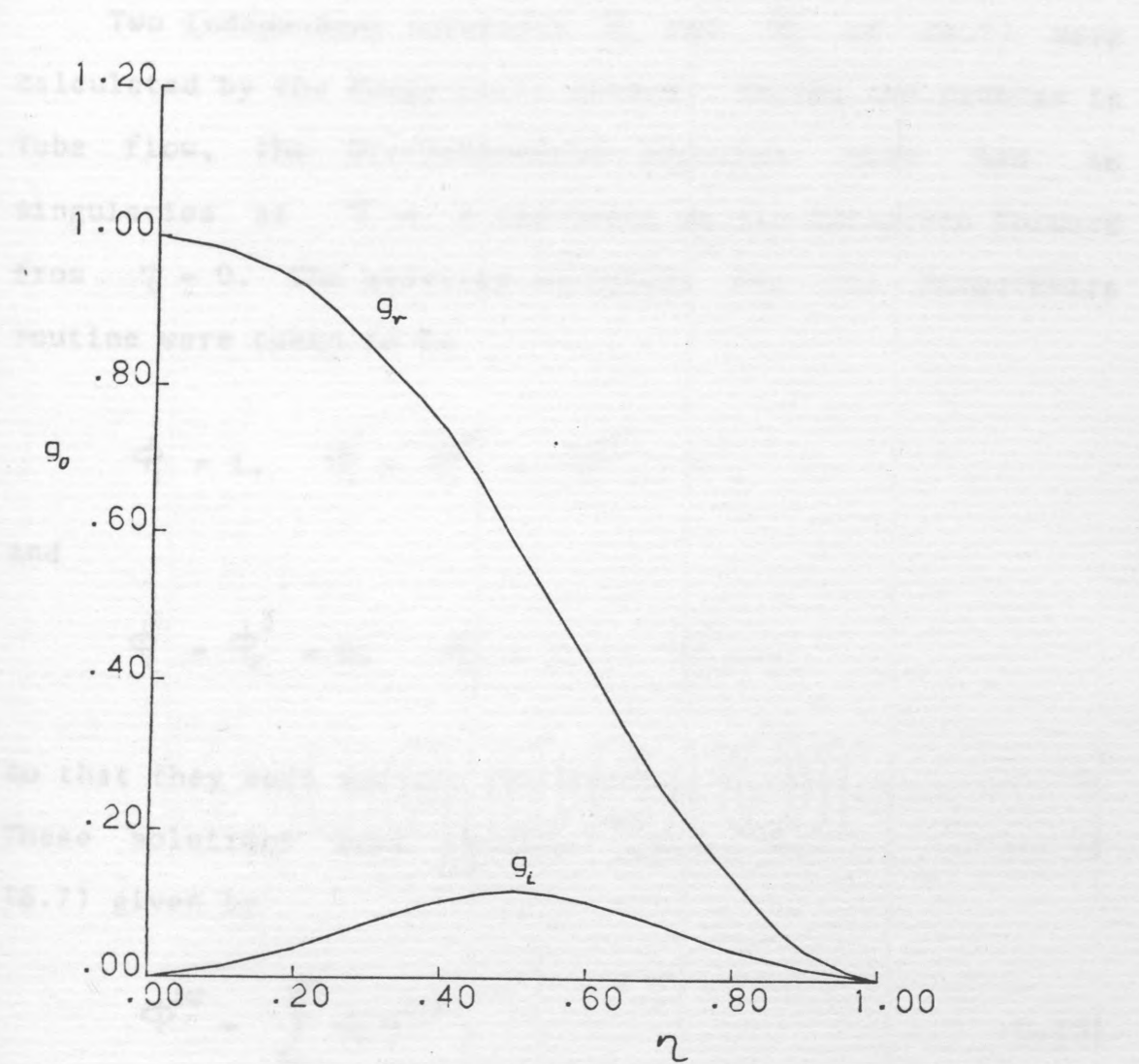


Fig. 6.1. Variation of the eigenfunction g_0 with η at $R = 60$, $\beta = 1$ and $Z = 1$.

changes from the Jeffrey-Hamel($J(\eta)$) flow to Poiseuille flow, $P(\eta)$. The roots at various values of R and β are given in Table 6.1.

Two independent solutions ϕ_1 and ϕ_2 of (6.7) were calculated by the Runge-Kutta method. Unlike the problem in Tube flow, the Orr-Sommerfeld equation here has no singularities at $\eta = 0$ and hence we may integrate forward from $\eta = 0$. The starting solutions for the Runge-Kutta routine were taken to be

$$\phi_1 = 1, \quad \phi_1' = \phi_1'' = \phi_1''' = 0,$$

and

$$\phi_2 = \phi_2' = 0, \quad \phi_2'' = 2, \quad \phi_2''' = 0.$$

so that they both satisfy the boundary conditions at $\eta = 0$. These solutions were checked against series solutions of (6.7) given by

$$\phi^{(0)} = \sum_{r=0}^{\infty} \phi_r \eta^{5+r}. \quad (6.13)$$

Having solved for $\phi^{(0)}$ we can now proceed to find $\phi^{(1)}$ which is determined from the $O(\epsilon)$ equation obtained from (6.6).

By equating the coefficients of λ to zero we get

$$\lambda^2 + K\lambda + JH = 0$$

β	R	K		JH	
1.2593	65.0	1.4888	0.2161	1.6025	-0.0205
	64.0	1.4871	0.2174	1.6025	-0.0180
	63.0	1.4854	0.2186	1.6026	-0.0546
	62.0	1.4836	0.2199	1.6027	-0.0129
	61.0	1.4819	0.2212	1.6028	-0.0102
	60.0	1.4802	0.2226	1.6029	-0.0074
1.0	65.0	1.2745	0.2266		
	60.0	1.2661	0.2343		

Table 6.1. Roots at various values of R for $\beta = 1$ and 1.2593. K is the Poiseuille Flow root and JH is the Jeffery-Hamel velocity profile.

By equating the coefficient of ϵ in (6.6) we obtain

$$L \phi^{(1)} = \frac{dA_0}{dz} (B_1 g_0 + B_2 g_0 \eta \eta) + A_0 (B_1 g_0 z + B_2 g_0 z \eta \eta + B_3) \quad (6.14)$$

where

$$B_1 = H(2\beta K - 3K^2 E_\eta^{(0)} - E_{\eta\eta}^{(0)} + \frac{4iK^3}{R}),$$

$$B_2 = H(E_\eta^{(0)} - \frac{4iK}{R}),$$

$$B_3 = g_0 (C_1 - iK^3 E_\eta^{(1)} - iK E_{\eta\eta}^{(1)}) + g_0 \eta (C_2 + g_0 \eta (C_3 + iK E_\eta^{(1)}) + g_0 \eta \eta (C_4)),$$

$$C_1 = \beta H^2 q' - 3KH^2 q' E_\eta^{(0)} + \frac{6iK^2 H^2 q'}{R},$$

$$C_2 = -2\beta K \eta H' + 2K^2 \eta H' E_\eta^{(0)} - 2H' E_\eta^{(0)} + K^2 H E_z^{(0)} + H E_{\eta z}^{(0)} - \frac{4iK^3 \eta H'}{R},$$

$$C_3 = -2H' E_\eta^{(0)} + \frac{8iKH'}{R} - \frac{2iH^2 q'}{R},$$

$$C_4 = -H E_z^{(0)} + \frac{4iK \eta H'}{R} \quad (6.15)$$

The boundary conditions on $\phi^{(1)}$ are

$$\begin{aligned} \phi_{\eta}^{(1)} = \phi_{\eta\eta}^{(1)} = 0 \quad \text{at } \eta = 0, \\ \phi^{(1)} = \phi_{\eta}^{(1)} = 0 \quad \text{at } \eta = 1. \end{aligned} \quad (6.16)$$

The functions $B_1, B_2, B_3, C_1, C_2, C_3$ and C_4 are the functions determined by Eagles & Smith(1980). They considered a channel whose walls are given by $H(Z) = 1 + (1/2)\tanh Z$. In the present study we confine ourselves to the case $H(Z) = Z$, the straight walled channel.

The equation for $\phi^{(1)}$ is inhomogeneous with an unknown amplitude function. It has a solution if and only if a certain solvability condition is satisfied. This is supplied by the adjoint function to $\phi^{(0)}$. Let \bar{L} be the adjoint operator and $\bar{\gamma}$ the adjoint to $\phi^{(0)}$. The governing equation and boundary conditions are

$$\bar{L}\bar{\gamma} = 0, \quad (6.17)$$

$$D\bar{\gamma} = D^3\bar{\gamma} = 0 \quad \text{at } \eta = 0,$$

$$\bar{\gamma} = D\bar{\gamma} = 0 \quad \text{at } \eta = 1$$

where

$$\bar{L} \equiv R^{-1} (D^2 - K^2)^2 - iK \left[(E_{\eta}^{(0)} - \beta/K)(D^2 - K^2) \right.$$

$$\left. + 2E_{\eta\eta}^{(0)} D \right],$$

$$D \equiv \frac{\partial}{\partial \eta}.$$

Provided that $\phi^{(1)}$ satisfies the boundary conditions, the required orthogonality condition is that

$$\int_0^1 \gamma L \phi^{(1)} d\eta = 0 . \quad (6.18)$$

From (6.14) we obtain the ordinary differential equation

$$H_1 A_0 + H_2 \frac{dA_0}{dZ} = 0 \quad (6.19)$$

where

$$H_1(Z) = \int_0^1 \gamma (B_1 g_{0Z} + B_2 g_{0Z} \eta \eta + B_3) d\eta ,$$

$$H_2(Z) = \int_0^1 \gamma (B_1 g_0 + B_2 g_0 \eta \eta) d\eta .$$

It follows from the normalisation (6.12) that

$$\frac{dA_0}{dZ} = - \frac{H_1}{H_2} \quad \text{at } Z = 1 .$$

The required solution $\phi^{(1)}$ is given by

$$\phi^{(1)} = g_1(\eta, Z) + A_1(Z) g_0(\eta, Z) \quad (6.20)$$

where g_1 is a particular integral and A_1 is the amplitude function associated with g_1 . The particular integral g_1 may be written in the form

$$g_1 = A \phi_1(\eta) + B \phi_2(\eta) + \phi_3(\eta)$$

where ϕ_1 and ϕ_2 are the solutions of the homogeneous

equation (6.7), A and B are arbitrary constants and ϕ_3 is a solution of (6.14) that satisfies boundary conditions

$$\phi_3' = \phi_3''' = 0 \quad \text{at } \eta = 0,$$

$$\phi_3 = 1 \quad \text{at } \eta = 0$$

The boundary conditions (6.16) require that

$$A \phi_1(1) + B \phi_2(1) + \phi_3(1) = 0,$$

$$A \phi_1'(1) + B \phi_2'(1) + \phi_3'(1) = 0,$$

which represent a system with a unique solution for A and B provided

$$\phi_1(1) \phi_2'(1) - \phi_2(1) \phi_1'(1) \neq 0.$$

However, this quantity is zero here by the eigenvalue relation. The equations are not independent and hence produce an infinite number of solutions provided (6.19) is satisfied. A particular solution was obtained by setting one of the arbitrary constants to zero, say $B = 0$, so that

$$A = - \frac{\phi_3(1)}{\phi_1(1)} = - \frac{\phi_3'(1)}{\phi_1'(1)}.$$

The normalisation (6.12) yields

$$\phi^{(1)}(0,1) = 0$$

so that

$$\begin{aligned} g_1(0, Z) &= -A_1(Z)g_0(0, Z) \\ &= -A_1(Z) \quad \text{at } Z = 1. \end{aligned}$$

The amplitude function $A_1(Z)$ may be chosen arbitrarily without affecting the growth rate, for details refer to section 7.4. Similarly, different choices of particular integrals will lead to different amplitude functions A_1 but will not affect the growth rate. Without loss of generality we may choose $A_1 = 0$ at $Z = 1$ so that equation (6.20) reduces to

$$\phi^{(1)} = g_1 \quad \text{at } Z = 1$$

and hence

$$g_1 = A\phi_1 + \phi_3.$$

where

The solution of the $O(\epsilon^2)$ equation for $\phi^{(2)}$ will be obtained in a similar manner and this is done in the next section.

6.23 Equation for $\phi^{(2)}$

By equating coefficients of ϵ^2 in (6.6) we obtain

$$\begin{aligned} L\phi^{(2)} &= \frac{dA_1}{dZ}(B_1g_0 + B_2g_0\eta\eta) \\ &+ A_1(B_1g_0Z + B_2g_0Z\eta\eta + B_3) \end{aligned}$$

$$\begin{aligned}
& + (D_1 A_0 + D_2 A'_0 + D_3 A''_0) g_0 \\
& + (D_4 A_0 + D_5 A'_0) g_0 \gamma \\
& + (D_6 A_0 + D_7 A'_0 - \frac{2}{R} H^2 A''_0) g_0 \gamma \gamma \\
& + (D_8 A_0 + \frac{2}{R} H H' \gamma A'_0) g_0 \gamma \gamma \gamma \\
& + (D_2 A_0 + 2 D_3 A'_0) g_0 z \\
& + D_3 A_0 g_0 z z + D_5 A_0 g_0 z \gamma + (D_7 A_0 - \frac{4}{R} H^2 A'_0) g_0 z \gamma \gamma \\
& + (-\frac{2}{R} H^2 A_0) g_0 z z \gamma \gamma + \frac{2}{R} H H' \gamma A_0 g_0 z \gamma \gamma \gamma \\
& + (C_1 - i K^3 F_\gamma^{(1)} - i K F_{\gamma \gamma}^{(1)}) g_1 + C_2 g_1 \gamma \\
& + (C_3 + i K F_\gamma^{(1)}) g_1 \gamma \gamma + C_4 g_1 \gamma \gamma \gamma + B_1 g_1 z \\
& + B_2 g_1 z \gamma \gamma , \tag{6.21}
\end{aligned}$$

where

$$\begin{aligned}
D_1 = & i H^3 q' F_\gamma^{(0)} - i K H'^2 (2 \eta F_\gamma^{(0)} + \eta^2 F_{\gamma \gamma}^{(0)}) \\
& - i K (2 H'^2 - H H') (F_\gamma^{(0)} + \eta F_{\gamma \gamma}^{(0)}) - 3 K H^2 q' F_\gamma^{(1)} \\
& + K^2 H F_\gamma^{(1)} - i K^3 F_\gamma^{(2)} - i K F_{\gamma \gamma}^{(2)} \\
& + \frac{H^3}{R} (3 H q'^2 + 4 K q'') ,
\end{aligned}$$

$$D_2 = - 3 K^2 H F_\gamma^{(1)} - H F_{\gamma \gamma}^{(1)} + 3 i H^3 q' F_\gamma^{(0)} + \frac{12}{R} K H^3 q' ,$$

$$D_3 = H^2 (- i \beta + 3 i K F_\gamma^{(0)} + \frac{6 K^2}{R}) ,$$

$$D_4 = i\gamma H^2 H' q' F_\eta^{(0)} - 2H' E_\eta^{(1)} + H E_{\eta\eta}^{(1)} + 2\gamma H' K^2 F_\eta^{(1)} \\ - \frac{12\gamma K H^2 H' q'}{R} - D_3 \gamma \left(\frac{H H'' - H'}{H^2} \right) - 2i\gamma H'^2 K F_\eta^{(0)},$$

$$D_5 = -D_3 \gamma \frac{H'}{H} + 2iK H H' \gamma F_\eta^{(0)},$$

$$D_6 = iK F_\eta^{(2)} - 2H' E_\eta^{(1)} - 2iK \gamma H'^2 F_\eta^{(0)} + \frac{4}{R} (H H'' - H'),$$

$$D_7 = H (E_\eta^{(1)} + \frac{4H'}{R}),$$

$$D_8 = \frac{2\gamma}{R} (H H'' - H') - H E_\eta^{(1)}. \quad (6.22)$$

The boundary conditions on $\phi^{(2)}$ are

$$\phi_\eta^{(2)} = \phi_{\eta\eta\eta}^{(2)} = 0 \quad \text{at } \eta = 0,$$

$$\phi^{(2)} = \phi_\eta^{(2)} = 0 \quad \text{at } \eta = 1.$$

As a check on the algebra note that the coefficients of A_0' and A_1' are equal and so are the coefficients of A_0 and A_1 . In B_3 the coefficients of g_0 , $g_{0\eta}$ and $g_{0\eta\eta}$ are equal to the coefficients of g_1 , $g_{1\eta}$ and $g_{1\eta\eta}$.

To obtain the equation for A_1 , we use the orthogonality condition (6.18) and obtain

$$H_2 \frac{dA_1}{dz} + H_3 A_1 + H_4 = 0 \quad (6.23)$$

where

$$H_3(z) = \int_0^1 \gamma (B_1 g_{0z} + B_2 g_{0z\eta\eta} + B_3) d\eta,$$

$$\begin{aligned}
H_4(Z) = & \int_0^1 \gamma \left[(D_1 A_0 + D_2 A_0' + D_3 A_0'') g_0 \right. \\
& + (D_4 A_0 + D_5 A_0') g_0 \eta \\
& + (D_6 A_0 + D_7 A_0' - \frac{2H^2 A_0''}{R}) g_0 \eta \eta \\
& + (D_8 A_0 + \frac{2\eta H H' A_0'}{R}) g_0 \eta \eta \eta \left. \right] d\eta \\
& + \int_0^1 \gamma \left[(D_2 A_0 + 2D_3 A_0') g_{0Z} + D_3 A_0 g_{0ZZ} \right. \\
& + D_5 A_0 g_{0Z} \eta + (D_7 A_0 - \frac{4H^2 A_0'}{R}) g_{0Z} \eta \eta \\
& - \frac{2H^2 A_0}{R} g_{0ZZ} \eta \eta + \frac{2HH' \eta A_0}{R} g_{0Z} \eta \eta \eta \left. \right] d\eta \\
& + \int_0^1 \gamma \left[B_4 + B_1 g_{1Z} + B_2 g_{1Z} \eta \eta \right] d\eta ,
\end{aligned}$$

where

$$\begin{aligned}
B_4 = & (C_1 - iK^3 F_2^{(1)} - iK F_\eta \eta^{(1)}) g_1 + C_2 g_1 \eta \\
& + (C_3 + iK F_\eta \eta^{(1)}) g_1 \eta \eta + C_4 g_1 \eta \eta \eta .
\end{aligned}$$

The amplitude equation (6.23) is given by

$$\frac{dA_1}{dZ} = - \frac{H_4}{H_2}$$

at $Z = 1$ from the normalisation.

The information so far obtained is adequate for calculating corrections to the Poiseuille flow growth rates to $O(\epsilon^2)$. This is dealt with in the next chapter.

7. GROWTH RATES

Eagles & Weissman(1975) defined three measures of growth rate, namely the growth rates based on the stream function, the mean kinetic energy and the relative mean kinetic energy. Similar growth rates will be defined here to $O(\epsilon^2)$. It will be shown that for the straight-walled channel, $H(Z) = Z$ the growth rate is a function of $f(\beta)/H$. We will also show that different choices of particular integrals will lead to different amplitude functions, but will not affect the growth rate. These results are very useful in making numerical checks to the growth rate.

7.1 Growth Rates Based on the Stream Function

The disturbance equation was defined by

$$\Psi = \phi(\eta, Z)e^{i(S(x) - \omega t)} + \text{C.C.} \quad (7.1)$$

The physical amplitude in terms of the stream function is given by

$$\begin{aligned} \text{amp } \Psi &= 2|\phi e^{i(S - \omega t)}| \\ &= 2|\phi| e^{-S_i} \end{aligned}$$

where $S = S_r + iS_i$.

The growth rate based on Ψ in the x space is defined as

$$G_x(\Psi) = \frac{1}{\text{amp } \Psi} \frac{\partial (\text{amp } \Psi)}{\partial x}$$

It is easy to show that

$$G_x(\Psi) = -\frac{K_i}{H} + \epsilon \frac{|\phi|}{|\phi|} z$$

which to $O(\epsilon^2)$ is equivalent to

$$G_x(\Psi) = -\frac{K_i}{H} + \text{REAL} \left[\epsilon \frac{\phi^{(0)}}{\phi^{(0)}} + \epsilon^2 \left(\frac{\phi^{(1)}}{\phi^{(0)}} - \frac{\phi^{(0)}}{\phi^{(0)}} \frac{\phi^{(1)}}{\phi^{(0)}} \right) \right]$$

where $K = K_r + iK_i$ and REAL indicates the real part of the complex number. Using equations (6.11) and (6.20) this may be rearranged as follows:

$$G_x(\Psi) = -\frac{K_i}{H} + \epsilon \text{REAL} \left[\frac{A'_0 g_{0z} + A_0 g_{0z}}{A_0 g_0} \right] + \epsilon^2 \text{REAL} \left[\frac{A'_1}{A_0} + \frac{g_{1z}}{A_0 g_0} - g_1 \left(\frac{A'_0}{A_0 A_0 g_0} + \frac{g_{0z}}{A_0 g_0 g_0} \right) - \frac{A_1 A'_0}{A_0 A_0} \right] \quad (7.2)$$

In general we may write the growth rate as

$$G_x(\Psi) = G_0(R) + \epsilon G_1(R) + \epsilon^2 G_2(R) + O(\epsilon^3) \quad (7.3)$$

where $G_0(R)$ is the quasi-parallel growth rate and higher order terms are the corrections to the growth rate.

Equation (7.2) was used in computing the growth rate $G_x(\Psi)$ used in obtaining the Figures and Tables given in Chapter 8. This was computed for the straight-walled channel $H(Z) = Z$ at $Z = 1$ and with $\beta = 1$. Theoretical results to be shown in section 7.3 show that these results should be the same and this was checked numerically.

The kinetic energy density E will be defined as in Eagles & Smith(1980) by

$$\begin{aligned}
 E(Z) &= \frac{\rho}{2} \int_0^{H(z)} \int_0^{2\pi/\omega} (u^2 + v^2) dt dy, \\
 &= \frac{\rho}{2} \int_0^l (u^2 + v^2) H d\eta \tag{7.4}
 \end{aligned}$$

where ρ is the fluid density, u and v are the velocity components of the disturbance. For the disturbance function (7.1), let

$$\sigma = i(S(x) - \omega t).$$

The velocity components of the disturbance will be given by

$$\begin{aligned}
 u &= \hat{\Psi}_y \\
 &= \frac{1}{H} \frac{\partial}{\partial \eta} (\phi e^\sigma) + \text{C.C.} \\
 v &= -\hat{\Psi}_x \\
 &= - \left[iq\phi + \epsilon \left(\phi_z - \gamma \frac{H'}{H} \phi_\eta \right) \right] e^\sigma + \text{C.C.}
 \end{aligned}$$

Note that the velocity components of the disturbance are real, and so are their squares, u^2 and v^2 .

Squaring each component and summing up, we obtain after simplifying

$$\begin{aligned}
 u^2 + v^2 = e^{-2S_i} & \left[\frac{1}{H^2} |\phi_\eta^{(0)}|^2 + |q \phi^{(0)}|^2 \right. \\
 & + \epsilon \left\{ \frac{1}{H^2} (\bar{\phi}_\eta^{(0)} \phi_\eta^{(1)} + \phi_\eta^{(0)} \bar{\phi}_\eta^{(1)}) \right. \\
 & + |q|^2 (\phi^{(0)} \bar{\phi}^{(1)} + \bar{\phi}^{(0)} \phi^{(1)}) \\
 & + i (q \phi^{(0)} \bar{\phi}_z^{(0)} - \bar{q} \bar{\phi}^{(0)} \phi_z^{(0)}) \\
 & \left. \left. + i \eta \frac{H'}{H} (\bar{q} \bar{\phi}^{(0)} \phi_\eta^{(0)} - q \phi^{(0)} \bar{\phi}_\eta^{(0)}) \right\} \right] + o(\epsilon^2).
 \end{aligned}$$

Using equations (6.11) and (6.20) this may be written as follows to $O(\epsilon)$

$$\begin{aligned}
 u^2 + v^2 = e^{-2S_i} & \left[\frac{|A_0|^2}{H^2} (|g_0 \eta|^2 + |K g_0|^2) \right. \\
 & + \frac{\epsilon}{H} \left\{ (\bar{A}_0 A_1 + A_0 \bar{A}_1) (|g_0 \eta|^2 + |K g_0|^2) \right. \\
 & + A_0 (g_0 \eta \bar{g}_1 \eta + |K|^2 g_0 \bar{g}_1) + \bar{A}_0 (\bar{g}_0 \eta g_1 \eta + |K|^2 \bar{g}_0 g_1) \\
 & + i |g_0|^2 (K A_0 \bar{A}_0 z - \bar{K} \bar{A}_0 A_0 z) + i |A_0|^2 (K \bar{g}_0 z g_0 - \bar{K} \bar{g}_0 g_0 z) \\
 & \left. \left. + i \eta H' |A_0|^2 (\bar{K} \bar{g}_0 g_0 \eta - K g_0 \bar{g}_0 \eta) \right\} \right].
 \end{aligned}$$

The energy equation (7.4) can be conveniently written as

$$E = \frac{\rho}{2} \frac{M e^{-2S_i}}{H} \tag{7.5}$$

where λ_1 is the imaginary part of the complex eigenvalue λ and N_1 is the partial derivative of N with respect to λ_1 .

$$M = M_1 + \epsilon M_2$$

and the functions M_1 and M_2 are given by

$$\begin{aligned}
 M_1 &= |A_0|^2 \int_0^1 (|g_{0\eta}|^2 + |kg_0|^2) d\eta, \\
 M_2 &= \int_0^1 \left[(\bar{A}_0 A_1 + A_0 \bar{A}_1) (|g_{0\eta}|^2 + |kg_0|^2) \right. \\
 &\quad + A_0 (g_{0\eta} \bar{g}_{1\eta} + |k|^2 g_0 \bar{g}_1) + \bar{A}_0 (\bar{g}_{0\eta} g_{1\eta} + |k|^2 \bar{g}_0 g_1) \\
 &\quad + i |g_0|^2 (k A_0 \bar{A}_{0z} - \bar{k} \bar{A}_0 A_{0z}) \\
 &\quad + i |A_0|^2 (k \bar{g}_{0z} g_0 - \bar{k} \bar{g}_0 g_{0z}) \\
 &\quad \left. + i \eta H' |A_0|^2 (\bar{k} \bar{g}_0 g_{0\eta} - k g_0 \bar{g}_{0\eta}) \right] d\eta. \tag{7.6}
 \end{aligned}$$

7.21 Growth Rate Based on Kinetic Energy Density

The growth rates based on kinetic energy density is defined as in Eagles & Weissman(1975) by

$$G_x(E) = \frac{1}{E} \frac{\partial}{\partial x} \left(\frac{\rho M e^{-2S_i}}{2H} \right).$$

Substituting the value of M given in (7.6) and using definitions (6.4) and (6.9) we have

$$G_x(E) = -\frac{2K_i}{H} + \epsilon \left(-\frac{H'}{H} + \frac{M_z}{M} \right) \tag{7.7}$$

where K_i is the imaginary part of the complex eigenvalue K and M_z is the partial derivative of M with respect to Z .

Equation (7.7) can be written in terms of M_1 , M_2 and their derivatives with respect to Z , so that

$$G_x(E) = -\frac{2K_i}{H} - \epsilon \frac{H'}{H} + \epsilon \left(\frac{M_{1Z}}{M_1} + \frac{\epsilon M_{2Z}}{\epsilon M_2} \right)$$

$$= -\frac{2K_i}{H} + \epsilon \left(-\frac{H'}{H} + \frac{M_{1Z}}{M_1} \right) + \epsilon^2 \left(\frac{M_{2Z}}{M_1} - \frac{M_2 M_{1Z}}{M_1 M_1} \right) \quad (7.8)$$

where

$$M_{1Z} = \int_0^1 \left[2|A_0| |A_0|_Z (|g_{0\eta}|^2 + |kg_0|^2) + |A_0|^2 (2|g_{0\eta}| |g_{0\eta}|_Z + 2|kg_0| |kg_0|_Z) \right] d\eta.$$

The partial derivative M_{2Z} is quite long. This is not surprising considering that M_2 contains a number of products which are functions of Z . Nevertheless, it will be given here for completeness. Hence, we have for M_{2Z}

$$M_{2Z} = \int_0^1 \left[\left\{ (\bar{A}_0)_Z A_1 + \bar{A}_0 A_{1Z} + A_0 Z \bar{A}_1 + A_0 (\bar{A}_1)_Z \right\} (|g_{0\eta}|^2 + |kg_0|^2) + (\bar{A}_0 A_1 + A_0 \bar{A}_1) (2|g_{0\eta}| |g_{0\eta}|_Z + 2|kg_0| |kg_0|_Z) + A_0 Z (g_{0\eta} \bar{g}_{1\eta} + |k|^2 g_0 \bar{g}_1) + A_0 \left\{ g_{0Z\eta} \bar{g}_{1\eta} + g_{0\eta} (\bar{g}_{1\eta})_Z + 2|k| |k|_Z g_0 \bar{g}_1 + |k|^2 g_{0Z} \bar{g}_1 + |k|^2 g_0 (\bar{g}_1)_Z \right\} \right] d\eta$$

The last term is

$$+ (\bar{A}_0)_z (\bar{g}_0 \eta g_1 + |K|^2 \bar{g}_0 g_1)$$

is zero in this case since we are considering the straight-...
 distinction between the derivative of the complex conjugate,
 e.g. $(\bar{K})_z$ and the complex...

$$+ \bar{A}_0 \left\{ (\bar{g}_0 \eta)_z g_1 \eta + \bar{g}_0 \eta g_{1z} \eta + 2|K| |K|_z \bar{g}_0 g_1 + |K|^2 (\bar{g}_0)_z g_1 + |K|^2 \bar{g}_0 g_{1z} \right\}$$

This was merely convenient for the purpose of this analysis,
 the derivative...

$$+ i \left\{ 2 |g_0| |g_0|_z (K A_0 \bar{A}_0)_z - \bar{K} \bar{A}_0 A_0 \right\}$$

$$7.27 \quad \text{Growth} + |g_0|^2 (K_z A_0 \bar{A}_0 + K A_{0z} \bar{A}_0 + K A_0 (\bar{A}_0)_z)$$

The growth rate $(\bar{K})_z \bar{A}_0 A_0 - \bar{K} (\bar{A}_0)_z A_0 - \bar{K} \bar{A}_0 A_{0z}$ is defined in terms of \bar{K} in equation (7.5) and E_0 , the kinetic energy density of...

$$+ 2|A_0| |A_0|_z (K g_0 \bar{g}_0)_z - \bar{K} \bar{g}_0 g_{0z} + |A_0|^2 (K_z g_0 \bar{g}_0 + K g_{0z} \bar{g}_0 + K g_0 (\bar{g}_0)_z)$$

For the basic flow we have

$$- (\bar{K})_z \bar{g}_0 g_{0z} - \bar{K} (\bar{g}_0)_z g_{0z} - \bar{K} \bar{g}_0 g_{0zz}$$

and

$$+ i \eta H' \left\{ 2|A_0| |A_0|_z (\bar{K} \bar{g}_0 g_0 \eta - K g_0 \bar{g}_0 \eta) + |A_0|^2 ((\bar{K})_z \bar{g}_0 g_0 \eta + \bar{K} (\bar{g}_0)_z g_0 \eta + \bar{K} \bar{g}_0 g_{0z} \eta - K_z g_0 \bar{g}_0 \eta - K g_{0z} \bar{g}_0 \eta - K g_0 (\bar{g}_0)_z \eta) \right\}$$

The sum of the squares of the velocity components gives

$$+ i \eta H'' |A_0|^2 (\bar{K} \bar{g}_0 g_0 \eta - K g_0 \bar{g}_0 \eta) \Big] d\eta.$$

The last term involves the second derivative of $H(Z)$, which

is zero in this case since we are considering the straight-walled channel $H(Z) = Z$. Note that we have made a distinction between the derivative of the complex conjugate, e.g. , $(\bar{K})_Z$ and the complex conjugate of the derivative \bar{K}_Z . This was merely convenient for the purpose of this analysis, the derivatives are equal.

7.22 Growth Rate Based on Relative Kinetic Energy

The growth rate based on relative kinetic energy \hat{E} is defined in terms of E in equation (7.5) and E_0 , the kinetic energy density of the basic flow so that

$$\hat{E} = \frac{E}{E_0} \quad (7.9)$$

For the basic flow we have

$$\Psi = F(\eta, Z)$$

and

$$u = \frac{1}{H} F_\eta \quad ,$$

$$v = -\epsilon (F_{ZZ} - \eta \frac{H'}{H} F_\eta) \quad .$$

The sum of the squares of the velocity components gives

$$u^2 + v^2 = \frac{1}{H^2} \left[(F_\eta^{(0)})^2 + 2\epsilon F_\eta^{(0)} F_\eta^{(1)} \right] + O(\epsilon^2).$$

From equation (7.4) we obtain for E_0

$$E_0 = \frac{\rho}{2} \int_0^1 (u^2 + v^2) H d\eta$$

$$= \frac{\rho}{2} \int_0^l \frac{1}{H} \left[(E_\eta^{(0)})^2 + 2\epsilon E_\eta^{(0)} E_\eta^{(1)} \right] d\eta .$$

This will be conveniently written as

$$E_0 = \frac{\rho N}{2H} \tag{7.10}$$

where

$$N = N_1 + \epsilon N_2 ,$$

$$N_1 = \int_0^l (E_\eta^{(0)})^2 d\eta ,$$

$$N_2 = 2 \int_0^l E_\eta^{(0)} E_\eta^{(1)} d\eta .$$

From definitions (7.5) and (7.10) we have

$$\hat{E} = \frac{E}{E_0}$$

$$= e^{-2S_i} \frac{M}{N}$$

which in terms of M_1 , M_2 , N_1 and N_2 becomes

$$\hat{E} = e^{-2S_i} \left[\frac{M_1}{N_1} - \epsilon \left(\frac{M_2}{N_1} - \frac{M_1 N_2}{N_1 N_1} \right) \right] \tag{7.11}$$

The growth rate based on relative energy may now be defined.

It is convenient to let

$$P = P_1 + \epsilon P_2$$

where

$$P_1 = \frac{M_1}{N_1} ,$$

$$P_2 = \frac{M_2}{N_1} - \frac{M_1 N_2}{N_1 N_1}$$

so that (7.11) becomes

$$\hat{E} = e^{-2S_i P} .$$

Therefore

$$G_x(\hat{E}) = \frac{1}{\hat{E}} \frac{\partial}{\partial x} (e^{-2S_i P})$$

$$= - \frac{2K_i}{H} + \frac{P_Z}{P}$$

where P_Z is the partial derivative of P with respect to Z . Writing this in terms of M and N , and grouping similar terms together we have after simplifying

$$G_x(\hat{E}) = - \frac{2K_i}{H} + \epsilon \frac{M_{1Z}}{M_1} + \epsilon^2 \left(\frac{M_{2Z}}{M_1} - \frac{M_{1Z} M_2}{M_1 M_1} - \frac{N_{2Z}}{N_1} \right) \quad (7.12)$$

Equation (7.12) was used in computing the relative energy growth rates $G_x(\hat{E})$ presented in Chapter 8. In the next section we look at the growth rate as a function of $f(\beta)/H$, where $f(\beta)$ means function of β .

7.3 Growth Rate as a Function of $f(\beta)/H$

At a given point Z for fixed R the growth rate is function of β and K only. However, K can be expressed as a function of β and so can all other quantities such as eigenfunctions and amplitude functions, that appear in the growth rate equation. By expressing the growth rate in the

form $f(\beta)/H$ it was possible to make numerical checks on the computed growth rate at different values of Z . This form is only applicable when $H(Z) = Z$ i.e. for the straight-walled channel.

In order to show that the growth rate is a function of $f(\beta)/H$, we need to calculate the derivatives of the various terms that are contained in the growth rate equation. This will be done here for the growth rate based on the stream function. The results derived here apply to all growth rates. The symbols $f(\beta)$, $f(\beta, \eta)$, $A_0(H_1, H_2)$, $H_2(B_1, B_2, g_0)$ etc are functional notations standing for functions of β or of β and η as the case may be. The resulting equations such as

$$A_0 = A_0(H_1, H_2),$$

or
$$C_3 = f(\beta, \eta) + H^2 q' f(\beta, \eta)$$

are to be understood in this context. They are only meant to show that a given variable e.g. C_3 is a function of the given quantities β , η in the forms shown.

The local frequency β was defined as

$$\beta(Z) = \omega H^2(Z) .$$

The first and the second derivatives of β are given by

$$\begin{aligned} \frac{d\beta}{dZ} &= 2\omega H \\ &= \frac{2}{H} \beta \\ &= \frac{1}{H} f(\beta) , \text{ for } H = Z , \end{aligned}$$

$$\frac{d^2\beta}{dZ^2} = \frac{1}{H^2} f(\beta) .$$

The derivatives of the local eigenvalue can also be expressed as functions of β as follows.

$$\frac{dK}{dZ} = \frac{dKd\beta}{d\beta dZ}$$

$$= \frac{2\beta dK}{H d\beta}$$

$$= \frac{1}{H} f(\beta) ,$$

$$\frac{d^2K}{dZ^2} = \frac{1}{H^2} f(\beta)$$

$$\frac{dq}{dZ} = \frac{1}{H^2} f(\beta) . \quad (7.13)$$

The eigenfunctions and their derivatives are functions of β as well as η so that we can express them as

$$g_0 = G(\beta, K, \eta) ,$$

$$g_{0Z} = \frac{\partial G dK}{\partial K dZ} + \frac{\partial G d\beta}{\partial \beta dZ}$$

$$= G_k \frac{1}{H} f(\beta) + G_\beta \frac{1}{H} f(\beta)$$

$$= \frac{1}{H} f(\beta, \eta) ,$$

and

$$\begin{aligned} g_{0ZZ} &= \frac{\partial G_k}{\partial Z} \frac{dK}{dZ} + G_k \frac{d^2 K}{dZ^2} + \frac{\partial G_\beta}{\partial Z} \frac{d\beta}{dZ} + G_\beta \frac{d^2 \beta}{dZ^2} \\ &= G_{kk} \frac{1}{H^2} 4\beta^2 \left(\frac{dK}{d\beta} \right)^2 + G_k \left[\frac{4\beta}{H^2} \frac{dK}{d\beta} - \frac{2\beta}{H^2} \frac{dK}{d\beta} + \frac{4\beta^2}{H^2} \frac{d^2 K}{d\beta^2} \right] \\ &\quad + G_{\beta\beta} \left(\frac{4\beta^2}{H^2} \right) + G_\beta \left(\frac{4\beta}{H^2} - \frac{2\beta}{H^2} \right) \end{aligned}$$

$$= \frac{1}{H^2} f(\beta, \eta) .$$

The functional relation for H_1 equals that of H_2 . These are
The functional relations for $g_{0\eta}$, $g_{0\eta\eta}$, g_1 , $g_{1\eta}$, $g_{1\eta\eta}$ and
 η are similar to that of g_0 , while those of $g_{0Z\eta}$, $g_{0Z\eta\eta}$
and g_{1Z} are similar to that of g_{0Z} .

We begin by analysing each function to show how it
The amplitude functions A_0 and A_1 are a little more
involved in that they contain most of the variables in the
stability equations. It will be easier to follow the various
variables when the amplitude functions are expressed
functionally as follows :

$$A_0 = A_0(H_1, H_2)$$

$$A_1 = A_1(H_2, H_3, H_4)$$

where

$$H_1 = H_1(B_1, B_2, B_3, g_{0Z}, g_{0Z\eta\eta}, \bar{\nu}, \eta)$$

$$H_2 = H_2(B_1, B_2, g_0, g_{0\eta\eta}, \bar{\nu}, \eta)$$

$$H_4 = H_4(B_4, D_i, A_0, A'_0, A''_0, g_0, g_{0\eta}, g_{0\eta\eta}, g_{0\eta\eta\eta}, g_{0Z},$$

$$g_{0Z\eta}, g_{0Z\eta\eta}, g_{0Z\eta\eta\eta}, g_{0ZZ}, g_{0ZZ\eta\eta}, g_1, g_{1Z},$$

$$g_{1Z\eta\eta}, \bar{\nu}, \eta, H) ,$$

and $i = 1, 2, 3, 4, 5, 6, 7, 8.$

The functional relation for H_3 equals that of H_1 . These are the coefficients of A_1 and A_0 respectively, which were shown to be equal.

We begin by analysing each function to show how it depends on $f(\beta)/H$. The functions $B_1, B_2, B_3, C_1, C_2, C_3$ and C_4 are defined in section 6.22, page 115 and the following may be deduced

$$B_1 = Hf(\beta, \eta) ,$$

$$B_2 = Hf(\beta, \eta) ,$$

$$B_3 = C_1 f(\beta, \eta) + f(\beta, \eta) + C_2 f(\beta, \eta) + C_3 f(\beta, \eta)$$

and hence

$$A_0 = \frac{1}{H} f(\beta) + f(\beta, \eta) + C_4 f(\beta, \eta) , \quad (7.14)$$

$$C_1 = H^2 q' f(\beta, \eta)$$

and using the result for q' in (7.13) we see that

$$C_1 = f(\beta) f(\beta, \eta)$$

$$= f(\beta, \eta) ,$$

$$C_2 = f(\beta, \eta) ,$$

$$C_3 = f(\beta, \eta) + H^2 q' f(\beta, \eta)$$

$$= f(\beta, \eta) ,$$

and $C_4 = f(\beta, \eta) .$

It follows from this analysis that

$$B_3 = f(\beta, \eta)$$

Having obtained B_i we can deduce H_1 and H_2 in (6.19) as

$$H_1 = f(\beta)$$

$$H_2 = H f(\beta)$$

and hence

and
$$A_0' = \frac{1}{H} f(\beta) , \tag{7.14}$$

The function
$$A_0'' = \frac{1}{H^2} f(\beta) .$$

substituting the functional terms into the expressions for H_4 given on page 138. Note that all H 's cancel out leaving

The variables for H_4 are defined in section 6.23 page 120. The analysis for B_4 and D_i is similar to that already carried out in the case of B_i and C_i .

$$B_4 = f(\beta, \eta) , \tag{7.15}$$

$$D_1 = H^3 q'' f(\eta) + f(\beta, \eta) + H^2 q' f(\beta, \eta) + (H^2 q')^2 + H^3 q'' f(\beta)$$

$$= f(\beta, \eta) ,$$

$$D_2 = H f(\beta, \eta) ,$$

$$D_3 = H^2 f(\beta, \eta) ,$$

$$D_4 = f(\beta, \eta) ,$$

$$D_5 = H f(\beta, \eta) ,$$

$$D_6 = f(\beta, \eta) ,$$

$$D_7 = H f(\beta) ,$$

and $D_8 = f(\eta)$.

The function H_4 can now be expressed in terms of β and H by substituting the functional terms into the expressions for H_4 given on page 136. Note that all H 's cancel out leaving

$$H_4 = f(\beta) .$$

From the amplitude equation we obtain

$$\frac{dA_1}{dZ_1} = \frac{1}{H} f(\beta) . \quad (7.15)$$

The growth rate based on the stream function is defined by equation (7.2). We can express the growth rate as function of β to $O(\epsilon^2)$ using the same procedure. Consider the growth rate based on the stream function as follows :

$$G_x(\Psi) = -\frac{K_i}{H} + \epsilon \text{REAL} \left(A'_0 + \frac{g_{0Z}}{g_0} \right) + \epsilon^2 \text{REAL} \left[A'_1 + \frac{g_{1Z}}{g_0} - g_1 \left(\frac{A'_0}{g_0} + \frac{g_{0Z}}{g_0 g_0} \right) \right] .$$

$$A'_0 + \frac{g_{0Z}}{g_0} = \frac{1}{H} f(\beta) ,$$

$$A'_1 + \frac{g_{1Z}}{g_0} = \frac{1}{H} f(\beta)$$

and $g_1 \left(\frac{A'_0}{g_0} + \frac{g_{0Z}}{g_0 g_0} \right) = \frac{1}{H} f(\beta) .$

Hence $G_x(\Psi) = \frac{1}{H} f(\beta) . \quad (7.16)$

7.4 Particular Integral g_p

The particular integral g_1 for which

$$\phi^{(1)} = g_1(\eta, Z) + A_1(Z)g_0(\eta, Z) \quad (7.17)$$

was shown to be associated with a stream function growth rate given by equation (7.2). The normalisation at $\eta = 0$ was chosen to be (6.12) which lead to

$$g_1(0, Z) = -A_1(Z) .$$

It follows that different normalisations would lead to different amplitude functions. For instance, if we choose instead

$$\phi^{(1)}(0, Z) = \alpha ,$$

then $g_1 = \alpha - A_1(Z)g_0$.

In general we could consider any particular integral g_p and ask whether this makes any difference to the growth rate. It turns out that different normalisations and hence different particular integrals do not alter the growth rate.

Let g_p be some particular integral given by

$$g_p = g_1 + M(Z)g_0 \quad (7.18)$$

so that

$$\begin{aligned}\phi_p^{(i)} &= g_p + \hat{A}_1(z)g_0 \\ &= g_1 + \left[M(z) + \hat{A}_1(z)g_0 \right]\end{aligned}\tag{7.19}$$

A glance at equations (7.17) and (7.19) tempts one to deduce that

$$\phi^{(i)} = \phi_p^{(i)}$$

and hence $A_1 = M + \hat{A}_1$, but this is wrong. It is worth remembering at this point that in equation (7.17) all we know about A_1 is that it satisfies the amplitude equation (6.23), which is

$$\frac{dA_1}{dz} + \frac{H_3}{H_2}A_1 + \frac{H_4}{H_2} = 0.\tag{7.20}$$

The function \hat{A}_1 satisfies a similar equation. However, from equation (6.17) we note that A_1 is only determined to within an additive multiple of the function A_0 , so that

$$\phi^{(i)} - \phi_p^{(i)} \neq 0$$

but
$$\phi^{(i)} - \phi_p^{(i)} = \alpha A_0 g_0$$

where α is a constant. It then follows that

$$\alpha A_0 g_0 = A_1 - (M - \hat{A}_1),$$

and $\hat{A}_1 = A_1 - M - \alpha A_0$. (7.21)

Equation (7.21) is consistent with equation (7.20) as the following analysis shows. In defining a new particular integral g_p , the terms which will be affected by the definition in the equation for $\phi^{(2)}$ are :

$$\phi^{(i)}, \phi_{\eta}^{(i)}, \phi_{\eta\eta}^{(i)}, \phi_{\eta\eta\eta}^{(i)}, \phi_z^{(i)} \text{ and } \phi_{\eta\eta z}^{(i)} \quad (7.22)$$

In each case A_1 is replaced by $(M + \hat{A}_1)$. The equation for $\phi^{(2)}$ remains the same except that A_0 is replaced by $(M + \hat{A}_1)$. The orthogonality condition yields

$$\frac{d}{dz} (M + \hat{A}_1) + \frac{H_3}{H_2} (M + \hat{A}_1) + \frac{H_4}{H_2} = 0. \quad (7.23)$$

Hence

$$\hat{A}_1 + M = A_1 + cA_0$$

which is equation (7.21) with an arbitrary constant c .

The growth rate is not affected by different normalisations. We can show this in equation (7.2) by replacing A_1 by \hat{A}_1 and g_1 by g_p . The resulting equation equals equation (7.2). In the growth rate as defined by (7.2) it can be seen that the $O(\epsilon)$ terms will not be

affected in view of (7.22). We can therefore look more closely at the $O(\epsilon^2)$ terms. On substituting for $\phi^{(0)}$, $\phi_z^{(0)}$, $\phi^{(1)}$ and $\phi_z^{(1)}$ in the $O(\epsilon^2)$ term we obtain in the notation of (7.3)

$$G_2(R) = \frac{A_1' g_0 + A_1 g_0 z + g_1 z}{A_0 g_0} - (g_1 + A_1 g_0) \left(\frac{A_0'}{A_0 A_0 g_0} + \frac{g_0 z}{A_0 g_0 g_0} \right) \quad (7.24)$$

If A_1 and g_1 are now replaced by \hat{A}_1 and g_p we obtain

$$\begin{aligned} \hat{G}_2(R) &= \left(\frac{A_1' - M' - \alpha A_0}{A_0} \right) + (A_1 - M - \alpha A_0) \frac{g_0 z}{A_0 g_0} \\ &\quad + \frac{g_1 z + M' g_0 + M g_0 z}{A_0 g_0} \\ &\quad - \left[g_1 + M g_0 + (A_1 - M - \alpha A_0) g_0 \right] \left(\frac{A_0'}{A_0 A_0 g_0} + \frac{g_0 z}{A_0 g_0 g_0} \right) \end{aligned}$$

which can be rearranged as

$$\begin{aligned} \hat{G}_2(R) &= \frac{A_1'}{A_0} + \frac{A_1 g_0 z}{A_0 g_0} + \frac{g_1 z}{A_0 g_0} - (g_1 + A_1 g_0) \left(\frac{A_0'}{A_0 A_0 g_0} + \frac{g_0 z}{A_0 g_0 g_0} \right) \\ &\quad - \frac{M'}{A_0} - \alpha \frac{A_0'}{A_0} - \frac{M g_0 z}{A_0 g_0} - \alpha \frac{g_0 z}{g_0} + \frac{M'}{A_0} + \frac{M g_0 z}{A_0 g_0} \\ &\quad - (M g_0 - M g_0 - \alpha A_0 g_0) \left(\frac{A_0'}{A_0 A_0 g_0} + \frac{g_0 z}{A_0 g_0 g_0} \right) \end{aligned}$$

and cancellation of terms involving M gives the $O(\epsilon^2)$ contribution as

$$\hat{G}_2(R) = \frac{A_1'}{A_0} + \frac{A_1 g_{0Z}}{A_0 g_0} + \frac{g_{1Z}}{A_0 g_0} - (g_1 + A_1 g_0) \left(\frac{A_0'}{A_0 A_0 g_0} + \frac{g_{0Z}}{A_0 g_0 g_0} \right)$$

$$= \frac{A_1'}{A_0} + \frac{g_{1Z}}{A_0 g_0} - g_1 \left(\frac{A_0'}{A_0 A_0 g_0} + \frac{g_{0Z}}{A_0 g_0 g_0} \right) - \frac{A_1 A_0'}{A_0 A_0}$$

which is the same as (7.24). Therefore $G_2(R) = \hat{G}_2(R)$.

Hence the growth rate has remained unchanged. This result is useful in making numerical calculations for growth rates.

Different ways of defining the particular integral used in calculating $\phi^{(1)}$ lead to different amplitude functions A_1 ,

but do not affect the growth rates.

8. NUMERICAL METHODS AND RESULTS

We now turn to the formidable task of the computing involved, numerical checks made and the difficulties encountered during the course of this work. The results on channel flow will also be presented here.

Most of the numerical results on channel flow were computed in single precision on the Cray-1S Computer. This is equivalent to double precision on the Honeywell or Amdahl Computer. Some results were checked by double precision on the Honeywell. The accuracy estimated will be described as we proceed.

8.1 Numerical Methods

The methods used and the checks that were carried out will be discussed as they arise. It is convenient to start with the Orr-Sommerfeld equation (6.7) which gave rise to earlier programs.

8.11 Orr-Sommerfeld Problem

The main program was designed to solve the Orr-Sommerfeld equation

$$(D^2 - K^2)^2 \phi - iKR \left[(F_\eta - \beta/K)(D^2 - K^2) - F_{\eta\eta\eta} \right] \phi = 0 ,$$

with boundary conditions

$$\phi = \phi_{,\eta} = 0 \quad \text{at } \eta = 1,$$

$$\phi = \phi_{,\eta\eta\eta} = 0 \quad \text{at } \eta = 0.$$

Note that we shall require subroutines to generate the basic flow F with its derivatives and also ϕ with its derivatives. The next problem was to find K , for fixed values of β , R and Z . Once the eigenvalue K is available, obtaining an eigenfunction ϕ that satisfies the boundary conditions is simple.

The following form of the Orr-Sommerfeld equation was found more convenient to use for the purpose of numerical integration.

$$\phi^{iv} + C_1 \phi'' + C_2 \phi = 0 \quad (8.1)$$

where

$$C_1 = -2K^2 + iR(\beta - KF)$$

$$\text{and } C_2 = K^4 + iKR(F_{,\eta}K^2 + F_{,\eta\eta\eta} - K\beta).$$

The constants C_1 and C_2 were calculated by a subroutine. A fourth order Runge-Kutta routine was used to calculate ϕ and its derivatives. We used a step length of $1/20$ and step length of $1/40$ for checks.

The Runge-Kutta routine requires starting points for and its derivatives, these were obtained from the series solution (6.13). Two even independent solutions ϕ_1 and ϕ_2 which satisfy boundary conditions at $\eta = 0$, are given by

$$\phi_1 = 1 - \frac{1}{24} C_2 \eta^4 + \frac{1}{720} C_1 C_2 \eta^6 + \frac{1}{40320} (C_2^2 - C_1^2 C_2) \eta^8 + \dots$$

and

$$\begin{aligned} \phi_2 = \eta^2 - \frac{1}{12} C_1 \eta^4 + \frac{1}{360} (C_1^2 - C_2) \eta^6 \\ + \frac{1}{20160} (2C_1 C_2 - C_1^3) \eta^8 + \dots \end{aligned}$$

The series solutions including the term containing η^{10} was used to check the computed values of ϕ , ϕ' , ϕ'' , ϕ''' and ϕ^{iv} for small values of η at $R = 40$, $\beta = 1$, $Z = 0.85$ and $Z = 1$. In Table 8.1 we give values of ϕ_1 and ϕ_2 computed by the Runge-Kutta (RK) and those calculated from the series (S). It is evident that the results are close for small values of η . The solutions ϕ_1 and ϕ_2 were also required to satisfy equation (8.1), which was also a check on the calculated values of C_1 and C_2 . By applying the boundary conditions (6.10) on the solution

$$\phi = A_1 \phi_1 + A_2 \phi_2 \quad (8.2)$$

Table 8.1. The

we obtain a set of homogeneous equations for the arbitrary constants A_1 and A_2 as in section 3.5. The requirement for a non-trivial solution to exist leads to the

Z	η	RK/S	ϕ_1		ϕ_2	
0.85	0.05	RK	0.9999	0.0000	0.0024	0.0000
		S	0.9999	0.0000	0.0024	0.0000
	0.10	RK	0.9999	0.0004	0.0098	0.0002
		S	0.9999	0.0004	0.0098	0.0002
	0.15	RK	0.9998	0.0021	0.0217	0.0012
		S	0.9995	0.0019	0.0216	0.0010
1.0	0.05	RK	1.00000	0.0000	0.0249	0.0000
		S	1.00000	0.0000	0.0249	0.0000
	0.10	RK	1.00005	0.0004	0.0988	0.0002
		S	1.00000	0.0004	0.0986	0.0002
	0.15	RK	1.00026	0.0022	0.0218	0.0014
		S	0.9998	0.0022	0.0217	0.0012

Table 8.1. The solutions ϕ_1 and ϕ_2 obtained by using the Runge-Kutta routine (RK) and the series (S) for $R = 40$, $\beta = 1$ at various values of η and Z .

familiar eigenvalue relation

$$F(R, \beta, K) = \phi_1(1) \phi_2'(1) - \phi_1'(1) \phi_2(1) = 0 .$$

This relation was our object function in the root finding routine and also in the contour plot programs.

Setting up the subroutine for the basic flow F was straight-forward except that it was worth remembering that the Runge-Kutta routine requires intermediate values of F . Therefore if N is the number of steps for the Runge-Kutta, the required number of steps for the base flow is $2N$. Once the routines for the Runge-Kutta and base flow were ready the next important task was to get an accurate value for K , the eigenvalue. This is dealt with in the next section.

8.12 The Eigenvalue K

The solution of the Orr-Sommerfeld equation depends on a good estimate of K . It was therefore important that we obtain as far as possible a good estimate of K . A simple root finding routine ROOTATZ was designed to locate roots at various values of Z , R and β . The routine uses the method of successive linear approximations. Convergence is not guaranteed, or in some cases the routine may converge to a different root. Despite these limitations of the method of successive approximations, the routine ROOTATZ worked remarkably well in locating roots which were revealed by contour plots or in tracing a given root.

An estimate for K was traced from a known root obtained by Eagles (Private communication). This root is believed to be the most unstable, or least stable root. The root was also revealed by contour plots and picked up by ROOTATZ. This was an important check on the program itself. The root obtained by tracing was further checked by plotting graphs of the eigenvalue K_i against R or β at fixed Z to ensure that the root was continuously connected. Table 6.1 gives the root traced by ROOTATZ and also shows numerical agreement to four decimal places.

Problems were encountered when the eigenvalue was allowed to vary with Z at step lengths of about $1/10$ or more. The routine converged to other roots more frequently. At smaller step lengths of about $1/20$ or $1/40$, the routine was more reliable. However, it was still necessary to check graphically whether the root was varying smoothly.

When the Orr-Sommerfeld equation was replaced by its adjoint the results for the eigenvalue K and the adjoint eigenvalue K_A were equal to four decimal places being given by

$$K = (1.266141, 0.234261)$$

and $K_A = (1.266062, 0.234324)$

at $R = 60$, $\beta = 1$ and $Z = 1$. This was an encouraging result since theoretically K and K_A are supposed to be equal.

The eigenfunction ϕ can easily be obtained from (8.2) by setting one of the arbitrary constants to unity, e.g. $A_1 = 1$. Applying the boundary conditions at $\eta = 1$ we obtain for the constant A_2

$$A_2 = - \phi_1(1) / \phi_2(1) .$$

The adjoint eigenfunction is obtained in a similar manner. Checks were made on both the eigenfunction and its adjoint by using different step lengths and also ensuring that the boundary conditions are satisfied.

8.13 Numerical Differentiation

In considering the computing involved in the non-parallel theory, it is necessary to recall the equations for $\phi^{(1)}$ and $\phi^{(2)}$ which are given by (6.14) and (6.21). For the solutions of (6.14) and (6.21) we require knowledge of the first and second derivatives of g_0 with respect to Z , other functions requiring only first derivatives.

A subroutine FINDIF consisting of finite central difference formulae was used to obtain the derivatives. We used 8 points with step length of $1/20$. In this way we were

able to find the second derivative with respect to Z at the centre point (usually $Z = 1$). The variable Z was usually varied from 0.85 to 1.2 so that the point $Z = 1$ lies somewhere close to the centre. An increase in the number of points to 10, for instance would increase the size of program considerably due to the complex matrices required to hold the finite differences. Even with 8 points it was not possible to run the program on the Honeywell Computer. An additional subroutine was required to find the derivatives of $g_1, g_{1\eta}, g_{1\eta\eta}, A_0, |g_0|, |g_{0\eta}|$ and $|K|$. The reason for this was that these functions were required later in the program and the subroutine required for them was very small compared with FINDIF.

This was a very important stage which required a lot of care to ensure that the derivatives are reasonably accurate. The computed derivatives were manually checked for accuracy using the computer generated table of differences and a calculator. The program was also checked against the derivatives of a known polynomial.

8.14 Amplitude Functions and Growth Rates

The equation for the amplitude function A_0 is given by (6.19). The functions $H_1(Z)$ and $H_2(Z)$ are integrals with respect to η . These were integrated using Simpson's Rule with a step length of $1/20$. The numerical

ratio H_1/H_2 was checked against equation (7.14) at $Z = 0.9$ for $R = 40$ and 60 . There was agreement to four significant figures. The growth rate results checked against (7.16) agree with the theory to three significant figures. From equation (6.9) we have

$$\beta(Z) = \omega H^2(Z)$$

so that ω can be chosen to ensure that $\beta = 1$ at selected values of Z . It was then possible to use the theory given in Section 7.3 to check the numerical results obtained for the growth rate. Some results for the growth rates are displayed in Table 8.2, and with $H(Z) = Z$ this confirms (to three figures) the expected relation that the growth rate is a function of $f(\beta)/H$, which is a useful check on the consistency of the numerical work. The frequency $\beta = 1$ was chosen for the purpose of comparison since it lies somewhere near the critical frequency for $\gamma = 3.57$ of the Eagles & Weissman(1975) neutral curve. Time did not allow computation with other values of β .

It was shown in Section 7.4 that different ways of defining the particular integral used in calculating $\phi^{(1)}$ lead to different amplitude functions but did not affect the growth rate. A subroutine RHSI was used to calculate the particular integral of equation (6.14) with starting value $(1,0,1,0)$. A different starting value like $(0,0,2,0)$ for instance, defines another particular integral and hence a different amplitude function. This was checked numerically for $R = 40, 50$ and 60 at $\beta = 1$,

$Z = 1$ and $\epsilon = 0.5$. Numerical results agree completely with the theory. The results are given in Table 8.2, where P_1 and P_2 represent particular integrals (PI) corresponding to the starting values (1,0,1,0) and (0.5,1,0) respectively.

8.2 Numerical Results

A brief survey of the numerical results on channel flow will be presented here. We begin with the case $\beta = 1$.

R	ϵ	Z	$G_x(\psi)$	$G_x(\hat{E})$	$HG_x(\psi)$	$HG_x(\hat{E})$
40	0.0	0.9	-0.307120	-0.614400	-0.276480	-0.552960
		1.0	-0.276480	-0.552960		
	0.0125	0.9	-0.287410	-0.562840	-0.258670	-0.506560
		1.0	-0.258800	-0.506910		
60	0.0	0.9	-0.260290	-0.520580	-0.234260	-0.468520
		1.0	-0.234260	-0.468200		
	0.0083	0.9	-0.235280	-0.462480	-0.211840	-0.416230
		1.0	-0.212120	-0.416820		

Table 8.2. The stream function and relative energy growth rates at various values of R, ϵ and Z for $\beta = 1$.

$$P_1 = \dots$$

$$P_2 = \dots$$

where P_1 and P_2 are the second and third eigenfunctions respectively.

$Z = 1$ and $\epsilon R = 0.5$. Numerical results agree completely with the theory. The results are given in Table 8.3, where P_1 and P_2 represent particular integrals (PI) corresponding to the starting values $(1,0,1,0)$ and $(0,0,2,0)$ respectively.

8.2 Numerical Results

A brief summary of the numerical results on channel flow will be presented here. We begin with the base flow discussed in chapter 5 and complete this section with a discussion on growth rates.

8.21 The Basic Flow

Recall that the stream function for base flow F was expanded in terms of ϵ to $O(\epsilon^2)$. The second and third approximations are functions of η , R and the shape function $H(Z)$ for fixed ϵ . Since we are mainly concerned with the straight-walled channel, $H(Z) = Z$ in this case. In Fig. 8.1 we show the second and third approximation to the velocity profile as a function of η at $Z = 1$. The approximations will be denoted by

$$\hat{F}_2 = F_\eta^{(0)} + \epsilon F_\eta^{(1)}$$

and

$$\hat{F}_3 = F_\eta^{(0)} + \epsilon F_\eta^{(1)} + \epsilon^2 F_\eta^{(2)}$$

where \hat{F}_2 and \hat{F}_3 are the second and third approximation respectively.

R	ϵ	PI	$G_x(\psi)$	$G_x(\hat{E})$
40	0.0125	P_1	-0.258799	-0.506906
		P_2	-0.258799	-0.506906
50	0.1	P_1	-0.231965	-0.455199
		P_2	-0.231965	-0.455199
60	0.0083	P_1	-0.212125	-0.416824
		P_2	-0.212125	-0.416828

Table 8.3. The stream function and relative energy growth rates with particular integrals P_1 and P_2 at $R = 40, 50, 60$ for $\beta = 1$ and $Z = 1$.

The approximations are compared at $R = 35$, $\epsilon = 0.1$ and $Z = 1$ with the appropriate Jeffery-Hamel ($J(\eta)$) profile at $Y = 3.5$. Note that the approximations get better with higher order terms. We would expect the fourth approximation to get even closer to the Jeffery-Hamel profile. This should imply better approximation to the growth rate in straight-walled channel flows.

8.22 Growth Rate Terms

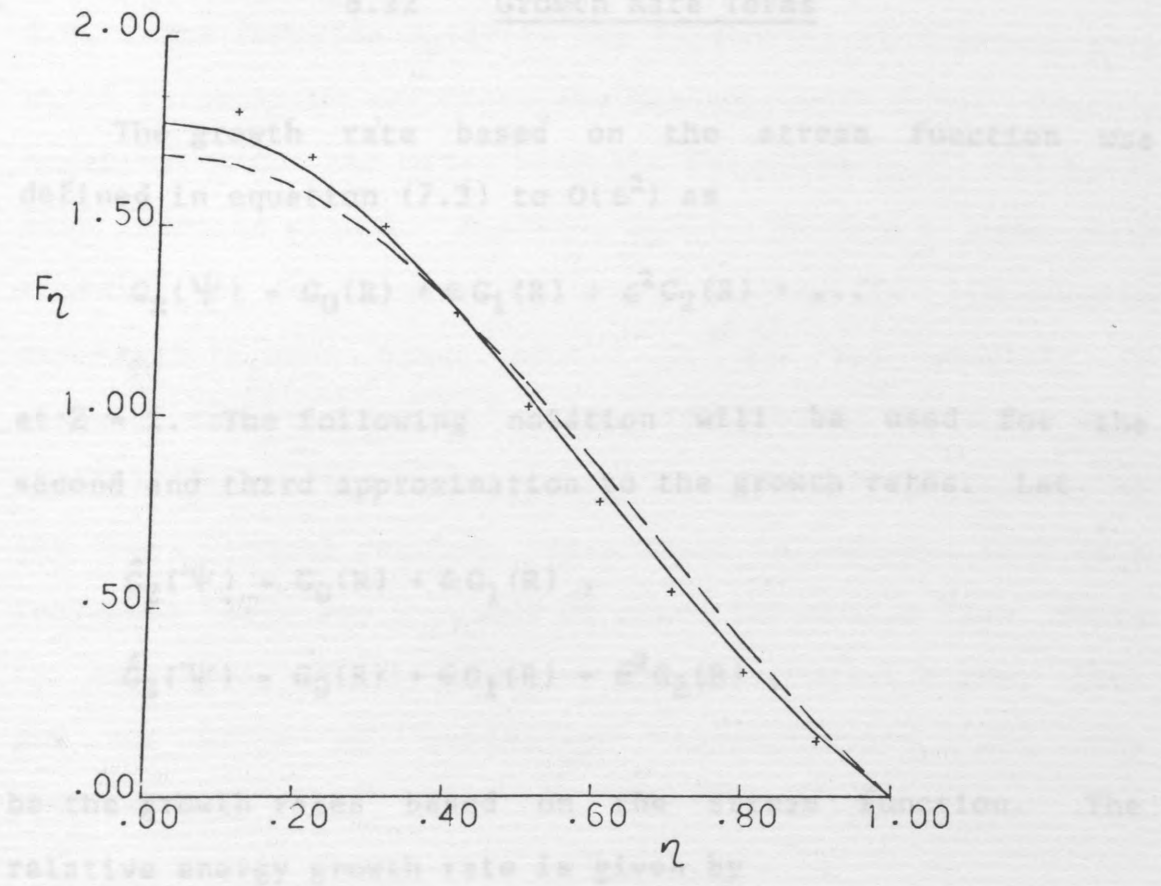


Fig. 8.1. Comparison of the second and third approximation for the velocity profile with the appropriate Jeffery-Hamel profile $J(\eta)$ at $R = 35$, $\epsilon = 0.1$ and $Z = 1$. - F_3 ; -- F_2 ; ++ $J(\eta)$.

The approximations are compared at $R = 35$, $\epsilon = 0.1$ and $Z = 1$ with the appropriate Jeffery-Hamel ($J(\gamma)$) profile at $\gamma = 3.5$. Note that the approximations get better with higher order terms. We would expect the fourth approximation to get even closer to the Jeffery-Hamel profile. This should imply better approximation to the growth rate in straight-walled channel flows.

8.22 Growth Rate Terms

The growth rate based on the stream function was defined in equation (7.3) to $O(\epsilon^2)$ as

$$G_x(\psi) = G_0(R) + \epsilon G_1(R) + \epsilon^2 G_2(R) + \dots$$

at $Z = 1$. The following notation will be used for the second and third approximation to the growth rates. Let

$$\hat{G}_2(\psi) = G_0(R) + \epsilon G_1(R) ,$$

$$\hat{G}_3(\psi) = G_0(R) + \epsilon G_1(R) + \epsilon^2 G_2(R) ,$$

be the growth rates based on the stream function. The relative energy growth rate is given by

$$G_x(\hat{E}) = H_0(R) + \epsilon H_1(R) + \epsilon^2 H_2(R) + \dots$$

so that the second and third approximations may be defined as

$$\hat{H}_2(\hat{E}) = H_0(R) + \epsilon H_1(R)$$

and $\hat{H}_3(\hat{E}) = H_0(R) + \epsilon H_1(R) + \epsilon^2 H_2(R).$

In Table 8.4 the terms $G_0(R)$, $G_1(R)$, and $G_2(R)$ for the stream function growth rate are given together with corresponding eigenvalues K at various values of the Reynolds number. The associated graphs with $G_1(R)$ as a function of R are also presented in Figures 8.2, 8.3 and 8.4. The function $G_0(R)$ is the Poiseuille flow growth rate which is negative and increases smoothly with R but remains negative. On the other hand the functions $G_1(R)$ and $G_2(R)$ both increase with R . However, $G_2(R)$ increases much more rapidly and at higher values of R ($R \approx 170$) the program converges to some other root. It was not possible to compute results for $R >$ about 170 because the basic most unstable Poiseuille flow root was not reliably picked out by the root finding routine. This seems to indicate that as R increases there are a number of other Poiseuille flow roots in existence, fairly close to the most unstable one. Time did not allow an exhaustive investigation of this phenomenon.

8.23 Growth Rates

In order to assess the accuracy of the present method, it was necessary to compare the second and third

R	K		G_0	G_1	G_2
50	1.2497	0.2516	-0.2516	1.7747	18.7215
60	1.2661	0.2343	-0.2343	2.4105	29.4890
70	1.2825	0.2193	-0.2193	3.0330	39.5743
80	1.2968	0.2060	-0.2060	3.5820	49.0837
100	1.3198	0.1844	-0.1844	4.5854	69.3896
120	1.3380	0.1684	-0.1684	5.6056	92.9291
140	1.3536	0.1561	-0.1561	6.6702	119.4171
150	1.3607	0.1509	-0.1509	7.2134	133.5622

Table 8.4. Values of the functions G_0 , G_1 and G_2 for the stream function growth rate with the corresponding Poiseuille flow eigenvalues K at various values of R for $\beta = 1$ and $Z = 1$.

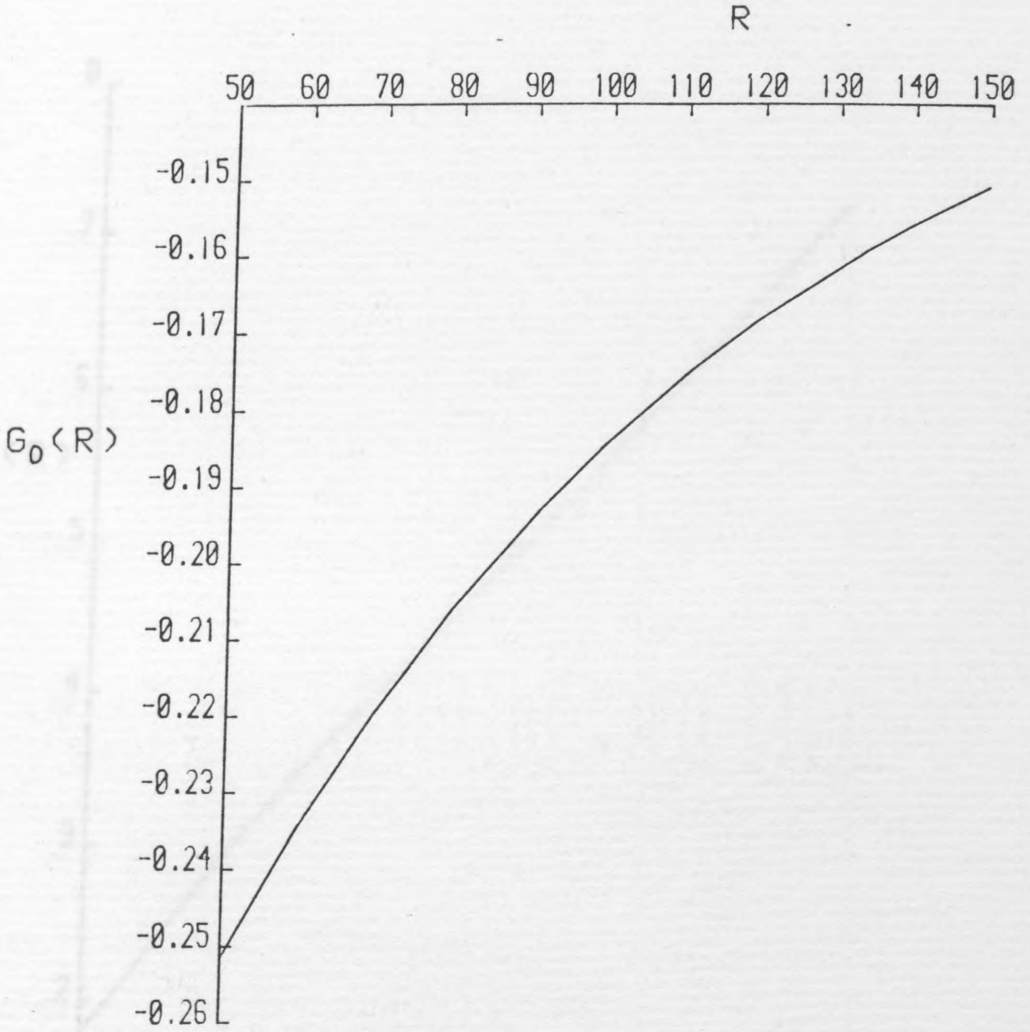


Fig. 8.2. The Poiseuille Flow stream Function growth rate as a function of R at $\beta = 1$ and $Z = 1$.

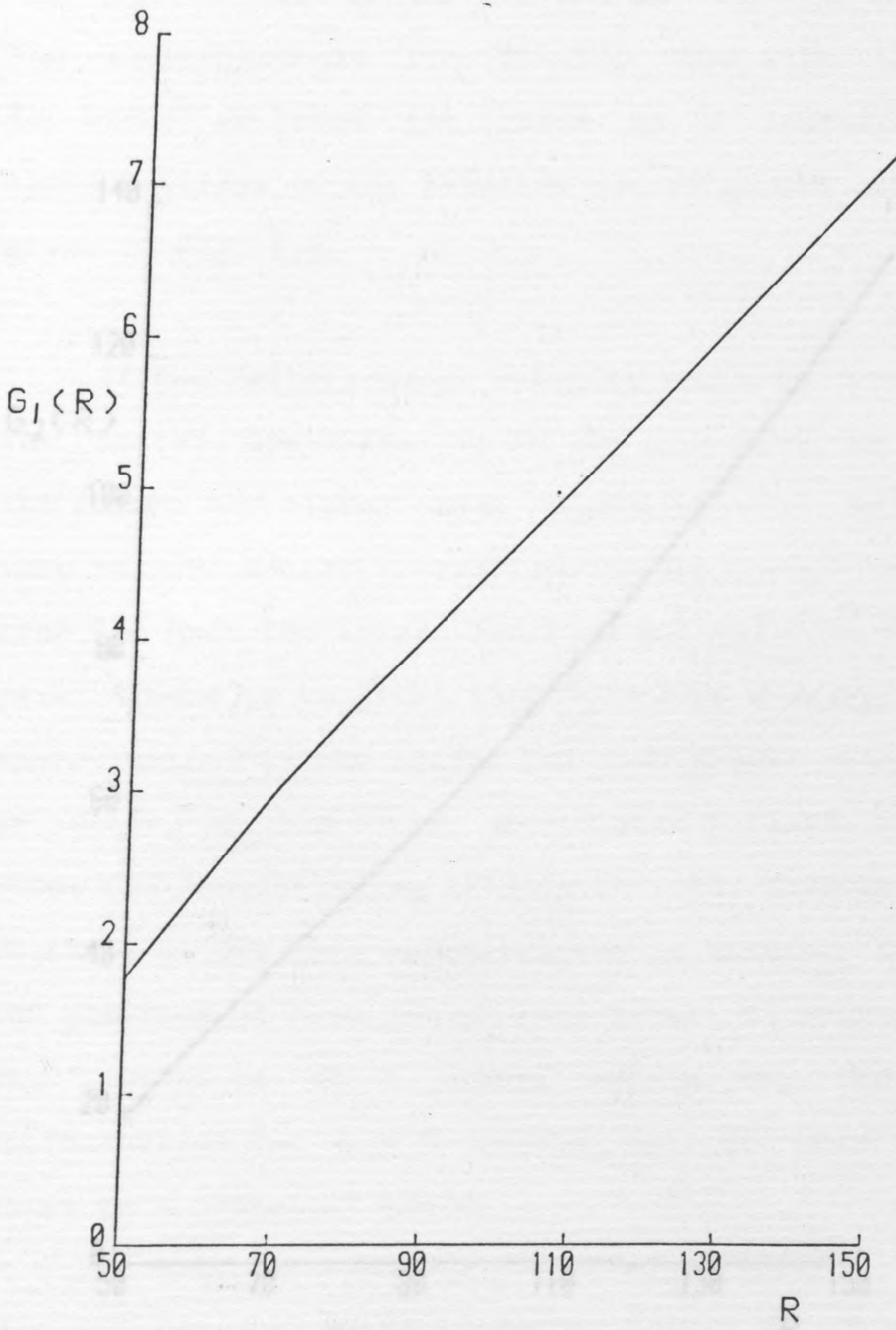


Fig. 8.3. The Function $G_1(R)$ in the stream function growth rate as a function of R at $\beta = 1$ and $Z = 1$.

approximations to the growth rate. The approximations as a function of δ are displayed in Figures 8.5 and 8.6. In Fig. 8.5 the stress function growth rates $\hat{G}_2(\psi)$ and $\hat{G}_3(\psi)$ are given at $R = 50$, $\beta = 1$ and $Z = 1$. The approximations for $R = 100$ have also been included in order to show the trend as R increases. The approximations to the relative energy growth rate $G_2(R)$ are given in Fig. 8.6.

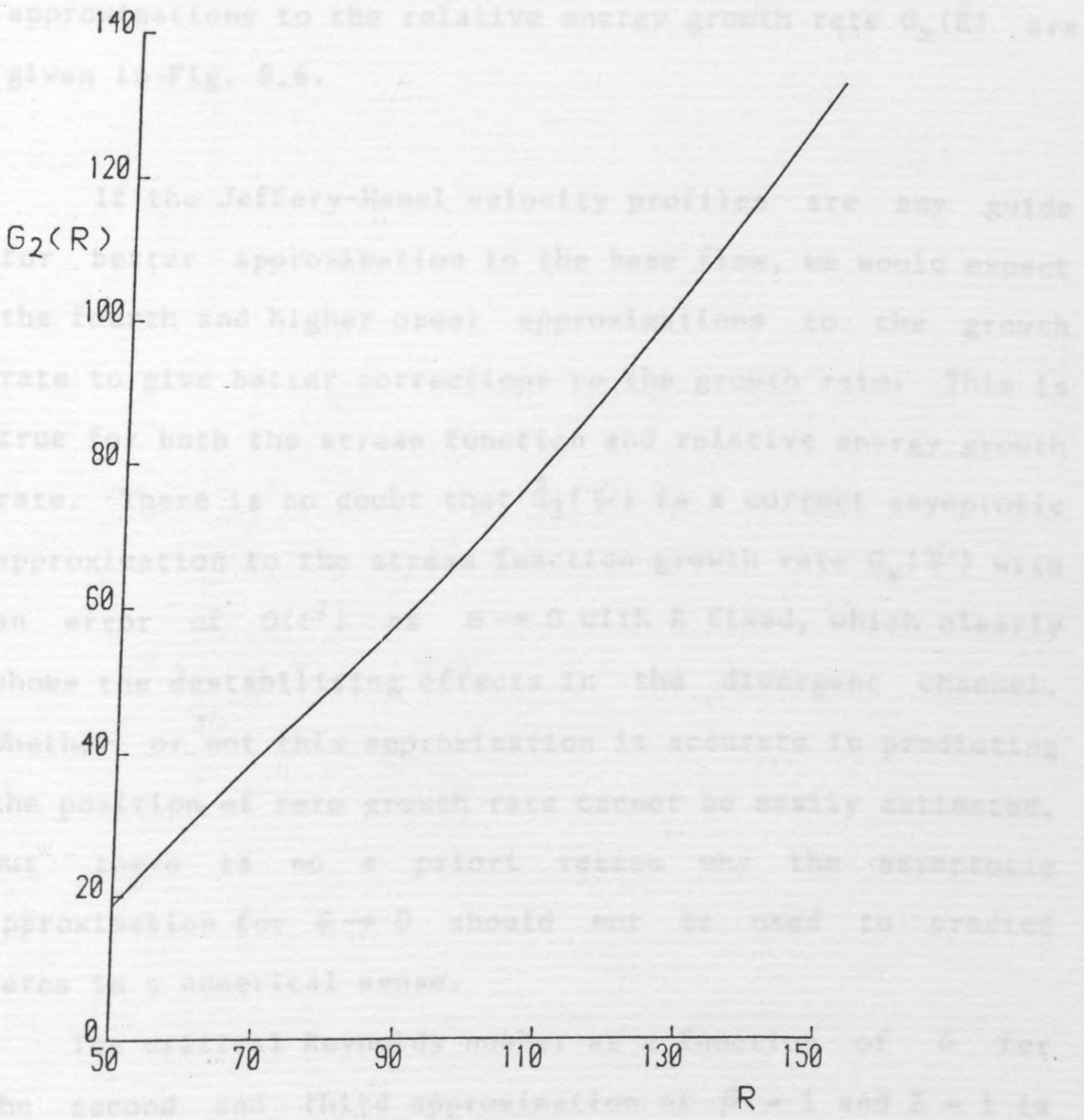


Fig. 8.4. The function $G_2(R)$ in the stream function growth rate as a function of R at $\beta = 1$ and $Z = 1$.

approximations to the growthrate. The approximations as a function of ϵ are displayed in Figures 8.5 and 8.6. In Fig. 8.5 the stream function growth rates $\hat{G}_2(\psi)$ and $\hat{G}_3(\psi)$ are given at $R = 60$, $\beta = 1$ and $Z = 1$. The approximations for $R = 150$ have also been included in order to show the trend as R increases. The approximations to the relative energy growth rate $G_x(\hat{E})$ are given in Fig. 8.6.

If the Jeffery-Hamel velocity profiles are any guide for better approximation to the base flow, we would expect the fourth and higher order approximations to the growth rate to give better corrections to the growth rate. This is true for both the stream function and relative energy growth rate. There is no doubt that $\hat{G}_3(\psi)$ is a correct asymptotic approximation to the stream function growth rate $G_x(\psi)$ with an error of $O(\epsilon^2)$ as $\epsilon \rightarrow 0$ with R fixed, which clearly shows the destabilising effects in the divergent channel. Whether or not this approximation is accurate in predicting the position of zero growth rate cannot be easily estimated, but there is no a priori reason why the asymptotic approximation for $\epsilon \rightarrow 0$ should not be used to predict zeros in a numerical sense.

The critical Reynolds number as a function of ϵ for the second and third approximation at $\beta = 1$ and $Z = 1$ is displayed in Figures 8.7 and 8.8. In Fig. 8.8 we also give the Eagles & Weissman(1975) neutral curve based on mean relative energy using Jeffery-Hamel profiles as the base

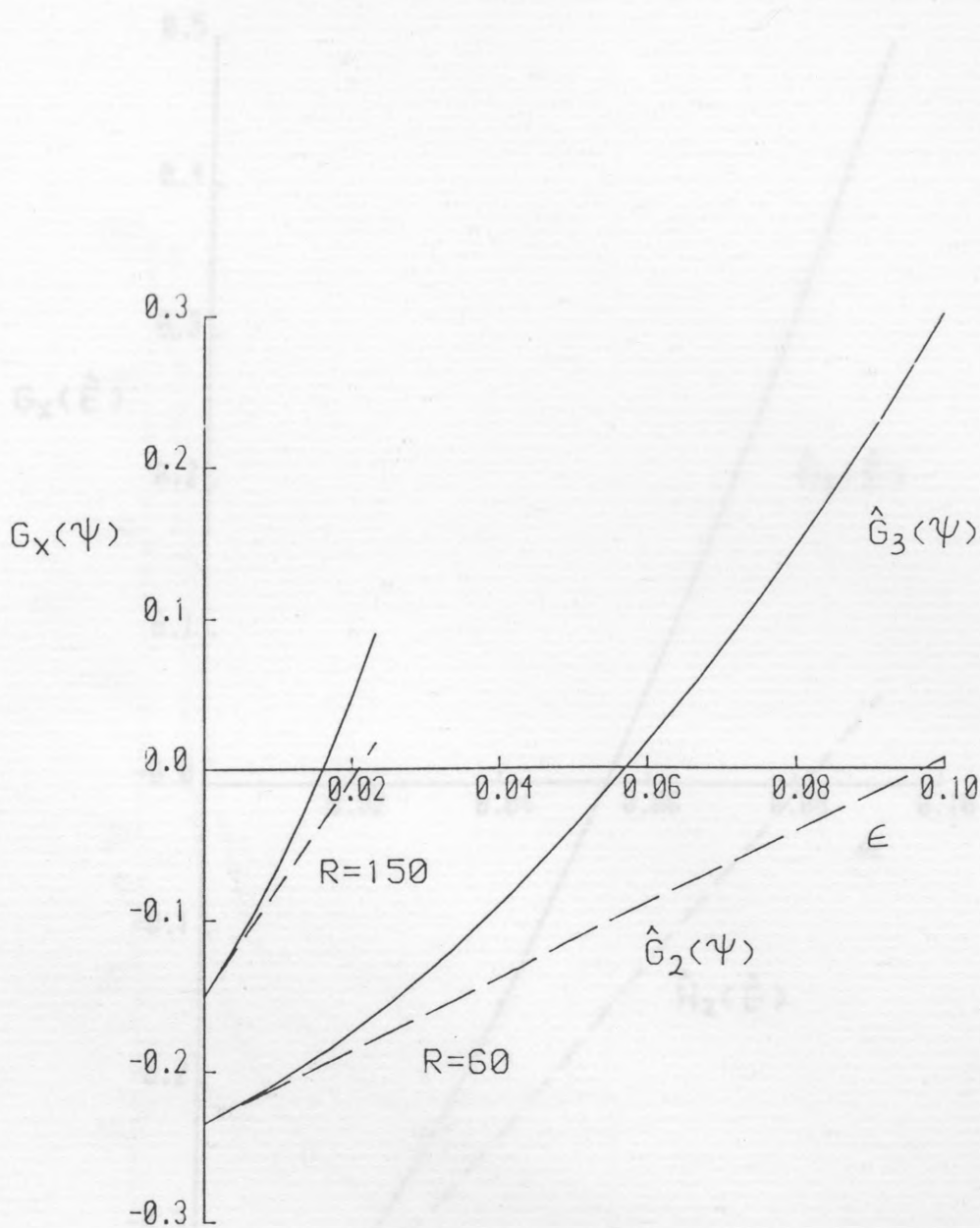


Fig. 8.5. The second (--) and third (-) approximation for the stream function growth rate $G_x(\psi)$, as a function of ϵ at $R = 60$ and 150 .

Fig. 8.5. The second (--) and third (-) approximation for the relative energy growth rate $G_x(\psi)$, as a function of ϵ at $R = 60$ for $\beta = 1$ and $\gamma = 1$.

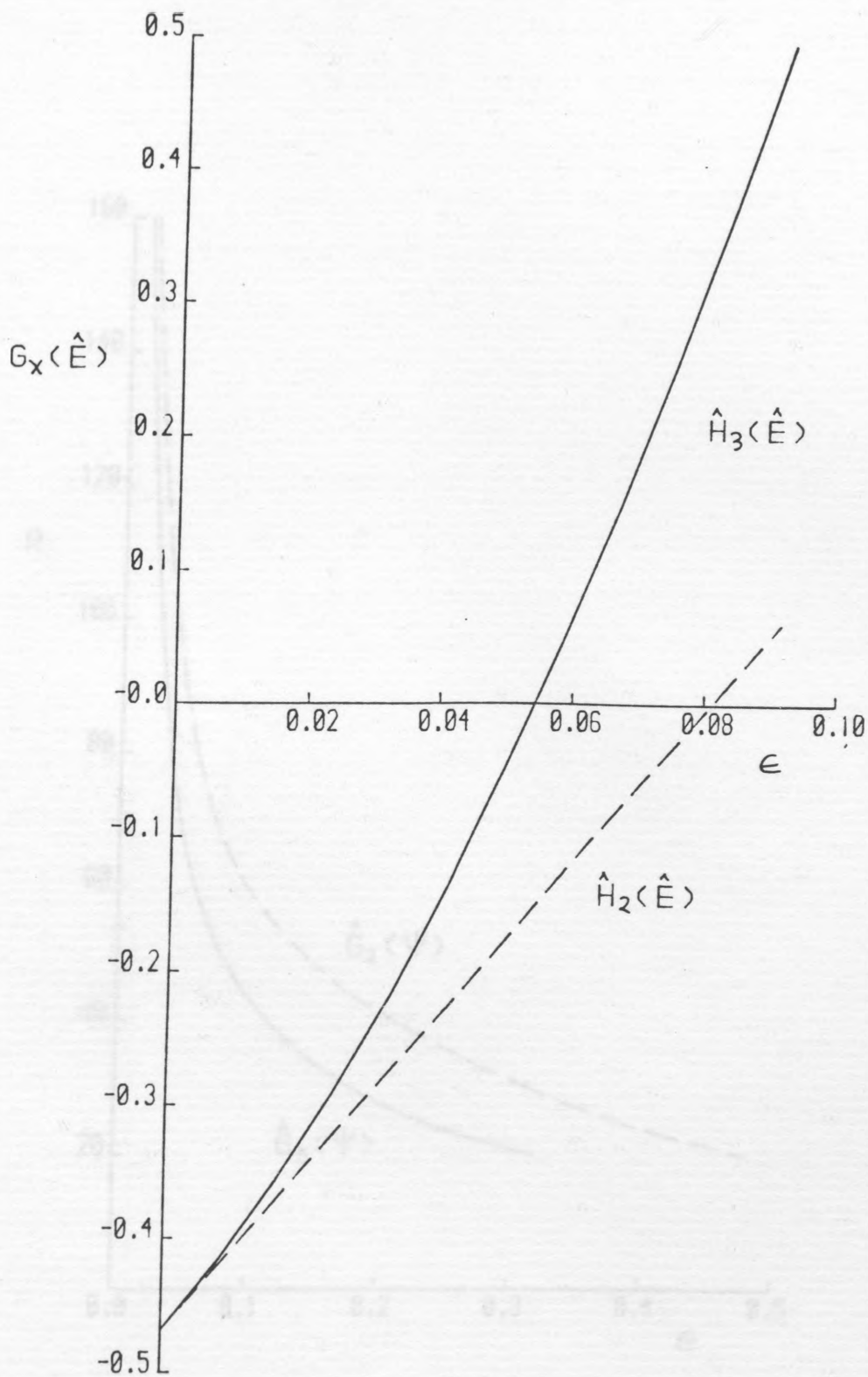


Fig. 8.6. The second (--) and third (-) approximation for the relative energy growth rate $G_x(\hat{E})$, as a function of ϵ at $R = 60$ for $\beta = 1$ and $Z=1$.

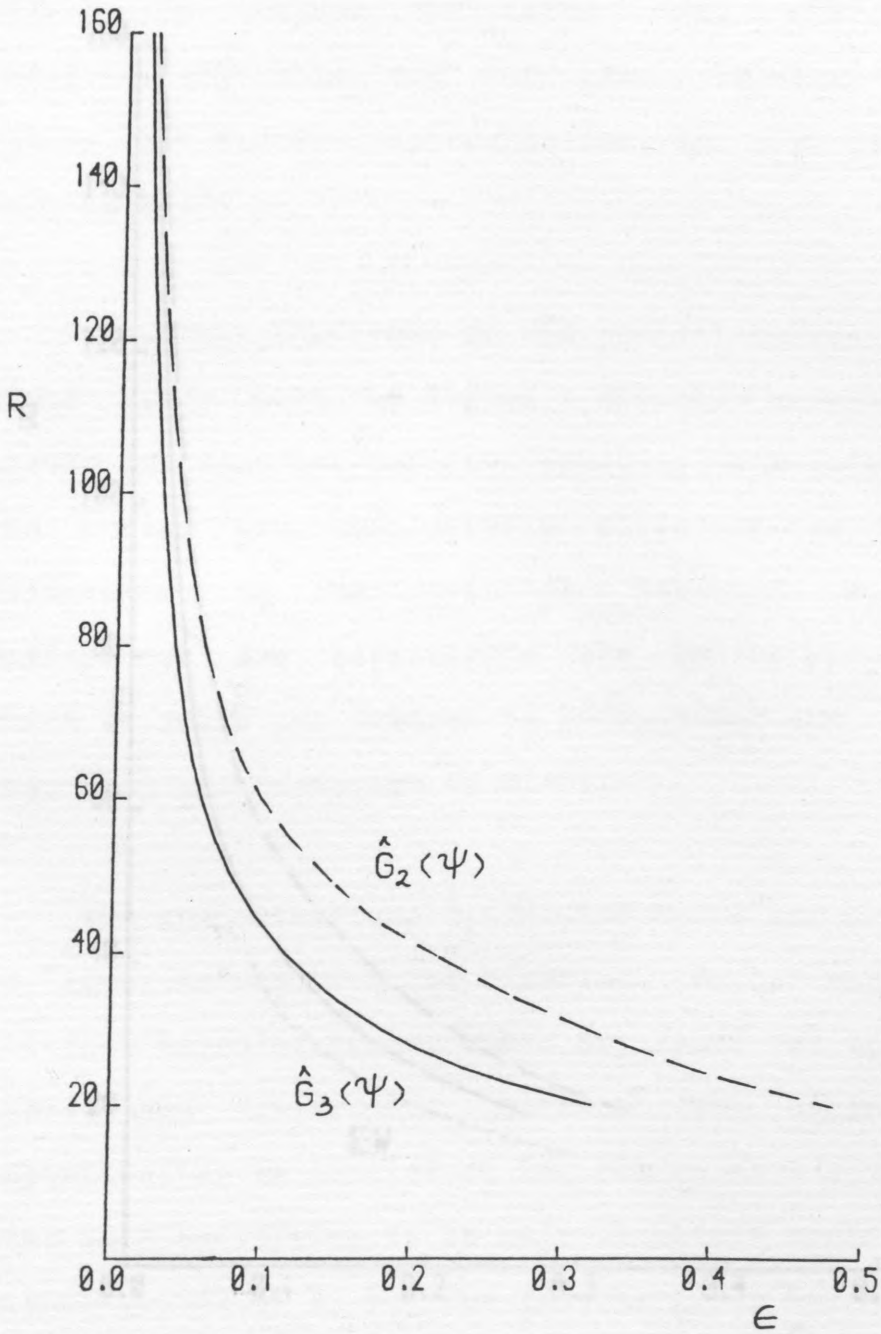


Fig. 8.7. The critical Reynolds number as a function of ϵ for the second (--) and third (-) approximation to the stream function growth rate at $\beta = 1$ and $Z = 1$.

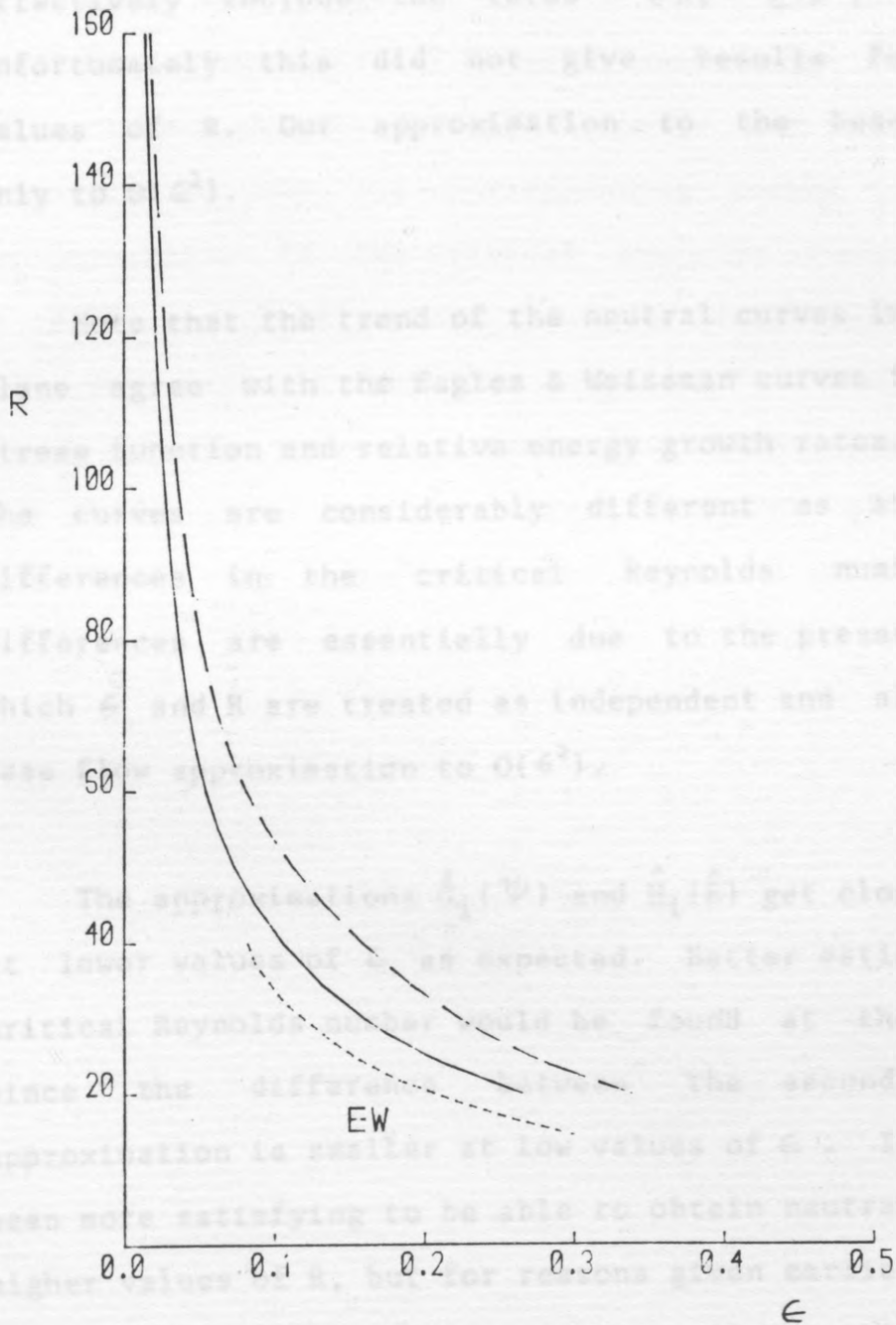


Fig. 8.8. The critical Reynolds number as a function of ϵ for the second (--) and third (-) approximation to the relative function growth rate at $\beta = 1$ and $Z = 1$. EW is the Eagles & Weissman (1975) mean relative energy growth rate.

flow. It is worth remembering at this point that the Eagles & Weissman growth rates were calculated using Jeffery-Hamel profiles (in the first approximation) which effectively include the terms ϵR , $\epsilon^2 R^2$, $\epsilon^3 R^3$ etc. Unfortunately this did not give results for lower values of R . Our approximation to the base flow is only to $O(\epsilon^2)$.

Note that the trend of the neutral curves in the R - ϵ plane agree with the Eagles & Weissman curves for both the stream function and relative energy growth rates. However, the curves are considerably different as shown by the differences in the critical Reynolds numbers. The differences are essentially due to the present method in which ϵ and R are treated as independent and also to the base flow approximation to $O(\epsilon^2)$.

The approximations $\hat{G}_1(\psi)$ and $\hat{H}_1(\hat{E})$ get closer together at lower values of ϵ as expected. Better estimates of the critical Reynolds number would be found at these values, since the difference between the second and third approximation is smaller at low values of ϵ . It would have been more satisfying to be able to obtain neutral curves for higher values of R , but for reasons given earlier about the method of successive approximations it was not possible to obtain reliable results beyond $R = 150$.

The second and third approximations to the critical Reynolds number are also given in Table 8.5. These were estimated from the graphs in Figures 8.7 and 8.8. A similar notation to that of growth rates was used, so that if $R(\Psi)$ and $T(\hat{E})$ are the critical Reynolds numbers for the growth rates based on the stream function and relative energy respectively, the the corresponding second and third approximations to the critical Reynolds number are given by $\hat{R}_i(\Psi)$ and $\hat{T}_i(\hat{E})$ where $i = 2,3$. Table 8.5 also shows that the critical Reynolds numbers for the relative energy growth rate are lower for both approximations than those given by the stream function growth rate. This trend is confirmed by Eagles & Weissman(1975).

0.10	38.8	41.8	33.8	41.5	35.8
0.15	48.2	33.5	41.8	31.1	25.8
0.20	41.5	27.5	33.8	25.2	20.1
0.25	35.2	23.1	25.7	20.5	15.9
0.30	31.7	20.5	22.6	17.5	14.5

Table 8.5. The second and third approximation to the critical Reynolds number at $\beta = 1$ and $Z = 1$ for the stream function and relative energy growth rate. R_c is the Eagles & Weissman (1975) eqq. relative energy growth rate.

ϵ	$\hat{R}_2(\psi)$	$\hat{R}_3(\psi)$	$\hat{T}_2(\hat{E})$	$\hat{T}_3(\hat{E})$	EW
0.02	130.0	100.0	122.3	98.0	-
0.05	90.0	65.0	80.0	60.0	-
0.10	60.0	43.0	53.0	41.5	35.0
0.15	48.2	33.5	41.8	31.1	25.0
0.20	41.5	27.5	33.0	25.0	20.3
0.25	35.2	23.4	26.7	20.5	16.8
0.30	31.7	20.8	22.6	-	14.5

Table 8.5. The second and third approximation to the critical Reynolds number at $\beta = 1$ and $Z = 1$ for the stream function and relative energy growth rate. EW is the Eagles & Weissman (1975) mean relative energy growth rate.

9. CONCLUSIONS

We looked at axisymmetric flows of a tube whose radius varied slowly with the streamwise coordinate. The radius was given in terms of a general shape function $r = H(Z)$ where Z is a slow variable. The basic flow was expanded in terms of λ to $O(\lambda^3)$ and a solution to the steady state equation was obtained to $O(\lambda^3)$. Getting the solution to higher order is a laborious task. An alternative approach would be necessary to extend the steady state solution and determine the solution as a general series such that given terms up to $n - 1$, the n^{th} term can be calculated. A similar attempt was made by Lucas(1972) who successfully calculated the 13th approximation for the general shape in a channel by computational methods, but did not give analytical forms so that it is difficult to reproduce.

Nevertheless, for the exponential tubes, the solution obtained by the expansion method is in good agreement with the exact solution for $|\lambda| \leq 3$. Outside this range the expansion method tends to under estimate the value of the velocity. This is an indication that more terms are required to make a contribution to the velocity profile.

The approximate solution obtained by the expansion method was used to advantage in the slender tube problem. Here the DE profiles were shown to be good approximations for more general slender tubes as anticipated by

Eagles(1982). In Table 2.3 the approximation for Tube 1 when $\lambda = 3$ is shown to be extremely good. The approximation for Tube 2 is expected to be even better since the flow is closer to Poiseuille flow.

The stability of the DE profiles was next considered by quasi-parallel theory. Contour plots were used in the search for eigenvalues in the complex q -plane. In the range $-10 \leq q_r \leq 10$ and $-4 \leq q_i \leq 4$, no unstable eigenvalues were found. The least stable eigenvalue was found to be $(1.7492, 1.3257)$ at $\gamma = 0$, $R = 40$ and $\omega = 1$. Stability tests were carried out on q by varying γ , R and ω . The eigenvalues remained stable to all the changes as shown in Figures 3.2, 3.3, 3.4 and 3.5.

The DE profiles were further tested for stability on the eigenvalues obtained by Davey & Drazin(1969). Tests were carried out on 9 eigenvalues that include the least stable eigenvalue. As γ , R and ω were varied the eigenvalues remained stable to all these changes. The various trends of the eigenvalues as shown in Figures 4.2, 4.3, 4.4 and 4.5 were checked against the modified Corcos & Sellars eigenvalue relation for centre modes. These results indicate that the DE profiles are stable for $-6 \leq \gamma \leq 6$. They also confirm one of the additional modes found by Davey & Drazin.

The link between our spatial and temporal roots was established. It was then possible to show that the least stable root in the spatial problem was linked continuously to the least stable root in the temporal problem. Using the same idea we obtained a link between the root confirmed by Eagles (Private communication) and the Davey-Drazin root B_1 . We also showed that the temporal root C_1 corresponds to the spatial root q_3 . This restored our confidence in q_1 as being the least stable root and hence in our conclusions concerning the stability of the DE profiles.

We next considered the stability of slightly non-parallel flow in a wedge. The special relation between R and ϵ assumed by Eagles & Weissman, i.e. $\epsilon R = O(1)$ for the basic flow was removed. Instead, the basic flow was expanded in terms of ϵ to $O(\epsilon^2)$ with R independent of ϵ . This mathematical procedure was not only satisfactory but it also removed the objections raised by Smith (1979).

Eagles & Weissman (1975) obtained their growth rate results to $O(\epsilon)$ using the Jeffery-Hamel profiles as the base flow which effectively contain terms ϵR , $\epsilon^2 R^2$, $\epsilon^3 R^3$ etc. In the present procedure it was necessary to go on to $O(\epsilon^2)$ in order to obtain adequate contribution from the basic flow. The third approximation to the basic flow as indicated by Fig. 8.1 is considerably closer to the Jeffery-Hamel profile than the second approximation so that

a better approximation to the growth rate is expected. However, our results for the relative energy growth rate given in Fig. 8.8 indicate that higher order terms would be required to get comparable results as in Eagles & Weissman(1975). This implies that our growth rate is under-estimated and consequently the critical Reynolds numbers are higher than those given by Eagles & Weissman as shown in Table 8.5. The difference could still be attributed to the present method in which ϵ and R are treated as independent of each other and also to the basic flow approximation to $O(\epsilon^2)$.

Despite the differences, the trends of the neutral curves in the R - ϵ plane agree with the Eagles & Weissman curves for the stream function and relative energy growth rates. In both cases the approximations to the critical Reynolds number are lower for the relative energy growth rate than those given by the stream function growth rate. The approximations $\hat{G}_1(\Psi)$ and $\hat{H}_1(\hat{E})$ get closer together at lower values of ϵ so that we expect better estimates of the critical Reynolds number at low values of ϵ . These trends and Table 8.5 only indicate that we have an order of magnitude agreement with the Eagles & Weissman results.

Since the present method is mathematically consistent, it is worth considering what effect higher order terms would have in narrowing the differences between our results and

those obtained by Eagles & Weissman. This would not only be an improvement on the $O(\epsilon^2)$ theory it would also shed more light on the two methods. Nevertheless, the alternative method is viable and could provide a satisfactory confirmation of the results obtained by Eagles & Weissman.

ALLMEN, H. (1980)

Ph.D. Thesis.

The City University, London.

BEAUMONT, D. M. (1981)

The stability of spatially periodic flows.

J. Fluid Mech. 108, 481.

BETCHOV, R. & STENKOVEK, A. (1963)

Stability of a shear layer between parallel streams.

Phys. Fluids 6, 1391.

BETCHOV, R. & CRIVINALE, W. O. (1967)

Stability of parallel flows.

Annals Phys.

BLASIUS, H. (1908)

Grenzschichten in Flüssigkeiten mit kleiner Reibung.

Z. Math. Phys. 59, 1.

BLASIUS, H. (1910)

Laminare Strömung in hohlen zylindrischen Röhren.

Z. Math. Phys. 59, 183.

BLOTTNER, F. G. (1971)

Numerical solution of slender channel laminar flows.

Comp. Math. in Appl. Math. 5 (2) 311.

CONFIDENTIAL (1966)

REFERENCES

ABRAMOWITZ, M. (1949)

On backflow of a viscous fluid in a diverging channel.
J. Math. Phys. 28, 1.

ALLMEN, M. (1980)

Ph.D. Thesis.
The City University, London.

BEAUMONT, D.N. (1981)

The stability of spatially periodic flows.
J. Fluid Mech. 108, 461.

BETCHOV, R. & SZEWCZYK, A. (1963)

Stability of a shear layer between parallel streams.
Phys. Fluids 6, 1391.

BETCHOV, R. & CRIMINALE, W.O. (1967)

Stability of parallel flows.
Academic Press.

BLASIUS, H. (1908)

Grenzschichten in Flüssigkeiten mit kleiner
Reibung.
Z. Math. V. Phys. 56, 1.

BLASIUS, H. (1910)

Laminare Strömung in Kanälen wechselnder
Breite.
Z. Math. Phys. 58, 225

BLOTTNER, F.G. (1977)

Numerical solution of slender channel laminar flows.
Comp. Meth. in Appl. Mech. & Eng. 11, 319.

CONTE,S.D. (1966)

The numerical solution of linear boundary value problems.
Siam Review 8, 309.

CORCOS,G.M. & SELLARS,J.R (1959)

On the stability of fully developed flow in a pipe.
J. Fluid Mech. 5, 97.

DANIELS,P.G & EAGLES,P.M. (1979)

High Reynolds number flows in exponential tubes of
slow variation.
J. Fluid Mech. 90,305.

DANIELS,P.G. & EAGLES,P.M. (1983)

Slender channel theory in flow between two cylinders.
J. Eng. Math. 17, 125.

DAVEY,A. (1973)

A simple numerical method for solving Orr-Sommerfeld
problems.
Q. Jl. Mech. Appl. Math. 26, 401.

DAVEY,A. (1978)

On the stability of flow in an elliptic pipe which is
circular.
nearly
J. Fluid Mech. 87,233.

DAVEY,A. & DRAZIN,P.G. (1969)

The stability of Poiseuille flow in a pipe.
J. Fluid Mech. 36, 209.

DAVEY,A & NGUYEN,H.P.F (1971)

Finite-amplitude stability of pipe flow.
J. Fluid Mech. 45,701.

DRAZIN, P.G. (1974)

On a model of instability of a slowly-varying flow.

Q. Jl Mech. appl. Math. 27, 69.

DRAZIN, P.G. & REID, W.H. (1982)

Hydrodynamic Stability.

Cambridge University Press.

EAGLES, P.M. (1966)

The stability of a family of Jeffery-Hamel solutions for divergent channel flow.

J. Fluid Mech. 24, 191.

EAGLES, P.M. (1973)

Supercritical flow in a divergent channel.

J. Fluid Mech. 57, 149.

EAGLES, P.M. (1982)

On the stability of slowly varying flow between concentric cylinders.

Proc. R. Soc. Lond. A 355, 209.

EAGLES, P.M. (1982)

Steady flow in locally exponential tubes.

Proc. R. Soc. Lond. A 383, 231.

EAGLES, P.M. & WEISSMAN, M.A. (1975)

On the stability of slowly varying flow: the divergent channel.

J. Fluid Mech. 69, 241.

EAGLES, P.M. & SMITH, F.T. (1980)

The influence of nonparallelism in channel flow stability.

J. Eng. Math. 14, 219.

EAGLES, P.M. & MUWEZWA, M.E. (1986)

Approximations to flow in slender tubes. *on flow stability.*

J. Engg. Sci. 17, 615.

EKMAN, V.W. (1910)

Arkiv. Nat. Astron. Fysik, 6. *problems with small wall curvature.*

FRAENKEL, L.E. (1962)

Laminar flow in symmetric channels with slightly curved walls. *problems for Orr-Sommerfeld problems.*

I. On the Jeffrey-Hamel solutions for flow between plane walls. *(1963)*

Proc. Roy. Soc. A 267, 119. *disturbances in Poiseuille flow*

FRAENKEL, L.E. (1963)

Laminar flow in symmetric channels with slightly curved walls. *YAMADA, H. & HIKUSHIMA, J. (1983)*

II. An asymptotic series for the stream function. *parallel*

Proc. Roy. Soc. A 272, 406.

GARG, V.K. (1983)

Stability of nonparallel developing flow in a pipe to nonaxisymmetric disturbances. *slight suspension in*

J. Appl. Mech. 50, 210.

GARG, V.K. & ROULEAU, W.T. (1972)

Linear spatial stability of flow in pipe Poiseuille flow.

J. Fluid Mech. 54, 113. *incompressible boundary layer in*

GASTER, M. (1965) *of compliant boundaries.*

On the generation of spatially growing waves in a boundary layer. *NO. 22-12 1965*

J. Fluid Mech. 22, 433.

LEE, L.H. & ROSENBLUTH, M.N. (1967)
On the generation of spatially growing waves in

GASTER, M. (1974)

On the effects of boundary-layer growth on flow stability.

J. Fluid Mech. 66, 465.

GEORGIU, G.A. & EAGLES, P.M. (1985)

The stability of flows in channels with small wall curvature.

J. Fluid Mech. 159, 259.

GERSTING, J.M. & JANKOWSKI, D.F. (1972)

Numerical methods for Orr-Sommerfeld problems.

Int. J. Num. Meth. Eng. 4, 195.

GILL, A.E. (1965)

On the behaviour of small disturbances to Poiseuille flow in a circular pipe.

J. Fluid Mech. 21, 145.

GOTOH, K., YAMADA, M. & MIZUSHIMA, J. (1983)

The theory of stability of spatially periodic parallel flows.

J. Fluid Mech. 127, 45.

KAIMAL, M.R. (1979)

Low Reynolds number flow of a dilute suspension in slowly varying tubes.

Int. J. Engg. Sci. 17, 615.

KAPLAN, R.E. (1964)

The stability of laminar incompressible boundary layers in the presence of compliant boundaries.

Aero-elastic and Structures Research Laboratory ,

Report No. ASRL-TR 166-1,

Massachusetts Institute of Technology.

LEE, L.H. & REYNOLDS, W.K. (1967)

On the approximate and numerical solution of

- Orr-Sommerfeld problems.
Quart. J. Mech. Appl. Math. 20, 1.
- LIN, C.C. (1955)
The theory of hydrodynamic stability.
Cambridge University Press.
- LIN, C.C. (1961)
Some mathematical problems in the theory of the stability
of parallel flows.
J. Fluid Mech. 10, 430.
- LUCAS, R.D. (1972)
A perturbation solution for viscous incompressible flow
in channels.
Ph.D. diss.,
Stanford University, USA.
- MANTON, M.J. (1971)
Low Reynolds number flow in slowly varying axisymmetric
tubes.
J. Fluid Mech. 49, 451.
- NAYFEH, A.H. (1973)
Perturbation Methods.
John Wiley and Sons.
- NACHTSHEIM, P.R. (1964)
An initial value method for the numerical treatment of the
Orr-Sommerfeld equation for case of plane Poiseuille flow.
Nat. Aero. Space Admin. Tech. Note No. D-2414,
- PATTERSON, G.N. (1934)
Canad. J. Res. 11, 770.

PATTERSON, V.W. (1935)

Canad. J. Res. 12, 676.

PEKERIS, C.L. (1948)

Stability of the laminar flow through a straight pipe of circular cross-section to infinitesimal disturbances which are symmetric about the axis of the pipe.

Proc. U.S. Nat. Acad. Sci. 34, 285.

PRANDTL, L. (1904)

Über Flüssigkeitsbewegung bei sehr kleiner Reibung.

Proceedings 3rd Intern. Math. Congr., 484-491, Heidelberg.

PRETSCH, J. (1941)

Die Laminare Reibungsschicht an elliptischen zylindern un Rotationsellipsoiden bei symmetrischer Anströmung.

Luftfahrtforschung 18, 397.

RAYLEIGH, LORD

On the stability of certain fluid motions.

Proc. London, Math. Soc. 11, 57 (1880) and 19, 67 (1887).

Scientific Papers I, 474-487 and III, 17.

Scientific Papers IV, 203 (1895) and VI, 197 (1913).

REYNOLDS, O. (1883)

On the experimental investigation of the circumstances which determine whether the motion of water shall be direct or sinuous, and the law of resistance in parallel channels.

Phil. Trans. Roy. Soc. 174, 935.

REYNOLDS, O. (1895)

On the dynamical theory of incompressible viscous fluids and the determination of the criterion.

Phil. Trans. Roy. Soc. 186A 123.

ROSENBROOK,G. (1937)

Instabilität der Gleitschichten im schwach divergenten Kanal.

Zamm. 17,8.

SALWEN,H. & GROSCH,C.E. (1972)

The stability of Poiseuille flow in a pipe of circular cross-section.

J. Fluid Mech. 4 93.

SEXL,Th. (1927)

Zur stabilitätsfrage der POISEUILLESchen un der COUETTE-Strömung.

Ann. Phy.(4),83,835.

SEXL,Th. & SPIELBERG,K. (1958)

Zum stabilitätsproblem der POISEUILLE-Strömung.

Acta Phy. Austriaca 12,9.

SMITH,F.T. (1976)

Flow throw constricted or dilated pipes and channels.

Q. Jl Mech. appl. Math. 29, 345 and 365.

STUART,J.T. (1960)

On the nonlinear mechanics of wave disturbances in stable and unstable parallel flows.

I. The basic behaviour in plane Poiseuille flow.

J. Fluid Mech. 9, 353.

TOLLMIEN,W. (1936)

Ein allgemeines Kriterium der instabilität laminarer Geschwindigkeitsverteilungen.

Nachr. Ges. Wiss. Göttingen, Math. Phys. Klasse,

Fachgruppe I,1,79.